UNIVERSITA' DEGLI STUDI DI NAPOLI FEDERICO II
A. D. MCCXXIV
**Dottorato di Ricerca in Ingegneria Informatica ed Automatica**
Comunità Europea
Fondo Sociale Europeo

# Multi-valued robust control techniques for uncertain systems and related implementation by means of microcontrollers

**FRANCESCO CALABRESE**

**Tesi di Dottorato di Ricerca**

**XX Ciclo**

**Novembre 2007**

**Il Tutore**

**Prof. Giovanni Celentano**

**Il Coordinatore del Dottorato**

**Prof. Luigi P. Cordella**

**Dipartimento di Informatica e Sistemistica**

# Multi-valued robust control techniques for uncertain systems and related implementation by means of microcontrollers

Francesco Calabrese

A Thesis submitted for the degree of Doctor of Philosophy

Dipartimento di Informatica e Sistemistica

University of Naples Federico II

November 2007

# Contents

# List of Figures

# List of Tables

**Abstract**

A variety of plants with high parametric uncertainties are usually controlled with signals that may assume only a finite number of values, in order to simplify actuator's construction and minimize the operation cost. This is, for instance, the case of the industrial plants' control where a power control signal is needed and then it is suitable to use simple and reliable actuators with a relatively low cost and high performance operation modes. The design of multi-valued control laws which provide a control signal that is discontinuous in time and quantized in magnitude is then of particular interest in many practical applications.

In this thesis we face the problem of designing new control laws for the multi-valued control, and their implementation by means of microcontrollers. In developing the synthesis technique, we make use of the concept of practical tracking, which allows imposing realistic constraints on the tracking of the reference signal with a reliable error tolerance over all the controlled time interval. The digital realization of the new multi-valued control law is addressed and the key issues associated with its microprocessor implementation are discussed. The efficiency of the design method and of the technology utilized for the realization are shown through a very interesting application: a temperature control system of a ceramic kiln.

# Chapter 1

# Introduction

In many practical applications the plants are controlled with signals that may assume only a finite number of values, the main reason being the choice of utilizing simple and reliable actuators with a relatively low cost and highly performing operation modes. This aspect originates the demand for developing new techniques in order to analyze, design and implement multi-valued controllers, i.e. systems which provide a control signal that is discontinuous in time and quantized in magnitude.

There are a lot of advantages and attractive features of deliberately introducing discontinuous controls [89], which have been applied for a long time in, for instance, relay systems. One interesting aspect of such control strategy is the motion of the trajectories in the set of discontinuities. In fact such motion is not inherent in any of the structures, but the trajectories describe a new type of motion called *sliding motion*, and the mode of behavior when sliding motions occur is called a sliding mode [46] [88] [89]. Systems with sliding modes can under certain circumstances be made insensitive to variations in the process dynamics and less sensitive to disturbances [89] [88] [90]. Furthermore, since the trajectories in the sliding mode are constrained to surfaces of lower dimension than that of the whole state space, the order of the differential equation describing the sliding mode is reduced. However, one disadvantage of variable structure systems may be that the control in the real process will change rapidly from one value to another on the discontinuous surface, which may wear out the physical actuators involved. The phenomenon of rapid switchings is called *chattering*. Chattering may be avoided by introducing hysteresis around the surfaces of discontinuity in the case of discrete actuators possibly combined with an equivalent continuous control (if sliding modes deliberately are introduced) such that the trajectory stays in the sliding mode. It is important to note, however, that the chattering effects the control even once the steady state is reached. It results then it is of particular interest the design of control laws that take the advantages of the above described robust controllers but avoid introducing the deleterious effects of the chattering.

Regarding the use of quantized control signals, various authors have studied problems concerning their definition and the properties of the derived control systems. In [17] the authors deal with feedback stabilization problems for LTI control systems with saturating quantized measurements. Problem relating to the structure of the reachable set for systems whose input sets are quantized are focused in [15]. In [43] the authors propose some stabilization methods for scalar linear systems by means of static quantized feedback controls, depending on the amount of information flow they require in the feedback loop. In [44] the authors analyze the stabilization problem for discrete time linear systems with multidimensional state and one-dimensional input using quantized feedbacks with a memory structure.

Most of the above mentioned control laws lack of practical implementations because they require strong computational effort and/or are based on theoretical assumptions that may be difficulty satisfied in practical applications. It follows that the plants commanded with quantized control signals are usually controlled with classical relay controllers or simple sliding mode controllers. Thanks to the increasing development of microprocessors, however, it is now possible to implement controllers through algorithms which describe both continuous, discrete and logical laws. Considering this new degree of freedom given by the development of microcontrollers, in this thesis we face the problem of designing new control algorithms, realized by means of microcontrollers, which implement multi-valued control laws. We make use of the concept of practical tracking by allowing imposing realistic constraints on the tracking of the reference signal with a reliable error tolerance over all the controlled time interval, without requiring a theoretical perfect tracking. It then becomes possible to design a logical robust control law that allows avoiding chattering and is able to solve the general practical tracking problem for stable and unstable plants, only imposing constraints on the minimum and maximum values of the control signal, which depend both from the plant and from the amplitude and variability of the reference trajectory.

Based on the developed control law synthesis technique, a prototypal embedded control system was developed and realized for the control of the temperature in a ceramic kiln. Electrical kilns, like many other power industrial plants, are commanded by means of relays which activate resistors (heating elements) and ventilation systems (cooling elements) in a discrete way [49]. Both PID controllers (whose output defines the duty cycle of a relay control signal, accordingly to a Pulse-Width Modulation technique) and relay controllers are usually adapted for the kiln control. Such controllers however do not provide good performance because they have not expressly been designed to be used for finite valued control and with complex plants respectively. The discussed control law instead allows tracking strict reference trajectories described in terms of temperature profile (reference trajectory and its first and second derivatives). The prototyped control system was applied to a classical ceramic kiln provided with a row of resistors, separately actuated. The reported experimental results have demonstrated that the proposed control law performs well in this application, also compared with the currently adopted controllers.

## 1.1 Summary of contents

This thesis deals with all the theoretical and technical aspect behind the design and implementation of multi-valued control laws. The following sections briefly present the main contents of the chapters of the thesis.

### 1.1.1 Analysis of stability

In many practical applications the main concern is the behavior of the system over a fixed finite time interval. It results that it could be of interest to define as stable a system whose state, given some initial conditions, remains within pre- scribed bounds in a prefixed time interval, and as unstable a system which does not. These bounds can be expressed as certain regions of the state space, e.g. boxes, and, depending on the constraints on the initial conditions, generate two classes of problems: finite-time stability and practical stability.

The finite-time stability (FTS) problem is presented in Section 2.2. Two approaches are presented for the analysis of FTS of a linear continuous system. The first approach deals with quadratic functions [6]. The second approach [4] instead deals with polyhedral functions. Indeed polytopic domains naturally arise in many practical problems, and it is shown with several examples that the polyhedral functions perform better because they allow to take directly into account polytopic domains.

The practical stability problem is presented in Section 2.3 [34] and is used to derive the synthesis theorem of the robust controller in Chapter 3.

The rest of the chapter deals with the analysis of discontinuous control systems [88] [89], and in particular the problem arising in the definition of solutions to discontinuous right hand side differential equations [46]. Theorems to verify the existence and uniqueness of the solution to differential inclusions are then stated.

### 1.1.2 Control law design

A novel method for the design of controllers that allow the state of a continuous system, to be stabilized within a certain region of the state space is presented in Chapter 3 [21]. The proposed controller is robust with respect to the plant's uncertain parameters and disturbances, and guarantees to follow the reference trajectory with prefixed values of the tracking error and of its derivatives until $n-1$, where $n$ is the order of the plant, and in particular with preassigned values of the error and of its first derivative. Moreover, the control law guarantees the convergence of the error in a prefixed time.

Section 3.5 discusses the characteristics of the control algorithm, the problem of existence and uniqueness of the solution and the choice of the control signal's range.

Considering the case when the control input can assume only a finite number of values, the control law is analyzed (see Section 3.6) and several examples are discussed.

### 1.1.3 Optimal filters for the delayed estimation

The problem of defining the optimal structure of a filter is presented in the Chapter 4, where it is supposed that a certain delay in the estimation is tolerable [20]. The main contribution is the formulation of an optimal filter design problem, taking into account the possibility that a delay in the signal's estimation can be tolerated. Various application of the proposed approach for the filtering design are described in this chapter, considering the wide class of Butterworth filters (see Section 4.3).

The proposed theory is then applied to design the optimal differentiation system which provides the derivatives of the reference trajectory for the implementation of the multi-valued control law of Section 3.6.

The theory presented in this chapter is also investigated to design optimal control systems for tracking reference signals, known with a certain advance, providing that an appropriate pre-processing system can be applied to the reference trajectory [19].

Finally, the application of the optimal filters to the estimation of the trajectory of mobile phone users is presented in Section 4.6. A collaboration was established to this end with Telecom Italia Lab and the Massachusetts Institute of Technology SENSEable City Laboratory [26], and a test bed was set up in the City of Rome during a three month exhibition in 2006 [25][76] to evaluate the accuracy of the developed mobile phones monitoring system.

### 1.1.4 Multi-valued controller implementation and experiments

The Chapter 5 deals with the digital realization of the new multi-valued control law synthesized in Section 3.6 and the key issues associated with its microprocessor implementation. The efficiency of the design method and of the technology utilized for the realization are shown through a very interesting application: a temperature control system of a ceramic kiln [23].

Using the implemented embedded control system, and, with reference to the test case of the ceramic kiln control, the Section 5.6 presents the performance of the proposed controller compared to the currently adopted controllers and the theoretical expectations.

# Chapter 2

# Analysis of stability

In this chapter the concept of stability within a certain region of the state space is provided, and the practical tracking control problem is stated. The rest of the chapter deals with the analysis of discontinuous control systems, and in particular the problem arising in the definition of solutions to discontinuous right hand side differential equations. This class of discontinuous control systems includes the class of feedback control systems characterized by a continuous plant and a controller whose output can assume only a finite number of levels, which is analyzed in this thesis.

## 2.1 Stability within a certain region of the state space

Since many practical applications deal with the analysis of the behavior of the system over a fixed finite time interval, it could be appropriate to introduce a new definition of stability, for which, we define as stable a system whose state, given some initial conditions, remains within prescribed bounds (trajectory domain) in a prefixed time interval, and as unstable a system which does not. These bounds can be expressed as certain regions of the state space, e.g. boxes, and, depending on the constraints on the initial conditions, generate two classes of problems:

1. *finite-time stability*, if the initial condition of the system is constrained by a domain of the state space contained in the trajectory domain. This case is analyzed in Section 2.2;

2. *practical stability*, if the initial condition of the system is constrained by a domain of the state space containing the trajectory domain. In this case, it is required that the state reaches the final domain by a certain time called convergence time. This case is analyzed in Section 2.3.

## 2.2 Finite time stability

Many are the practical problems in which this kind of stability, called finite-time stability (FTS) (see [40] and [91]) plays an important role: for instance the problem of controlling the trajectory of a space vehicle from an initial point to a final point in a prescribed time interval, or the problem of controlling a system when some saturation elements are present in the feedback loop. This section presents the definition of finite-time stability and describes the currently available methods to analyze the FTS of a continuous time system.

### 2.2.1 Problem statement

Let us consider the following linear system

$$\dot{x}(t) = Ax(t)\,, \quad t \in [0, T]\,, \tag{2.1}$$

where $A \in \mathbb{R}^{n\times n}$. Roughly speaking, system (2.1) is said to be finite-time stable if, given a certain initial domain, its state remains, over a finite-time interval, within a prescribed trajectory domain.

**Definition 1 (Finite-time stability)** *The linear system* (2.1) *is said to be FTS with respect to* $(T_0, T_\rho, T)$*, where* $T$ *is a positive scalar,* $T_0$ *is a domain containing the origin of* $\mathbb{R}^n$*,* $T_0 \subset T_\rho$*, if*

$$x(0) \in T_0 \Rightarrow x(t) \in T_\rho \quad \forall t \in [0, T]. \tag{2.2}$$

$\Diamond$

**Remark 1** *It is important to recall that FTS and Lyapunov Asymptotic Stability (LAS) are independent concepts; indeed a system can be FTS but not LAS, and vice versa. While LAS deals with the behavior of a system within a sufficiently long (in principle infinite) time interval, FTS is a more practical concept, useful to study the behavior of the system within a finite (possibly short) interval. Therefore FTS finds application whenever it is desired that the state variables do not exit a given domain (for example to avoid saturations or the excitation of nonlinear dynamics) during the transients.*

### 2.2.2 Stability analysis using quadratic functions

Stability analysis was first studied in [6] considering the case when $T_0$ and $T_\rho$ are ellipsoidal domains. The main result provided was a sufficient condition for FTS analysis and robust finite-time stabilization via state feedback. This condition was then reduced to a feasibility problem involving linear matrix inequalities (LMIs).

The definition of FTS considered in [6] is the following.

**Definition 2 (Finite-time stability)** *The linear system* (2.1) *is said to be FTS with respect to* $(R, c_1, c_2, T)$*, where* $R \in \mathbb{R}^{n\times n}$ *is a positive definite matrix,* $c_1$*,* $c_2$ *and* $T$ *are positive scalars, if*

$$x^T(0)Rx(0) \le c_1 \Rightarrow x^T(t)Rx(t) < c_2 \quad \forall t \in [0, T]. \tag{2.3}$$

$\Diamond$

Observe that the standard weighted quadratic norm is used to define both the initial state domain (*initial domain*) and the domain where the trajectory is requested to be confined over a prescribed time interval (*trajectory domain*),

The following Theorem states a sufficient condition for FTS.

**Theorem 1 (Sufficient condition for FTS)** *[6] System* (2.1) *is finite-time stable with respect to* $(R, c_1, c_2, T)$ *if there exist a positive scalar* $\alpha$ *and a symmetric positive definite matrix* $Q \in R^{n \times n}$ *such that*

$$A\tilde{Q} + \tilde{Q}A^T - \alpha\tilde{Q} \leq 0 \tag{2.4}$$

$$\frac{c_1}{c_2} e^{\alpha T} I < Q < I \tag{2.5}$$

*where* $\tilde{Q} = R^{-(1/2)} Q R^{-(1/2)}$.

### 2.2.3 Stability analysis using polyhedral functions

In this section we consider the finite-time stability problem, but, differently from Section 2.2.2, propose to perform the analysis with the aid of polyhedral Lyapunov functions rather than the classical quadratic Lyapunov functions [4]. In this way we are able to manage more realistic constraints on the state variables; indeed, in a way which is naturally compatible with polyhedral functions, we assume that the sets to which the state variables must belong to satisfy the finite-time stability requirement are boxes (or more in general polytopes) rather than ellipsoids.

The main result, derived using polyhedral Lyapunov functions, is a sufficient condition for FTS of linear systems, which can also be used in the controller design context. Detailed analysis and design examples are presented to illustrate the advantages of the proposed methodology over existing methods.

#### Polytopic versus ellipsoidal domains

The definition given in Section 2.2.2 exploits the standard weighted quadratic norm to define both the initial state domain (*initial domain*) and the domain where the trajectory is requested to be confined over a prescribed time interval (*trajectory domain*); therefore such domains turn out to be ellipsoidal. The definition of the above domains is consistent with the fact that quadratic Lyapunov functions are used to derive the main results of [5] and [6].

In this section we propose a new definition for the initial and trajectory domains that makes use of polytopes rather than ellipsoidal domains. Polytopic domains naturally arise in many practical problems when, for instance, we consider constraints on the state variables in the form $a_i \leq x_i \leq b_i$.

If the domains are defined by means of polytopes, the FTS analysis based on the ellipsoidal domains introduces conservatism since it is needed to approximate the polytopic initial domain by an appropriate ellipsoidal domain containing it, and the polytopic trajectory domain by another ellipsoidal domain contained in it. For example let us consider the mass-spring-friction system

$$M\ddot{y} + K_f\dot{y} + K_s y = 0\,, \tag{2.6}$$

where $y$ [m] is the position of the mass, $M = 1$ Kg, $K_f = 0.25$ Ns/m, $K_s = 1$ N/m and assume that the following constrains on the state variables are

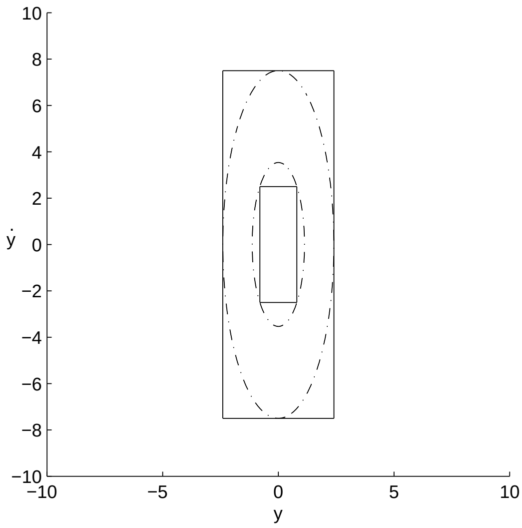


Figure 2.1: *Initial domain* and *trajectory domain* for system (2.6).

imposed

$$-0.8 \leq y(0) \leq 0.8 \tag{2.7a}$$
$$-2.5 \leq \dot{y}(0) \leq 2.5 \tag{2.7b}$$
$$-2.4 \leq y(t) \leq 2.4,\ t \in [0, T] \tag{2.7c}$$
$$-7.5 \leq \dot{y}(t) \leq 7.5,\ t \in [0, T]\,, \tag{2.7d}$$

where $T = 0.8$ s.

If we analyze this FTS problem by the approach proposed in [6], we need to approximate the initial domain and the trajectory domain by ellipsoidal domains, as done in Fig. 2.1; it is therefore evident that the approximation of the domains introduces conservatism in the FTS analysis.

Moreover, as we will see in the next sections, in some cases the technique proposed in [6] cannot be applied; this happens when the ellipsoid approximating the trajectory domain does not contain the ellipsoid approximating the initial domain.

To avoid this problem, in this section we provide a technique based on polyhedral Lyapunov functions [16] which allows us to take directly into account polytopic domains in the FTS analysis; the main result is a sufficient condition for FTS of linear time-invariant systems, which can also be used to design a state feedback finite-time stabilizing controller. Then we present some numerical examples to show the advantages of the proposed approach over the existing techniques.

### Notation

We denote by $q_i$, $i = 1, ..., m$ the $i - th$ column of a matrix $Q \in \mathbb{R}^{n \times m}$. If $Q \in \mathbb{R}^{n \times m}$ is a full row rank matrix, we indicate with $\wp(Q)$ the polytope defined as (see [78], p. 6)

$$\mathcal{P} = \wp(Q) = \{x \in \mathbb{R}^n : \|Q^T x\|_\infty \leq 1\}\,, \tag{2.8}$$

where, given a vector $v \in \mathbb{R}^m$, $\|v\|_\infty := \max\{|v_1|, \ldots, |v_m|\}$ denotes the infinity norm of $v$. By $\partial\wp(Q)$ we indicate the boundary of the polytope $\wp(Q)$. Finally, $\mathbb{N}_n$ indicates the set $\{1, \ldots, n\}$.

### Problem statement

**Definition 3 (Finite-time stability)** *The linear system* (2.1) *is said to be FTS with respect to* $(P_0, P, T)$*, where* $T$ *is a positive scalar,* $P_0 \in \mathbb{R}^{n\times m_0}$ *and* $P \in \mathbb{R}^{n\times m}$ *are two full-row rank matrices with* $\wp(P_0) \subset \wp(P)$*, if*

$$x(0) \in \wp(P_0) \Rightarrow x(t) \in \wp(P) \quad \forall t \in [0, T]. \tag{2.9}$$

$\Diamond$

**Remark 2** *Note that, given a full row rank matrix* $P$*, the set* $\wp(P)$ *is a polytope symmetric with respect to the origin (see* (2.8)*). It follows that, by Definition 3, we are restricting our attention to the class of initial and trajectory domains that are symmetric polytopes.* $\Diamond$

**Remark 3** *A sufficient condition for system* (2.1) *to be FTS with respect to* $(P_0, P, T)$ *can be derived by using the approach proposed in [6]. The main result of [6] states that system* (2.1) *is FTS with respect to* $(P_0, P, T)$ *if there exist three positive scalars* $\alpha, c_1, c_2$*, with* $c_2 > c_1$ *and two positive definite matrices* $R, Q \in \mathbb{R}^{n\times n}$ *such that*

$$\wp(P_0) \subseteq \mathcal{E}_1 = \{x \in \mathbb{R}^n : x^T R x \leq c_1\} \tag{2.10a}$$

$$\wp(P) \supseteq \mathcal{E}_2 = \{x \in \mathbb{R}^n : x^T R x < c_2\} \tag{2.10b}$$

$$A\tilde{Q} + \tilde{Q}A^T - \alpha\tilde{Q} < 0 \tag{2.10c}$$

$$\frac{c_1}{c_2} e^{\alpha T} I < Q < I\,, \tag{2.10d}$$

*where* $\tilde{Q} = R^{-1/2}\, Q\, R^{-1/2}$*. First note that this way of proceeding unavoidably introduces conservatism in the FTS analysis. Even worse, there are some cases where it is not possible to find a matrix* $R$ *and two scalars* $c_1$ *and* $c_2$*,* $c_2 > c_1$*, such that conditions* (2.10a) *and* (2.10b) *are satisfied. In these cases, the procedure derived in [6] cannot be applied. For example assume that the initial and trajectory domains are*

$$\wp(P_0) = \{x \in \mathbb{R}^2 :\ |x_1| \leq 1,\ |x_2| \leq 1\}$$
$$\wp(P) = \{x \in \mathbb{R}^2 :\ |x_1| \leq 1 + \epsilon,\ |x_2| \leq 2,\ \epsilon > 0\}\,.$$

*It is easy to see that, regardless the system under consideration and the time* $T$*, there exists a lower bound* $\bar{\epsilon}$ *to the value of* $\epsilon$ *for which the approach proposed in [6] cannot be exploited because it is not possible to find two ellipsoidal domains* $\mathcal{E}_1$ *and* $\mathcal{E}_2$ *which verify* $\wp(P_0) \subseteq \mathcal{E}_1 \subset \mathcal{E}_2 \subseteq \wp(P)$*.* $\Diamond$

In the following we provide some preliminary definitions and results on polytopes.

**Definition 4 (Affine space)** *An* affine space *over a field* $\mathbb{K}$ *is a triplet* $(A, V, \pi)$ *composed of a nonempty set* $A$*, a vector space* $V$ *over* $\mathbb{K}$ *and an application* $\pi : (a, b) \in A \times A \to \pi(a, b) \in V$ *such that*

*i) for all* $a \in A$ *and* $v \in V$*, there exists a unique element* $b \in A$ *such that* $\pi(a, b) = v$ *;*

*ii)* $\forall a, b, c \in A,\ \pi(a, b) + \pi(b, c) = \pi(a, c)$ *.*

$\diamondsuit$

For example, $\mathbb{R}^n$ can be interpreted both as a point set or as a vector space. Indeed to a given point $a \in \mathbb{R}^n$ we can associate the vector $v_a \in \mathbb{R}^n$ going from the origin to the point $a$. It is simple to verify that the triplet $(\mathbb{R}^n, \mathbb{R}^n, \pi)$ is an affine space once we define

$$\pi(a, b) := v_a - v_b\,. \tag{2.11}$$

**Definition 5 (Affine subspace)** *Let* $(A, V, \pi)$ *be an affine space. Let* $H$ *be a subset of* $A$ *and* $V_H$ *the set of vectors* $\{\pi(a, b)\ :\ a, b \in H\}$*. Let us restrict the domain and codomain of* $\pi$ *to* $H \times H$ *and* $V_H$*, respectively, and denote the resulting application with* $\pi_H$*. The triplet* $(H, V_H, \pi_H)$ *is an* affine subspace *of* $(A, V, \pi)$ *if a)* $V_H$ *is a vector subspace of* $V$ *and b)* $(H, V_H, \pi_H)$ *is an affine space. The* dimension *of the affine subspace* $(H, V_H, \pi_H)$ *is the dimension of the vector subspace* $V_H$*.* $\diamondsuit$

Let us consider the affine space $(\mathbb{R}^2, \mathbb{R}^2, \pi)$, with $\pi$ defined as in (2.11), and the line $L := \{x \in \mathbb{R}^2\ :\ x_1 + x_2 = 1\} \subset \mathbb{R}^2$. Note that $\mathbb{R}^2_L$ is the subspace of $\mathbb{R}^2$ given by the bisector of the second and fourth quadrant. It is simple to recognize that the triplet $(L, \mathbb{R}^2_L, \pi_L)$ is an affine subspace of $(\mathbb{R}^2, \mathbb{R}^2, \pi)$ of dimension one.

In the following we will consider the affine space associated to the standard vector space $\mathbb{R}^n$ over the field $\mathbb{R}$, and the related affine subspaces; correspondingly, the operator $\pi(a, b)$, with $a, b \in \mathbb{R}^n$, will always coincide with the one defined in (2.11). Concerning Definition 5, without loss of generality and for the sake of simplicity, we shall refer to the "affine subspace $H$" rather than to the "affine subspace $(H, V_H, \pi_H)$".

**Definition 6 (Convex and affine hull [97], p. 3)** *Given a set* $A \subset \mathbb{R}^n$ *the convex hull of* $A$ *is defined as the subset of* $\mathbb{R}^n$ *composed of all vectors obtained via convex combination from the elements of* $A$*, namely*

$$\begin{aligned}\mathrm{conv}(A) := \Bigg\{ v \in \mathbb{R}^n\ :\ v = \sum_{i=1}^{k} \lambda_i v^{(i)}, \sum_{i=1}^{k} \lambda_i = 1, \\ \lambda_i \geq 0\,,\ v^{(i)} \in A, i = 1, \dots, k\,,\ k = 1, 2, \dots \Bigg\}\,.\end{aligned} \tag{2.12}$$

*If in* (2.12) *we eliminate the requirement that the numbers* $\lambda_i$ *be nonnegative, the resulting set is said to be the* affine hull *of* $A$*.* $\diamondsuit$

It is worth noticing that the convex hull of a set $A$ is the smallest convex set containing $A$, while the affine hull turns out to be an affine subspace of $\mathbb{R}^n$.

If we deal with a finite set $K = \{x^{(1)}, \dots, x^{(k)}\} \subset \mathbb{R}^n$ the *convex hull* of $K$ turns out to be a *polytope*, whose *dimension* ([97], p. 5), is given by the dimension of the affine hull of $K$. Moreover, as stated in the next lemma, the set of vertices of a given polytope $\mathcal{P}$ defined as the convex hull of $K$ is a subset of $K$.

**Lemma 1 ([97])** *Given a polytope defined as the convex hull of*

$$K = \{x^{(1)}, \ldots, x^{(k)}\} \subset \mathbb{R}^n \tag{2.13}$$

*the vertices of the polytope are the points $x^{(i)} \in K$ which satisfy the following property*

$$x^{(i)} \notin \operatorname{conv}\left(K - \{x^{(i)}\}\right).$$

$\diamondsuit$

**Remark 4** *Note that, given a collection of symmetric points $K = \{x^{(1)}, \ldots, x^{(2l)}\}$, $x^{(i)} = -x^{(l+i)}, i = 1, \ldots, l$, if $x^{(i)}$ is a vertex of* $\operatorname{conv}(K)$*, then also $x^{(l+i)} = -x^{(i)}$ is a vertex of* $\operatorname{conv}(K)$*.* $\diamondsuit$

**Remark 5** *Note that a given symmetric polytope $\mathcal{P}$ admits two different equivalent descriptions: the first one as convex hull of its vertices, the other one in the matrix form* (2.8)*. As we will see later, a fundamental point in our approach will be the development of an efficient algorithm to pass from one representation to the other one.* $\diamondsuit$

**Definition 7 (Affinely independent points [97], p. 3)** *A set of $k > 0$ points is* affinely independent *if its affine hull has dimension $(k-1)$.* $\diamondsuit$

**Lemma 2 ([97])** *The convex hull of any $(n+1)$ affinely independent points in $\mathbb{R}^n$ is a polytope of dimension $n$.* $\diamondsuit$

Finally, the next definition generalizes for our purposes, the concept of "points in general position" given in [97].

**Definition 8 (Set of points in generic position)** *A set of $k \geq n$ points in $\mathbb{R}^n$, $n \geq 2$, is said to be in* generic position *if there is no $n$-tuple composed of such points lying on a common affine plane of dimension $(n-2)$. If $n = 1$ any set of points is in generic position.* $\diamondsuit$

**Remark 6** *Note that, requiring that $k$ points are in generic position in $\mathbb{R}^n$, implies that,* i) *they are distinct for $n = 2$;* ii) *there is no triplet of such points lying on a common line for $n = 3$;* iii) *there is no quadruplet of such points lying on a common plane for $n = 4$; etc.* $\diamondsuit$

**Remark 7** *The minimum number of vertices that define a symmetric polytope in $\mathbb{R}^n$ of dimension $n$ is $2n$. An example of symmetric polytope with minimum number of vertices is the* crosspolytope *of dimension $n$*

$$\mathcal{C} := \{x \in \mathbb{R}^n : \sum_i |x_i| \leq 1\} = \operatorname{conv}\{e_1, -e_1, \ldots, e_n, -e_n\},$$

*where $e_i$ are the unit vectors in $\mathbb{R}^n$. Note that these points are in generic position.* $\diamondsuit$

**Machinery**

The solution to the following Problem will be useful to derive the main result of the section.

**Problem 1** *Given a polytope $\mathcal{P}$ defined as the convex hull of $2l$ symmetric points $K = \{x_Q^{(1)}, \dots, x_Q^{(2l)}\}$ in generic position in $\mathbb{R}^n$, $x_Q^{(i)} = -x_Q^{(l+i)}, i = 1, \dots, l$, with $l \geq n$, where $(n+1)$ of them are affinely independent, find a matrix $Q$ such that* (2.8) *is satisfied.* $\Diamond$

The following procedure solves Problem 1.

**Procedure 1 (Solution to Problem 1)** *First of all, note that Lemma 2 guarantees that $\mathcal{P}$ has dimension $n$. Next, using Lemma 1, it is possible to select the $2k$ vertices of $\mathcal{P}$, $k \leq l$, from $\{x_Q^{(1)}, \dots, x_Q^{(2l)}\}$. Let us reorder the points such that $\{x_Q^{(1)}, \dots, x_Q^{(k)}, x_Q^{(l+1)}, \dots, x_Q^{(l+k)}\}$ are the vertices of $\mathcal{P}$. Note that, given the assumption that the set of points is in generic position, each vertex $x_Q^{(i)}$, $i = 1, \dots, k$, of $\mathcal{P}$ is the intersection of $s_i$ half-planes $q_{i,h} \in \mathbb{R}^n, h = 1, \dots, s_i$, $s_i \geq n$; such half-planes are univocally determined by $n$ vertices. These half-planes are columns vectors satisfying, for $i = 1, \dots, k$, the following conditions*

*a)*

$$q_{i,h}^T x_Q^{(i)} = 1\,; \tag{2.14}$$

*b) there exists a $(n-1)$-tuple of indexes $i_1 \neq i_2 \neq \cdots \neq i_{n-1} \in \{1, \dots, k, l+1, \dots, l+k\} - \{i\}$ such that*

$$q_{i,h}^T x_Q^{(i_t)} = 1\,, \quad \forall t = 1, \dots, n-1 \tag{2.15a}$$

$$q_{i,h}^T x_Q^{(j)} \leq 1\,, \quad \forall j \in \{1, \dots, k, l+1, \dots, l+k\} - \{i, i_1, \dots, i_{n-1}\}\,. \tag{2.15b}$$

*Once the half-planes $q_{i,h}$ have been found, we can equivalently define the polytope $\mathcal{P}$ as in* (2.8)*, where the matrix $Q$ can be constructed as follows*

$$Q = \begin{pmatrix} q_{1,1} & \dots & q_{1,s_1} & \dots & q_{k,1} & \dots & q_{k,s_k} \end{pmatrix}\,. \tag{2.16}$$

$\Diamond$

**Remark 8** *It is easy to see that for all $i = 1, \dots, k$ and $h = 1, \dots, s_i$, there exist at least $(n-1)$ vertices $x_Q^{(i_t)}$, $t = 1, \dots n-1$, such that one of its associated half-plane is equal to $q_{i,h}$, i.e. $q_{i,h} = q_{i_t, m_t}, m_t \in \{1, 2, \dots, s_{i_t}\}$. Therefore the matrix $Q$ presents several repeated columns that, without loss of generality, can be cancelled in order to lighten the computational burden.* $\Diamond$

In the sequel we will make use of the following definition.

**Definition 9 (Candidate set of points)** *A collection of points*

$$K = \{x_Q^{(1)}, \dots, x_Q^{(2l)}\} \subset \mathbb{R}^n,$$

*with $l \geq n$, is said to be a candidate set of points if*

- *the points are in generic position in* $\mathbb{R}^n$*;*
- *the points are symmetric, i.e.* $x_Q^{(i)} = -x_Q^{(l+i)}, i = 1, \ldots, l$*;*
- $(n+1)$ *of the points are affinely independent.*

*Without any loss of generality, we assume that the vertices of the polytope defined as* $\mathrm{conv}(K)$ *are the first* $k$ *points,* $k \leq l$*, of* $K$ *and their symmetric. Finally, we denote by* $q_{i,h}$*,* $h = 1, \ldots, s_i$*, the half-planes associated to the vertex* $x_Q^{(i)}$*,* $i = 1, \ldots, k$*, of the polytope.* $\Diamond$

To conclude this subsection, we present a lemma that will be used in the proof of the main result.

**Lemma 3** *Let* $P_0 \in \mathbb{R}^{n \times m_0}$ *and* $P \in \mathbb{R}^{n \times m}$ *be two full-row rank matrices. If* $\wp(P_0) \subseteq \wp(P)$ *then*

$$\|P^T x\|_\infty \leq \|P_0^T x\|_\infty \quad \forall x \in \mathbb{R}^n \tag{2.17}$$

***Proof 1*** *Consider a vector* $x \in \mathbb{R}^n$*. There exist two points* $\bar{x} \in \partial\wp(P)$ *and* $\bar{x}_0 \in \partial\wp(P_0)$*, and two positive scalars* $\beta$ *and* $\beta_0$ *such that*

$$x = \beta\bar{x} = \beta_0\bar{x}_0.$$

*From the definition of boundary point of a polytope, we have*

$$\begin{aligned} \|P^T x\|_\infty &= \beta\|P^T\bar{x}\|_\infty = \beta \\ \|P_0^T x\|_\infty &= \beta_0\|P_0^T\bar{x}_0\|_\infty = \beta_0 \end{aligned}$$

*Taking into account that* $\wp(P_0) \subseteq \wp(P)$*, it results that*

$$\bar{x} = \gamma\bar{x}_0, \quad \gamma \leq 1$$

*which implies* $\beta \leq \beta_0$*.*
*From the last statement, the proof follows.*

**Main result**

**Theorem 2 (Sufficient condition for FTS)** *System* (2.1) *is finite-time stable with respect to* $(P_0, P, T)$ *if there exist a positive scalar* $\alpha$ *and a candidate set of points as given in Definition 9 such that the following conditions hold*

$$q_{i,h}^T (A - \alpha I)\, x_Q^{(i)} \leq 0 \tag{2.18}$$

*for all* $i = 1, \ldots, k$*,* $h = 1, \ldots, s_i$*, and*

$$\max_i \|Q^T x_{P_0}^{(i)}\|_\infty \max_i \|P^T x_Q^{(i)}\|_\infty \, e^{\alpha T} \leq 1 \tag{2.19}$$

*where* $x_{P_0}^{(i)}$ *are the vertices of the polytope* $\wp(P_0)$*, and*

$$Q = \begin{pmatrix} q_{1,1} & \ldots & q_{1,s_1} & \ldots & q_{k,1} & \ldots & q_{k,s_k} \end{pmatrix}. \tag{2.20}$$

**Proof 2** *Consider a polytope $\wp_v$ assigned as the convex hull of the set $\{x_Q^{(1)}, ..., x_Q^{(2l)}\}$; by using Procedure 1, let us determine the half-planes $q_{i,h}$ associated to the $2k$ vertices, $k \leq l$, and let us construct the $Q$ matrix as*

$$Q = \begin{pmatrix} q_{1,1} & \dots & q_{1,s_1} & \dots & q_{k,1} & \dots & q_{k,s_k} \end{pmatrix} ,$$

*such that*

$$\wp_v = \wp(Q) = \{x \in \mathbb{R}^r : \|Q^T x\|_\infty \leq 1\} .$$

*Now let us consider the function*

$$V(x) = \|Q^T x\|_\infty . \tag{2.21}$$

*We denote by $\dot{V}$ the Dini derivative of $V$ along the solution of the system* (2.1) *(see [55]). Assume that the condition*

$$\dot{V}(x(t)) \leq \alpha V(x(t)) \tag{2.22}$$

*holds for all $t \in [0, T]$. We will first demonstrate that conditions* (2.19) *and* (2.22) *imply that system* (2.1) *is FTS with respect to $(P_0, P, T)$. Then, to conclude the proof, we will show that condition* (2.22) *is implied by* (2.18)*.*

*Dividing both sides of* (2.22) *by $V(x(t))$, and integrating from 0 to $t$, with $t \in (0, T]$, we obtain*

$$\log \frac{V(x(t))}{V(x(0))} \leq \alpha t . \tag{2.23}$$

*It follows that*

$$\|Q^T x(t)\|_\infty \leq \|Q^T x(0)\|_\infty e^{\alpha t} \qquad \forall t \in [0, T] . \tag{2.24}$$

*Since $x(0) \in \wp(P_0)$ and $\|Q^T x\|_\infty$ enjoys a radial property, an upper bound to the quantity $\|Q^T x(0)\|_\infty$ is attained at one of the vertices of $\wp(P_0)$, i.e.*

$$\|Q^T x(0)\|_\infty \leq \max_i \|Q^T x_{P_0}^{(i)}\|_\infty . \tag{2.25}$$

*Let us choose $h > 0$ such that $\wp(Q) \subseteq \wp(hP)$. Using account Lemma 3, this can be equivalently written as*

$$\|Q^T x\|_\infty \geq h\|P^T x\|_\infty \qquad \forall x \in \mathbb{R}^n . \tag{2.26}$$

*Recalling the definition of vertices of a polytope, we have*

$$\max_i h\|P^T x_Q^{(i)}\|_\infty \leq 1 . \tag{2.27}$$

*Equation* (2.27) *gives an upper bound to the values of $h$ that satisfy* (2.26)

$$h \leq h_{max} := \frac{1}{\max_i \|P^T x_Q^{(i)}\|_\infty} . \tag{2.28}$$

*From* (2.26) *and* (2.28) *we have along the system trajectories*

$$\|Q^T x(t)\|_\infty \geq h_{max}\|P^T x(t)\|_\infty = \frac{\|P^T x(t)\|_\infty}{\max_i \|P^T x_Q^{(i)}\|_\infty} . \tag{2.29}$$

*Putting together* (2.24), (2.25) *and* (2.29), *we obtain*

$$\|P^T x(t)\|_\infty \leq \max_i \|Q^T x_{P_0}^{(i)}\|_\infty \max_i \|P^T x_Q^{(i)}\|_\infty e^{\alpha t}. \tag{2.30}$$

*From* (2.30) *it readily follows that* (2.19) *implies, for all* $t \in [0,T]$, $\|P^T x(t)\|_\infty \leq 1$*; from this last consideration our first claim follows.*

*Now we will prove that condition* (2.18) *guarantees* (2.22). *The derivative of* $V$ *can be expressed as*

$$\dot{V}(x) = \max_{j \in I(x)} \tilde{q}_j^T Ax, \tag{2.31}$$

*where* $\tilde{Q} = \begin{pmatrix} Q & -Q \end{pmatrix}$ *and* $I(x)$ *is the set of the indexes* $j$ *such that* $V(x) = \tilde{q}_j^T x$ *(see [16]).*

*Condition* (2.22) *is guaranteed if*

$$\max_{j \in I(x)} \tilde{q}_j^T Ax \leq \alpha V(x). \tag{2.32}$$

*Since, by definition of* $I(x)$, $V(x) = \tilde{q}_j^T x$ *for all* $j \in I(x)$, *then* (2.32) *can be rewritten*

$$\max_{j \in I(x)} \tilde{q}_j^T (A - \alpha I)x \leq 0. \tag{2.33}$$

*The last condition is equivalent to the fact that* $V(x) = \|Q^T x\|_\infty$ *is a polyhedral Lyapunov function for the system* $\dot{x} = (A - \alpha I)x$. *From Fact 1 in [7], it follows that* (2.33) *is equivalent to*

$$q_{i,h}^T (A - \alpha I)\, x_Q^{(i)} \leq 0 \tag{2.34}$$

*for all* $i = 1, \ldots, k, l+1, \ldots, l+k$, $h = 1, \ldots, s_i$. *Eventually, condition* (2.18) *follows noticing that it is sufficient to check* (2.34) *for all* $i = 1, \ldots, k$, $h = 1, \ldots, s_i$, *because of the symmetry of the polytope.*

In order to find a polyhedral Lyapunov function satisfying the conditions of Theorem 2, the following procedure can be adopted.

**Procedure 2 (Implementation of Theorem 2)**

1. *Fix a positive* $\alpha$ *and a number* $l \geq n$. *Let* $K_0 = \{x_Q^{(i)}\}_{i=1,\ldots,2l}$ *be a* candidate set of points, *in the sense of Definition 9, whose convex hull is a regular polytope of* $2k$ *(*$k \leq l$*) vertices and radius* 1. *We assume that the vertices of the polytope defined as* $\mathrm{conv}(K_0)$ *are the first* $k$ *points of* $K_0$ *and their symmetric.*

2. *Find a candidate set of points* $K$ *solving the problem*

$$\min_K \max\{f(K), g(K)\} \tag{2.35}$$

*with initial condition* $K_0$, *where*

$$f(K) = \max_{i=1,\ldots,k} \max_{h=1,\ldots,s_i} q_{i,h}^T (A - \alpha I)\, x_Q^{(i)} \tag{2.36}$$

$$g(K) = \max_i \|Q^T x_{P_0}^{(i)}\|_\infty \max_i \|P^T x_Q^{(i)}\|_\infty e^{\alpha T} - 1. \tag{2.37}$$

*3. Let* $M = \min_K \max\{f(K), g(K)\}$*. If* $M < 0$ *then set*

$$K_{opt} = \arg M, \tag{2.38}$$

*and go to step 4, else set*

$$\begin{aligned} K_0 &= K \cup \left\{x_Q^{(l+1)}, -x_Q^{(l+1)}\right\}, \; x_Q^{(l+1)} \in \mathbb{R}^n && \text{(2.39a)} \\ l &= l+1\,, && \text{(2.39b)} \end{aligned}$$

*assume that the vertices of the polytope defined as* $\mathrm{conv}(K_0)$ *are the first* $k$ *points of* $K_0$ *and their symmetric, and go to step 2.*

*4. The polyhedral Lyapunov function which proves the FTS of system* (2.1) *wrt* $(P_0, P, T)$ *is*

$$V(x) = \|Q^T x\|_\infty \tag{2.40}$$

*where* $Q$ *is obtained from* $K_{opt}$ *using Procedure 1.*

$\diamondsuit$

**Remark 9** *To solve problem* (2.35)*, we have made use of the Matlab Optimization Toolbox routine* fminimax *[1], with variables* $x_Q^{(i)}, i = 1, \ldots, l$*.* $\diamondsuit$

**Remark 10** *The choice of* $x_Q^{(l+1)}$ *in step 3 is done putting such point on one of the faces of* $\wp(Q)$*. In particular, if* $\max_i \max_h q_{i,h}^T (A - \alpha I)\, x_Q^{(i)}$ *is obtained in correspondence of* $h = r \in \{1, \ldots, s_i\}$*,* $i = t \in \{1, \ldots, k\}$*, the point is put in the middle of the face defined by the half-plane* $q_{t,r}$*. In this way, since at each step the algorithm begins from the solution found in the previous step, the value* $M$ *decreases (or, at least, does not increase) at each step.* $\diamondsuit$

**Numerical Examples**

In this subsection two examples are discussed. The former considers a second order mass-spring system and is useful to illustrate the application of Theorem 2 and to compare our approach with the approach of [6]. The second example shows how the proposed methodology can be applied in a design context.

**Comparison with the previous literature**

Let us reconsider the FTS problem described earlier in this section. We will show that Theorem 2 allows us to prove that system (2.6), under the constraints (2.7), is FTS while the sufficient condition proposed in [6] does not.

First of all note that system (2.6) can be rewritten in the form (2.1) where

$$A = \begin{pmatrix} 0 & 1 \\ -1 & -0.25 \end{pmatrix}, \; x = \begin{pmatrix} x_1 \\ x_2 \end{pmatrix} := \begin{pmatrix} y \\ \dot{y} \end{pmatrix}. \tag{2.41}$$

Our goal is to check whether system (2.1), (2.41) is FTS with respect to $(P_0, P, T)$, where $P_0$ and $P$ are the 4-vertices polytopes selected accordingly to the constraints (2.7) (see Fig. 2.1), and $T = 0.8s$.

We first tried to verify the FTS stability of system (2.6) by using the approach described in Remark 3. To this end, we selected $R$ and $c_2$ imposing the ellipsoid $\mathcal{E}_2$ to be symmetric with respect to the coordinated axis and with maximum volume. Consequently, $c_1$ was computed by a scaling operation (see Fig. 2.1). The conditions (2.10c)–(2.10d) were evaluated with the aid of the Matlab LMI Toolbox [50] and the derived problem was found unfeasible for all $\alpha > 0$.

Then, we tried to solve the problem with the application of Theorem 2. Since $r = 2$, we can order the symmetric points $\{x^{(1)}, ..., x^{(2l)}\}$ counterclockwise. Therefore, conditions (2.18) of Theorem 2 and (2.14), (2.15) of Procedure 1 can be rewritten as follows

$$q_i^T\,(A - \alpha I)\,x_Q^{(i)} < 0 \tag{2.42a}$$
$$q_i^T\,(A - \alpha I)\,x_Q^{(i+1)} < 0 \tag{2.42b}$$
$$q_l^T\,(A - \alpha I)\,x_Q^{(l)} < 0 \tag{2.42c}$$
$$-q_l^T\,(A - \alpha I)\,x_Q^{(1)} < 0 \tag{2.42d}$$
$$q_i^T\,x_Q^{(i)} = 1 \tag{2.42e}$$
$$q_i^T\,x_Q^{(i+1)} = 1 \tag{2.42f}$$
$$q_l^T\,x_Q^{(l)} = 1 \tag{2.42g}$$
$$-q_l^T\,x_Q^{(1)} = 1 \tag{2.42h}$$
$$\pm q_i^T\,x_Q^{(j)} < 1,\ j \neq i\,,\ j \neq i+1 \tag{2.42i}$$
$$\pm q_l^T\,x_Q^{(j)} < 1,\ j \neq 1\,,\ j \neq l \tag{2.42j}$$

for all $i = 1, ..., l-1$, $j = 1, ...l$, where $q_i := q_{i,2} = q_{i+1,1}$.

In the case of second order systems, the problem simplifies since for each vertex we have only two associated half-spaces. Then, by using (2.42e)–(2.42h), we can express the row vectors $q_i^T, i = 1, ..., l$ as functions of the vertices $x_Q^{(i)}, i = 1, ..., l$. Therefore, the original problem is reduced to find $x_Q^{(i)}, i = 1, ..., l$ so as to satisfy the set of strict inequality constraints (2.42a)–(2.42d), (2.42i)–(2.42j). This feasibility problem can then be solved using standard optimization routines.

We used the Matlab Optimization Toolbox routine *fminimax*, with variables $x_Q^{(i)}, i = 1, ..., l$, and with the cost function derived by (2.18) and (2.19). We verified that system (2.6) is FTS with respect to $(P_0, P, T)$, by using the polyhedral Lyapunov function of 40 vertices shown in Fig. 2.2, with $\alpha = 0.3$.

Now consider again the mass-spring-friction system with an external force $u$ [N] applied to the mass

$$M\ddot{y} + K_f\dot{y} + K_s y = u. \tag{2.43}$$

We analyzed the FTS of the third order closed-loop system consisting of the connection of system (2.43) with an integral controller $u(t) = K_i \int y(t)dt$, with $K_i = 0.1$. The dynamic matrix of the closed-loop system reads

$$A = \begin{pmatrix} 0 & 1 & 0 \\ 0 & 0 & 1 \\ -0.1 & -1 & -0.25 \end{pmatrix}, \tag{2.44}$$

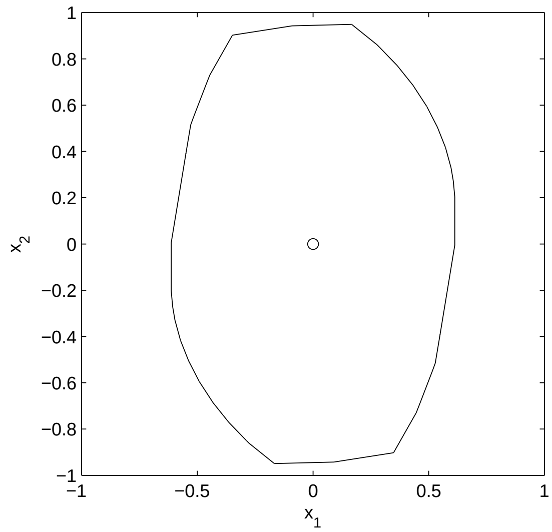


Figure 2.2: Polyhedral Lyapunov function with 40 vertices.

where $x_1 = u$, $x_2 = y$, $x_3 = \dot{y}$. Consider the following boxes in $\mathbb{R}^3$

$$\begin{aligned} P_0 &= \{x \in \mathbb{R}^3 : |x_1| \leq 0.5, |x_2| \leq 0.8, |x_3| \leq 2.5\} \\ P &= \{x \in \mathbb{R}^3 : |x_1| \leq 2.0, |x_2| \leq 3.2, |x_3| \leq 10.0\}\,; \end{aligned}$$

moreover let $T = 0.5$ s. We found that the system is FTS for $\alpha = 1.05$, with the polyhedral Lyapunov function of 12 vertices shown in Fig. 2.3.

**State Feedback Design**

Consider the linear system

$$\dot{x}(t) = Ax(t) + Bu(t)\,, \tag{2.45}$$

where $A \in \mathbb{R}^{n \times n}$, $B \in \mathbb{R}^{n \times s}$, $t \in [0, T]$, and the following state feedback controller

$$u(t) = Hx(t)\,, \quad H \in \mathbb{R}^{s \times n}\,. \tag{2.46}$$

The closed-loop connection between (2.45) and (2.46) reads

$$\dot{x}(t) = (A + BH)x(t)\,, \quad t \in [0, T]\,. \tag{2.47}$$

From Theorem 2 we can easily derive the following corollary, namely a sufficient condition for finite-time stabilization of the closed loop system (2.47).

**Corollary 1 (State feedback design)** *The closed loop system* (2.47) *is finite-time stabilizable with respect to* $(P_0, P, T)$ *if there exist a positive scalar* $\alpha$*, a candidate set of points as given in Definition 9, and a matrix* $H \in \mathbb{R}^{s \times n}$ *such that the following conditions hold*

$$q_{i,h}^T\,(A + BH - \alpha I)\,x_Q^{(i)} \leq 0 \tag{2.48}$$

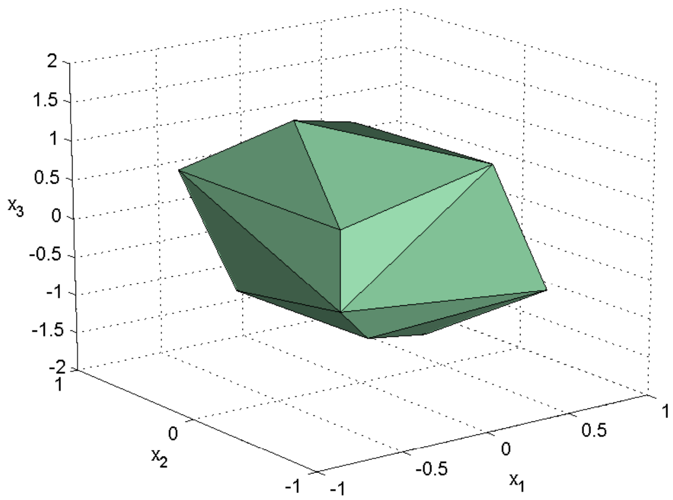


Figure 2.3: Polyhedral Lyapunov function with 12 vertices.

*for all* $i = 1, \ldots, k$*,* $h = 1, \ldots, s_i$*, and*

$$\max_i \|Q^T x_{P_0}^{(i)}\|_\infty \, \max_i \|P^T x_Q^{(i)}\|_\infty \, e^{\alpha T} \leq 1 \,, \tag{2.49}$$

*where* $x_{P_0}^{(i)}$ *are the vertices of the polytope* $\wp(P_0)$*, and* $Q$ *has been defined in* (2.20)*.* $\Diamond$

Now consider again system (2.43); we solved the finite-time stabilization problem via state feedback for such system with the same constraints of Example 1 and $T = 1.6$s. Note that, for this value of $T$, the open loop system is not FTS.

We obtained that the closed-loop system is FTS for $H = (-1.895 \; -1.806)$, by using the polyhedral Lyapunov function of 40 vertices shown in Fig. 2.4 and $\alpha = 0.2$.

### Discussion

From the above results we can conclude that the method proposed in this section improves the existing literature when, as often it happens in practical engineering problems, the initial and trajectory domains, to which the state variables are constrained to belong, are boxes or, more in general, polytopes in the state space.

Indeed, in this case, the problem data may be such that the method proposed in [6] cannot be applied for the FTS analysis of the system under consideration (see Remark 3).

On the other hand the proposed approach suffers from the fact that the feasibility problem with constraints given by (2.18) and (2.19) is, in general, not convex, and therefore the convergence to the optimal solution is not guaranteed. Conversely, the approach of [6] is based on LMIs conditions which leads to a convex optimization problem. However, even in this case, when the initial and

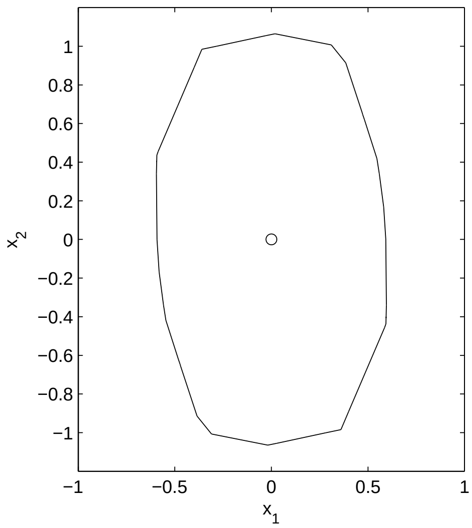


Figure 2.4: Polyhedral Lyapunov function for the state feedback case.

trajectory domains are polytopes, the technique proposed in [6] may introduce a so high level of conservatism that, as shown in Section 2.2.3, it is more convenient to apply Theorem 2 for FTS analysis.

Another concern with the proposed approach is related to the computational burden which increases with the order $r$ of the system. Indeed condition (2.18) introduces $\sum_{i=1}^{k} s_i$ constraints, where $s_i \geq r$ is related to the number of half-planes associated to the $i$-th vertex of the polytope and $k$ is related to the number of polytope vertices ($k \leq l$).

Therefore as the system order increases, the numbers $s_i$ increase and, in order to keep low the computational burden, we have to limit the number of polytope vertices.

## 2.3 Practical stability and stabilization

This kind of stability is often considered in practical problems where the state is required to converge to a certain region surrounding the origin in a given time called convergence time. The stability is not to be intended as in the classical way, since here we do not require the state trajectory to perfectly converge to the origin. The rigorous definition is the following.

### 2.3.1 Problem statement

Let us consider a continuous-time plant of the form

$$\dot{x}(t) = f(x(t), u(t), p(t)) \tag{2.50a}$$

$$y(t) = g(x(t), u(t), p(t)) \tag{2.50b}$$

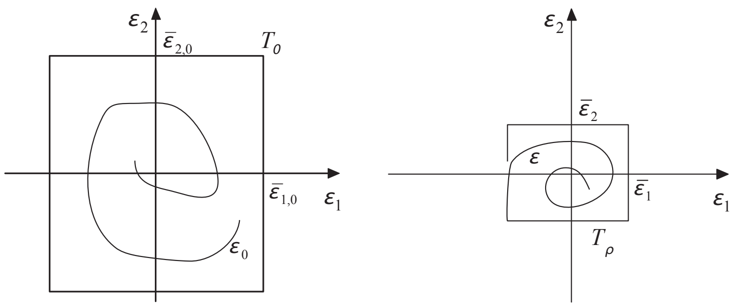


Figure 2.5: Domains defined in the practical tracking problem.

where $x(t) \in \mathbb{R}^n$ is the state, $u(t) \in R$ is the input, $p(t)$ is a vector of uncertain parameters $p \in \wp_p$, $y(t) \in R$ is the output. Consider, moreover the controller

$$u(t) = k(y(t), \hat{y}(t)), \tag{2.51}$$

where $\hat{y}(t)$ is the reference trajectory.

**Definition 10 (Practical stability)** *Given a region $T_0$ (containing the origin of $\mathbb{R}^n$), a region $T_\rho \subset T_0$, $t_0 \in \wp_t$ and $t_c > 0$, we say that system* (2.50) *is practical stable with respect to* $(t_0, t_c, T_0, T_\rho)$ *if and only if, for all functions $p : \wp_t \to \wp_p$ and $\forall x_0 \in T_0$ the solution of the system* (2.50)*, denoted by $x\left(t, t_0, x_0, u_{[t_0,t]}, p\right)$, is bounded and $\forall t > t_0 + t_c$ satisfies the condition $x\left(t, t_0, x_0, u_{[t_0,t]}, p\right) \in T_\rho$.*

From a control design point of view, the practical tracking control problem can be stated as follows.

**Problem 1 (Practical tracking problem)** *Given the plant* (2.50)*, a reference trajectory $\hat{y}$, a region $T_0$ (containing the origin of $\mathbb{R}^n$) of admissible initial errors $\epsilon_0$ at time $t_0$ and a region $T_\rho \subset T_0$ of tolerable errors after the time $t_c$ (see, for instance, Fig. 2.5), design a control law* (2.51) *that guarantees the practical stability with respect to* $(t_0, t_c, T_0, T_\rho)$ *of the associate error system characterized by the state vector*

$$\epsilon = \begin{pmatrix} \epsilon_1 & \epsilon_2 & \dots & \epsilon_n \end{pmatrix}^T, \ \epsilon_1 = \hat{y} - y, \ \epsilon_i = \epsilon_1^{(i-1)}, \ i = 2, \dots, n. \tag{2.52}$$

Imposing the practical stability of the error system implies that we are aiming at bound both the tracking error $\hat{y} - y$ and its derivatives up to the order of the plant minus one. This constraint is often required in practical applications where not only the error needs to be bounded, but also a slow variation of the state trajectory around the reference trajectory is necessary.

The Chapter 3 will provide the theoretical framework to tackle this problem and some new results in order to synthesize controllers.

## 2.4 Analysis of discontinuous control systems

In this section, we analyze the discontinuous control systems [88] [89], and in particular the problem arising in the definition of solutions to discontinuous right hand side differential equations [46]. Theorems to verify the existence and uniqueness of the solution to differential inclusions are then stated.

### 2.4.1 Discontinuous control

Let us consider the simplest example of discontinuous control system. Let $s : \mathbb{R}^n \to \mathbb{R}$ be a function for which $s(x) = 0$ describes a hypersurface $\mathcal{S}$ in $\mathbb{R}^n$ and let

$$\dot{x} = f(x, u) \tag{2.53}$$

be a continuous vector field with respect to $x$ and $u$. By defining the control such that

$$u = \begin{cases} u^+(x), & \text{if } s(x) > 0, \\ u^+(x), & \text{if } s(x) < 0, \end{cases} \tag{2.54}$$

where $u^+$ and $u^-$ are continuous functions designed in such a way that the trajectory reaches the hypersurface $s(x) = 0$, the result is a differential equation (2.53) with discontinuous right-hand side at the states satisfying $s(x) = 0$. This motivates the need for a generalization of the concept of solution at the set of discontinuities of the vector field. The motion of the trajectories in the set of discontinuities is not inherent in any of the structures, but the trajectories describe a new type of motion called *sliding motion*, and the mode of behavior when sliding motions occur is called a sliding mode [46] [88] [89]. For system (2.53) the surface $s(x) = 0$ is the set of points where the sliding motion occurs. Systems that change their structure by switching between different continuous control functions are commonly called *variable structure systems* [89] [90] and sliding motion is the major mode of operation in such systems.

There are a lot of advantages and attractive features of deliberately introducing discontinuous controls and sliding motions on certain surfaces [89], which have been applied for a long time in, for instance, relay systems. For example, systems with sliding modes can under certain circumstances be made insensitive to variations in the process dynamics and less sensitive to disturbances [89] [88] [90]. Furthermore, since the trajectories in the sliding mode are constrained to surfaces of lower dimension than that of the whole state space, the order of the differential equation describing the sliding mode is reduced. However, one disadvantage of variable structure systems may be that the control in the real process will change rapidly from one value to another on the discontinuous surface, which may wear out the physical actuators involved. The phenomenon of rapid switchings is called *chattering*. Chattering may be avoided by introducing hysteresis around the surfaces of discontinuity in the case of discrete actuators possibly combined with an equivalent continuous control (if sliding modes deliberately are introduced) such that the trajectory stays in the sliding mode. It should be mentioned that chattering is not always a disadvantage. In some cases, the performance can be improved by building electric inertialess actuators which may operate in switching mode only. Therefore, even in the case of continuous-control algorithms, the control is shaped as a high-frequency discontinuous signal whose mean value is equal to the desired continuous control. Such actuators are well suited when using discontinuous controls.

**Remark 11 (Discontinuous control systems as hybrid systems)** *Systems described by differential equations with discontinuous right-hand sides are included in the class of hybrid systems. In fact, it is possible that the right-hand side of the differential equation which describes the continuous-time motion of* *an hybrid system is discontinuous at certain continuous states $x$. Furthermore, vector field switchings may also imply that the resulting system behaves as a system with discontinuous right-hand sides.*

**Differential equations with discontinuous right-hand sides**

Differential equations with discontinuous right-hand sides arise naturally for a large class of systems [46] [89]. Different structures of the physical plant may introduce different structures of the continuous dynamics describing the behavior. Discrete actuators may also introduce discontinuities in the continuous dynamics. It is also possible to design discontinuous continuous time control-laws resulting in differential equations with discontinuous righthand sides. Switching phenomena were first studied from a dynamical systems point of view by Filippov [46], and from a control theory perspective by Utkin [88]. Switching controllers are widely used in the control literature. In fact, the history of switching controllers began in the 1960s when Utkin established the sliding mode control scheme.

The discontinuous right hand side presents a number of theoretical and practical problems when dealing with such systems:

1. The ambiguity in the meaning of solution of such differential equations. In fact the classical Caratheodory solutions (C-solutions) defined for ordinary differential equations some times are not valid. So we have to define the solution in some other sense. For example Filippov solutions (F-solutions) arise from considering an appropriate differential inclusion.

2. Proving the uniqueness and boundedness of solutions to this system is not straightforward, indeed, the solutions may not be unique.

3. Theoretically, a controlled system can operate by switching infinitely fast between two control signals on the switching surface. However, in the real world sensors and actuators cannot operate instantaneously. Therefore system trajectories travel back and forth within a neighborhood of the switching surface at high frequency, leading to the undesirable phenomenon known as chattering. Chattering is often harmful as it may excite un-modeled high-frequency dynamics of the system [84].

4. Simulating such a system is difficult due to the stiff differential equations which are difficult to investigate numerically. Runge-Kutta is commonly used for integrating discontinuous systems as it is less sensitive to discontinuities in the r.h.s. of differential equations [84] than multi-step or extrapolation methods. However, switching at an infinite rate in sliding motion forces the fixed step-size Runge- Kutta integrator to limit its step-size resulting in consuming considerable time to simulate the behavior of the system at the discontinuity surface and the high frequency chattering close to the switching surface which do not provide any significant information from the design point of view.

### 2.4.2 Definition of solutions

The unknown dynamic behavior in the sliding motion gives freedom in choosing an adequate mathematical model description. However, some requirements must necessarily be met if the model is going to be of any use [46]. Of major interest are the definitions where the dynamics accurately describes a fairly wide class of processes in real physical systems. Most of the known definitions of a solution to a differential equation with discontinuous right-hand side may be presented as follows [46]. At each point in the continuous domain, a set $F(x)$ consisting of n-dimensional vectors is specified. If the vector field $f$ is continuous at a point $x$ then the set $F(x)$ consists of $f(x)$. If $x$ is a point of discontinuity of $f$, the set $F(x)$ is given in some other way. A solution to (2.53) over an interval $[t_0, t_1]$ is a solution to the differential inclusion

$$\dot{x} \in F(x) \tag{2.55}$$

which is a continuous function $x : [t_0, t_1] \rightarrow \mathbb{R}^n$ for which $\dot{x}(t) \in F(x(t))$ almost everywhere on $[t_0, t_1]$. The meaning of almost everywhere is that the set of times where the solution does not satisfy (2.3) has measure zero [38] (for instance a countable number of times). This definition of a solution coincides with the usual definition of a solution as a continuous function satisfying (2.53) at every point of continuity of the vector field in (2.53). When the vector field is discontinuous but the vector field on both sides of a discontinuity has the same direction, the solution is continuous and passes through the discontinuity. In this case, the solution satisfies (2.53) almost everywhere except at the intersection points at which the solution does not have a derivative. Finally, in the case of sliding motions, uncertainty of the behavior of discontinuous systems gives freedom in choosing an appropriate definition of the dynamics, and the value of the vector field at the set of discontinuity, whether defined or not, is described by a differential inclusion.

Filippov [46] discusses several possible definitions of the set $F(x)$ and the dynamics of the sliding motion at the set of discontinuities of the vector field $f$. In some cases, the definitions will not accurately describe the motion in sliding mode in certain real physical systems. The dynamics should then be defined using some (further) information about the system at the points of discontinuity [46] [89].

### Convex definition

In the convex definition, the dynamics at the points of discontinuity is determined from the dynamics at the points of continuity. The dynamics in the sliding motion is the net effect obtained when switching rapidly between the vector fields around the discontinuity.

More formally, the set $F(x)$ is given by the smallest convex closed set containing all the limit values of the function $f$

$$\lim_{x^* \rightarrow x, x^* \notin S, x \in S} f(x^*)$$

where $S$ is a set with zero measure containing the points of discontinuities of the vector field $f$, which usually is given by a number of hyperplanes or hypersurfaces. At points of continuity, the set $F(x)$ consists of one point as mentioned above; but in the case of discontinuities, the set $F(x)$ contains several elements forming for instance segments, polygons or polyhedrons.

The dynamics of the sliding motion satisfies

$$\dot{x} = f^0(x), \tag{2.56}$$

where $f^0(x)$ is a vector in $F(x)$ pointing in the direction of the discontinuity of $S$. A continuous function $f(x)$ that satisfies (2.53) at the points of continuity of $f$ under some time interval and (2.56) when in sliding motion during the rest of the time is a solution of (2.53) in the sense of a differential inclusion.

Let us illustrate the method in the case when $S$ is a surface separating the vector field $f$ into two domains $\Omega^-$ and $\Omega^+$. Let $x^*$ be a point approaching the value $x \in S$ from the domains $\Omega^-$ and $\Omega^+$ and define

$$f^-(x) = \lim_{x^* \to x, x^* \in \Omega^-} f(x^*), \qquad f^+(x) = \lim_{x^* \to x, x^* \in \Omega^+} f(x^*).$$

The set $F(x)$ then becomes the linear segment joining the endpoints of the vectors $f^-(x)$ and $f^+(x)$. Let $P$ be the plane tangent to the surface $S$ at the point $x$. The intersection point of the segment and the plane $P$ determines the vector field $f^0$ describing the sliding motion (2.56) along the surface $S$. The vector field $f^0$ is given by

$$f^0 = \alpha f^+ + (1-\alpha) f^-, \quad \alpha = \frac{f_N^-}{f_N^- - f_N^+}, \quad 0 \le \alpha \le 1,$$

where $f_N^-$ and $f_N^+$ are the projections of the vectors $f^-$ and $f^+$ onto the normal of the surface $S$ at the point $x$. In the case when the surface $S$ is given by an equation $\phi(x) = 0$ and $\nabla\phi(x) = \frac{\partial \phi}{\partial x} \neq 0$, then

$$f_N^- = \frac{\nabla\phi f^-}{|\nabla\phi|}, \quad f_N^+ = \frac{\nabla\phi f^+}{|\nabla\phi|}, \quad \alpha = \frac{\nabla\phi f^-}{\nabla\phi(f^- - f^+)}.$$

**Equivalent control**

Another way to define a solution at the points of discontinuity is by the equivalent control method [46] [89]. The equivalent control method implies a replacement of the undefined discontinuous dynamics on the discontinuous boundary with continuous dynamics which directs the vector field along the discontinuity surface intersection. The name equivalent control originally refers to systems with continuous control inputs which are defined, for instance, as in (2.54) resulting in a discontinuous vector field (2.53). Even though the name equivalent control method is somewhat misleading when applied to systems without inputs, the name is still used for historical reasons. However, the symbol $z$ is used instead of $u$ to stress that it is not necessarily equal to the continuous control input. To explain the method more formally, consider a system

$$\dot{x} = f(x, z(x))$$

where $f$ is continuous in the set of arguments, and the components $z_i(x)$ of $z(x)$ are scalar functions that are discontinuous on the smooth surfaces $S_i$ given by $\phi_i(x) = 0$. Let $Z_i(x)$ denote the (closed convex) set of points which is possible for $z_i$ at $x$. At the points of continuity of $z_i$ the set $Z_i(x)$ contains one point $z_i(x)$, but at the points of discontinuity, the set $Z_i(x)$ contains all points in the closed interval $[z_i^-(x), z_i^+(x)]$, where $z_i^-(x)$ and $z_i^+(x)$ are the limit points of the function $z_i$ on both sides of the surface $S_i$. The set $F(x)$ is obtained by the function $f(x, z(x))$, where $z_1(x) \in Z_1(x), \ldots, z_r(x) \in Z_r(x)$ vary independently of each other. The dynamics of the sliding motion satisfies

$$\dot{x} = f(x, z^{eq}(x)) \tag{2.57}$$

where $z_1^{eq}(x) \in Z_1(x), \ldots, z_r^{eq}(x) \in Z_r(x)$ are defined so that the vector $f$ in (2.57) is tangent to the surfaces of discontinuity. The functions $z_i^{eq}(x)$ are determined from

$$\nabla\phi_i(x)f(x, z^{eq}(x)) = 0. \tag{2.58}$$

The vector fields $f^-$, $f^+$ and $f^{eq}$ are shorthand for $f(x, z^-(x))$, $f(x, z^+(x))$ and $f(x, z^{eq}(x))$ respectively. The set $F(x)$ becomes the arc segment obtained when $z$ varies from $z^-$ to $z^+$. The intersection point of the arc segment and the plane $P$ determines the vector field $f(x, z^{eq}(x))$ describing the sliding motion (2.57) along the surface $S$.

**General definition**

Another way to define $F(x)$ is to let it be the smallest convex closed set containing the set obtained in the equivalent control method. If the function $f$ is nonlinear in $z_1, \ldots, z_r$, then the intersection of $F(x)$ and the plane $P$ consists in general of more than one point, implying that the dynamics in sliding mode along S is not uniquely determined.

### 2.4.3 Existence and uniqueness of solution

The different definitions of a solution in sliding mode differ in general. A solution defined by the convex combination and equivalent control method is also a solution using the general definition. The solutions according to the equivalent and general definitions coincide if the function $f$ is affine in $z$:

$$\dot{x} = f_0(x) + B(x)z(x). \tag{2.59}$$

If, besides, all $S_i$ are different, and at the points of their intersection the normal vectors are linearly independent, then the sets $F(x)$ in the different methods coincide, implying that the definitions of the vector field in all three methods are the same [46]. This also implies that the vector field describing the dynamics in the sliding mode is uniquely determined. To see this, let $G(x)$ be equal to a matrix where the $i$th row is equal to $\nabla\phi_i(x)$. Then, according to (2.58),

$$G(x)(f_0(x) + B(x)z^{eq}(x)) = 0.$$

Hence, if $\det GB \neq 0$, then

$$z^{eq}(x) = -(G(x)B(x))^{-1}G(x)f_0(x).$$

If each component of $z^{eq}$ satisfies $z_i^-(x) \leq z_i^{eq} \leq z_i^+(x)$ (otherwise there is no motion along $S$), then substituting $z^{eq}$ into (2.59) results in the dynamics [89]

$$\dot{x} = f_0(x) - B(x)(G(x)B(x))^{-1}G(x)f_0(x).$$

The case when $\det GB = 0$ is treated in [89].

Consider, moreover, the case of differential inclusions with smooth discontinuity surfaces, which covers the case of systems

$$\dot{x} = f(x,t) = \begin{cases} f^+(x,t), & x \in \Omega^+; \\ f^-(x,t), & x \in \Omega^-, \end{cases} \tag{2.60}$$

where the regions $\Omega^+$ and $\Omega^-$ are separated by the smooth surface $S = \{x : s(x) = 0\}$.

Theorems 4,5 in [46] state that the solution to the differential inclusion exists if $f^+(x)$, $f^-(x)$ are locally Lipschitz in $x$ away from $S$ (i.e. in $\Omega^-$ and $\Omega^+$). Moreover, (see Lemma 2 and Theorem 2 in [46]) the solution is unique if it is disallowed the case when trajectories point away from $S$ along both $f^+$ and $f^-$ (i.e. $f_N^- < 0$, $f_N^+ > 0$).

Explicating the theorems, we can say that, if $f^+$ and $f^-$ are locally Lipschitz in $x$ in the regions $\Omega^-$ and $\Omega^+$, the existence and uniqueness of the differential equation (2.60) is guaranteed if at least one of the inequalities

$$f_N^-(x,t) > 0 \quad or \quad f_N^+(x,t) < 0. \tag{2.61}$$

hold for each point $(x,t) \in S$.

# Chapter 3

# Control law design

This chapter presents a new technique for robust control design in order to force a SISO linear plant, subject to disturbances and parametric uncertainties, to track a given sufficiently regular reference trajectory.

The used approach is based on Lyapunov method and allows designing a control law which guarantees to follow the reference trajectory with prefixed values of the tracking error and of its derivatives until $n-1$, where $n$ is the order of the plant, and in particular with preassigned values of the error and of its first derivative. Moreover, the control law is quite robust and guarantees the convergence of the error in a prefixed time.

The technique is then applied to design controllers characterized by control signals that may assume only a finite number of values. In this case, the control law can be seen as a generalization of the traditional relay control laws and of the sliding mode ones, with a relatively low switching frequency. Finally, a simple example shows the advantages of the control law obtained with the proposed design methodology with respect to the ones obtained using sliding mode and classical relay approaches.

## 3.1 Introduction

Plants with high parametric uncertainties are usually controlled with signals that may assume only a finite number of values, in order to simplify actuator's construction and minimize the operation cost. This is, for instance, the case of the industrial plants control where there is a power control signal and it is suitable to use simple and reliable actuators with a relatively low cost and highly performing operation modes. Such plants are usually controlled with classical relay controllers that, as it is well-known, perform well only if the plant is approximated with a first order system. In the other cases the performance of the whole system mainly depends on the plant to control, reducing the possibility of imposing severe constraints on the reference trajectory and on the tracking error and, for this reason, the performance is often unacceptable. Moreover, since the relay controller only uses two control levels, the switching frequency of the control signal can become excessive and this is not always realizable and/or convenient from a practical point of view.

This chapter presents a new method for controllers synthesis, characterized by a control signal that may assume only a finite number of values. This method allows a controller to force a SISO linear plant, belonging to a class of sufficiently general plants and subject to disturbances and parametric uncertainties, to follow a given sufficiently regular reference trajectory.

In [69] and [70] controllers with control signals without amplitude constraints, but constant in assigned time intervals, are presented. In [60], [88], [89] and [96] sliding mode control laws with two or an infinite number of levels and with an infinite switching frequency are proposed. Various authors have studied problems concerning quantized control (see, for example, [39], [17], [41] [73], [15], [43], [44]). In [17] the authors deal with feedback stabilization problems for LTI control systems with saturating quantized measurements. The use of logarithmic quantizers in order to stabilize a discrete system is described in [41]. On the other hand, a uniformly quantized control set is used in [73]. Problem relating to the structure of the reachable set for systems whose input sets are quantized are focused in [15]. In [43] the authors propose some stabilization methods for scalar linear systems by means of static quantized feedback controls, depending on the amount of information flow they require in the feedback loop. In [44] the authors analyze the stabilization problem for discrete time linear systems with multidimensional state and one-dimensional input using quantized feedbacks with a memory structure. The proposed control law solves a more general tracking problem for stable and unstable plants, only imposing constraints on the minimum and maximum values of the control signal, which depend both from the plant and from the amplitude and variability of the reference trajectory. In [31] a similar problem is treated but the method proposed in their work is not very robust and does not allow satisfying specification about the error derivatives because of a severe limitation in the Lyapunov function used in the control law design.

The proposed control law [21] allows using intermediate levels, which allow reducing the amplitude of the control signal and the average switching frequency. The theory of the practical stability is used, with reference not only to the output error but also to its derivatives; this approach often allows satisfying process vital specifications; in thermal processes, for example, small but fast temperature variations with respect to the reference can generate defects in the manufactured objects (see [77], [66] and [42]).

## 3.2 Problem statement

Consider the continuous-time SISO linear plant

$$y^{(n)} = \sum_{i=1}^{n} a_i(p(t),t)y^{(n-1)} + b(p(t),t)u + d(p(t),t) \tag{3.1}$$

where: $t \in \wp_t \subseteq \mathbb{R}$ is the time; $u \in \wp_u \subset \mathbb{R}$ is the control input; $y \in \mathbb{R}$ is the output to be controlled; $d \in \wp_d \subset \mathbb{R}$ is the effect of some disturbances acting on the plant; $p(t) \in \wp_p \subset \mathbb{R}^\gamma$, $t \in \wp_t$ is a vector of uncertain parameters;

$$a_1(p,t) \quad a_2(p,t) \quad \ldots \quad a_n(p,t) \ \in \wp_a \subset \mathbb{R}^n, \tag{3.2a}$$

$$b(p,t) \cdot sgn(b(p,t)) \in \wp_p \subset \mathbb{R}^+, \tag{3.2b}$$

$$d(p,t) \in \wp_d, \forall t \in \wp_t,\ \forall p \in \wp_p, \tag{3.2c}$$

$$\wp_a, \wp_b, \wp_d \text{ compact sets.} \tag{3.2d}$$

Let $\hat{y}(t)$ be the trajectory that the plant (3.1) must track, with bounded $n$-th derivative. The equation of the tracking error vector

$$\epsilon = \begin{pmatrix} \epsilon_1 & \epsilon_2 & \ldots & \epsilon_n \end{pmatrix}^T,\ \epsilon_1 = \hat{y} - y,\ \epsilon_i = \epsilon_1^{(i-1)},\ i = 2, \ldots, n, \tag{3.3}$$

can be rewritten as

$$\dot{\epsilon} = E\epsilon - Bw \tag{3.4}$$

where:

$$E = \begin{pmatrix} 0 & 1 & 0 & \ldots & 0 \\ 0 & 0 & 1 & \ldots & 0 \\ \cdot & \cdot & \cdot & \ldots & \cdot \\ 0 & 0 & 0 & \ldots & 1 \\ -k_1 & -k_2 & -k_3 & \ldots & -k_n \end{pmatrix}, \quad B = \begin{pmatrix} 0 \\ 0 \\ \cdot \\ 0 \\ 1 \end{pmatrix}, \tag{3.5}$$

$$k_i \in \mathbb{R}, i = 1, \ldots, n, \tag{3.6}$$

$$w = b(p,t)u - \sum_{i=1}^{n} (a_i(p,t) + k_i)\epsilon_i + d(p,t) + \left[ \sum_{i=1}^{n} a_i(p,t)\hat{y}^{(i-1)} - \hat{y}(n) \right]. \tag{3.7}$$

Particularizing the concept of practical stability given in Section 2.3, we introduce the following definition.

**Definition 11 (Practical stability)** *Given a reference trajectory $\hat{y}(\cdot)$, a region $T_0$ (containing the origin of $\mathbb{R}^n$), a region $T_\rho \subset T_0$, $t_0 \in \wp_t$ and $t_c > 0$, we say that system* (3.4)-(3.7) *is practical stabilizable with respect to $(t_0, t_c, T_0, T_\rho)$ if and only if, for all functions $p : \wp_t \to \wp_p$ and $\forall \epsilon_0 \in T_0$, there exists a control law $u(t,\epsilon) : \wp_t \times T_0 \to \wp_u$ such that the solution of the system* (3.4)-(3.7)*, denoted by $\epsilon\left(t, t_0, \epsilon_0, u_{[t_0,t]}, p\right)$, is bounded and $\forall t > t_0 + t_c$ satisfies the condition $\epsilon\left(t, t_0, \epsilon_0, u_{[t_0,t]}, p\right) \in T_\rho$.*

The general tracking problem is stated as follows.

**Problem 2 (Practical tracking problem)** *Given the plant* (3.1)*, a reference trajectory $\hat{y}$, a region $T_0$ (containing the origin of $\mathbb{R}^n$) of admissible initial errors $\epsilon_0$ at time $t_0$ and a region $T_\rho \subset T_0$ of tolerable errors after the time $t_c$, design a control law with values in $\wp_u$ that guarantees the practical stability with respect to $(t_0, t_c, T_0, T_\rho)$ of the associate error system* (3.4)-(3.7)*.*

## 3.3 Preliminary results

For the solution of Problem 2 we introduce the following lemmas.

**Lemma 4** *Let $S_\rho = \{\epsilon \in \mathbb{R}^n : \|\epsilon\|_P \le \rho, \rho > 0\}$, where $\|\epsilon\|_P = \sqrt{\epsilon^T P \epsilon}$ and $P \in \mathbb{R}^{n\times n}$ is a symmetric and positive definite (p.d.) matrix, be an hyper-ellipsoid of $\mathbb{R}^n$ and $T_\rho$ be the most little hyper-rectangle that includes $S_\rho$ and with it faces orthogonal to the coordinated axis (see Fig. 3.1). Then the semi-length of the edges of $T_\rho$ parallel to the $i$-th axes is*

$$\bar{\epsilon}_i = \rho\sqrt{p_{ii}^{inv}}, \quad i = 1, \ldots, n, \tag{3.8}$$

*where $p_{ii}^{inv}$ denotes the $(i,i)$-element of the matrix $P^{-1}$.*

**Proof 3** *Let $\bar{\epsilon}$ be the tangency point of the hyper-ellipsoid $S_\rho$ with the hyper-plain normal to positive semi-axis $i$. Since the gradient of $\epsilon^T P \epsilon$ in $\bar{\epsilon}$ is parallel to axis $i$, that is*

$$2P\bar{\epsilon} = \mu \begin{pmatrix} 0 & \ldots & 0 & 1 & 0 & \ldots & 0 \end{pmatrix}^T, \quad \mu \in \mathbb{R}, \tag{3.9}$$

*it is*

$$\bar{\epsilon} = 1/2 \begin{pmatrix} ? & \ldots & ? & p_{ii}^{inv} & ? & \ldots & ? \end{pmatrix}^T \mu \;= \begin{pmatrix} ? & \ldots & ? & \bar{\epsilon}_i & ? & \ldots & ? \end{pmatrix}^T, \tag{3.10}$$

*where the ? denote elements which do not need to be specified for the purpose of the proof.*

*From* (3.10) *it follows that*

$$\mu = \frac{2\bar{\epsilon}_i}{p_{ii}^{inv}} \tag{3.11}$$

*and*

$$\bar{\epsilon} = P^{-1} \begin{pmatrix} 0 & \ldots & 0 & 1 & 0 & \ldots & 0 \end{pmatrix}^T \frac{\bar{\epsilon}_i}{p_{ii}^{inv}}. \tag{3.12}$$

*Since $\bar{\epsilon}$ is on the boundary of $S_\rho$, it must be that $\bar{\epsilon}^T P \bar{\epsilon} = \rho^2$, that is*

$$\rho^2 = p_{ii}^{inv} \frac{\bar{\epsilon}^2}{(p_{ii}^{inv})^2} = \frac{\bar{\epsilon}^2}{p_{ii}^{inv}} \tag{3.13}$$

*which proves the* (3.8).

**Lemma 5** *Let $E \in \mathbb{R}^{n\times n}$ be a matrix with $v$ distinct and real eigenvalues $\lambda_i$, $i = 1, \ldots, n$, and $2l = n - v$ distinct and complex conjugate eigenvalues $\lambda_{i\pm} = \alpha_i \pm j\omega_i$, $i = 1, \ldots, l$. Moreover, let $u_i$, $i = 1, \ldots, n$ and $u_{i\pm} = u_{ai} \pm j u_{bi}$, $i = 1, \ldots, l$ be the corresponding eigenvectors. Then, denoting with $Z^*$ the complex conjugate transposed matrix of $Z \in \mathbb{C}^{n\times n}$, the matrices:*

$$P = (ZZ^*)^{-1} = \left[ \sum_{i=1}^{v} u_i u_i^T + 2 \sum_{i=1}^{l} (u_{ai} u_{ai}^T + u_{bi} u_{bi}^T) \right]^{-1} \tag{3.14}$$

$$Q = -(Z^*)^{-1}(\Lambda + \Lambda^*)Z^{-1} = -\left[ \frac{1}{2} \sum_{i=1}^{v} \frac{1}{\lambda_i} u_i u_i^T + \sum_{i=1}^{l} \frac{1}{\alpha_i} (u_{ai} u_{ai}^T + u_{bi} u_{bi}^T) \right]^{-1} \tag{3.15}$$

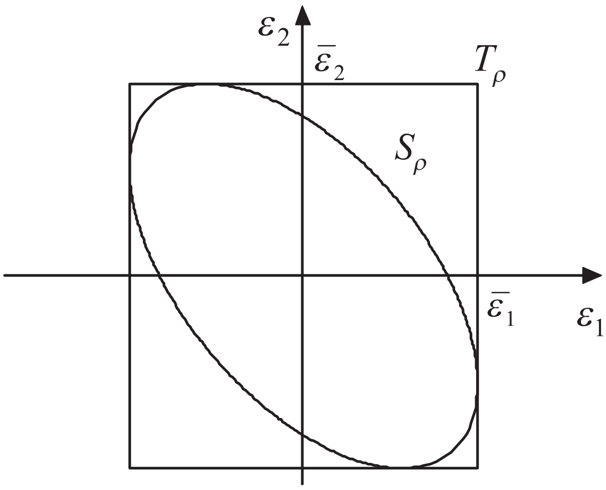


Figure 3.1: Regions $S_\rho$ and $T_\rho$.

*with*

$$Z = \begin{pmatrix} u_1 & \dots & u_v & u_{a1} + ju_{b1} & u_{a1} - ju_{b1} & \dots & u_{al} + ju_{bl} & u_{al} - ju_{bl} \end{pmatrix} \tag{3.16}$$

$$\Lambda = diag \begin{pmatrix} \lambda_1 & \dots & \lambda_v & \lambda_{1+} & \lambda_{1-} & \dots & \lambda_{l+} & \lambda_{l-} \end{pmatrix} \tag{3.17}$$

*satisfy the Lyapunov equation*

$$E^T P + PE = -Q. \tag{3.18}$$

*Moreover, if the eigenvalues of $E$ have negative real part then the matrices $P$ and $Q$ are both p.d. and*

$$\lambda_{max}(Q^{-1}P) = -\frac{1}{2\max_{i=1,\dots,n} \Re(\lambda_i)} = \frac{1}{2}\tau_{max}(E), \tag{3.19}$$

*where $\lambda_{max}(Q^{-1}P)$ denotes the maximum eigenvalue of the matrix $Q^{-1}P$ and $\tau_{max}(E)$ denotes the maximum time constant of the modes of the system $\dot{\epsilon} = E\epsilon$.*

**Proof 4** *Since $Z^{-1}EZ = \Lambda$, it results*

$$\begin{aligned} E^T P + PE &= E^* P + PE & (3.20)\\ &= (Z^*)^{-1}\Lambda^* Z^* (Z^*)^{-1} Z^{-1} + (Z^*)^{-1} Z^{-1} Z \Lambda Z^{-1} & (3.21)\\ &= (Z^*)^{-1} (\Lambda + \Lambda^*) Z^{-1}, & (3.22) \end{aligned}$$

*and then* (3.18)*. From* (3.15)*, $\forall x \in \mathbb{R}^n - \{0\}$ it is*

$$\begin{aligned} x^T Q x = x^* Q x &= -Z^* (\Lambda + \Lambda^*) z & (3.23)\\ &= -2\sum_{i=1}^{v} \lambda_i z_i z_i^* - 2\sum_{i=1}^{l} \alpha_i \left(z_{v+2i-1} z_{v+2i-1}^* + z_{v+2i} z_{v+2i}^*\right), & (3.24) \end{aligned}$$

*where*

$$z = Z^{-1}x = \begin{pmatrix} z_1 & z_2 & \dots & z_n \end{pmatrix}^T \neq 0. \tag{3.25}$$

*If* $\lambda_i < 0$, $i = 1, \dots, v$ *and* $\alpha_i < 0$, $i = 1, \dots, l$, *from* (3.23), *it results*

$$x^T Q x > 0 \quad \forall x \in \mathbb{R}^n - \{0\}, \tag{3.26}$$

*and then* $Q$ *is p.d. .*

*It is simple to prove that* $P$ *is p.d. in a similar way or remembering that* $P$ *is the solution of the Lyapunov equation* (3.18) *where* $Q$ *is p.d. and all the eigenvalues of* $E$ *have negative real part.*

*In order to prove* (3.19), *it can be noted that*

$$P^{-1}Q = -ZZ^*(Z^*)^{-1}(\Lambda + \Lambda^*)Z^{-1} = -Z(\Lambda + \Lambda^*)Z^{-1}, \tag{3.27}$$

*and then the eigenvalues of* $P^{-1}Q$ *are*

$$-(\lambda_i + \lambda_i^*) = -2\Re(\lambda_i), \quad i = 1, \dots, n, \tag{3.28}$$

*and the eigenvalues of* $Q^{-1}P$ *are*

$$-\frac{1}{2\Re(\lambda_i)}, \quad i = 1, \dots, n. \tag{3.29}$$

**Lemma 6** *Consider the system* (3.4) *with* $\epsilon_0 \in T_0$, *where all the eigenvalues of* $E \in \mathbb{R}^{n\times n}$ *are distinct and with negative real part,* $B \in \mathbb{R}^{n\times 1}$ *and* $P$ *is given by* (3.14). *Let us define the linear function of the tracking error and of its derivatives* $v = B^T P\epsilon$ *and two subsets* $S_\sigma$ *and* $S_\rho$ *of* $\mathbb{R}^n$ *such that*

$$S_\sigma = \{\epsilon \in \mathbb{R}^n : \|\epsilon\|_P \leq \sigma, \sigma > 0\} \supseteq T_0, \tag{3.30}$$

$$S_\rho = \{\epsilon \in \mathbb{R}^n : \|\epsilon\|_P \leq \rho, 0 < \rho < \sigma\} \subseteq T_\rho. \tag{3.31}$$

*If*

$$v \cdot w \geq 0 \quad \forall \epsilon \notin \mathring{S}_\rho, \tag{3.32}$$

*where* $\mathring{S}_\rho$ *denotes the interior of* $S_\rho$, *then the system* (3.4) *is finite-time practically stable with respect to* $(t_0, t_c, T_0, T_\rho)$ *for every* $t \in \wp_t$ *and*

$$t_c \geq \tau_{max}(E) \ln \frac{\sigma}{\rho}. \tag{3.33}$$

**Proof 5** *The Lyapunov function* $V(\epsilon) = \epsilon^T P \epsilon$ *for the system* (3.4) *is chosen. Taking into account* (3.18), *it results* $-\dot{V}(\epsilon) = \epsilon^T Q\epsilon + 2vw$. *Using* (3.32) *it follows that*

$$\frac{\dot{V}(\epsilon)}{V(\epsilon)} \leq -\inf_\epsilon \frac{\epsilon^T Q \epsilon}{\epsilon^T P \epsilon} \quad \forall \epsilon \notin \mathring{S}_\rho. \tag{3.34}$$

*Since*

$$\frac{\epsilon^T Q\epsilon}{\epsilon^T P\epsilon} \geq \frac{1}{\lambda_{max}(Q^{-1}P)} \quad \forall \epsilon \neq 0, \tag{3.35}$$

*for any symmetric and p.d. matrices $P$ and $Q$ (see, for example [51]), and by Lemma 5 it results*

$$\frac{\dot{V}(\epsilon)}{V(\epsilon)} \leq -\frac{1}{\tau_{max}(E)} \quad \forall \epsilon \notin \mathring{S}_\rho, \tag{3.36}$$

*and then*

$$\|\epsilon(t)\|_P \leq \|\epsilon(t_0)\|_P \exp\left(-(t - t_0)/\tau_{max}(E)\right). \tag{3.37}$$

*From last inequality it follows that $\epsilon$ converges into the hyper-ellipsoid $S_\rho$ in a time not greater than*

$$t_{c0} = \tau_{max}(E) \ln \frac{\|\epsilon(t_0)\|_P}{\rho}. \tag{3.38}$$

*Since $\epsilon_0 \in S_\sigma$, the proof easily follows.*

**Remark 12** *It is important to note that the matrix $P$ given by* (3.14) *is optimal with respect to the estimation of the convergence velocity, according to the Lyapunov approach, of the system $\dot{\epsilon} = E\epsilon$. This is due to the fact that the time constant of $\|\epsilon(t)\|_P$ coincides with the maximum time constant of $E$.*

## 3.4 Control law synthesis

It is now possible to state the following main result.

**Theorem 3** *Given the plant* (3.1)*, a reference trajectory $\hat{y}$ with bounded $n$-th derivative, a region $T_0$ (containing the origin of $\mathbb{R}^n$) of admissible initial errors $\epsilon_0$ at time $t_0$ and a region $T_\rho \subset T_0$ of tolerable errors after a prefixed time $t_c$.*

*Then it is possible to solve the practical tracking problem with respect to $(t_0, t_c, T_0, T_\rho)$ choosing:*

- *$\sigma$, $\rho$ and the values $k_i$, $i = 1, \ldots, n$ such that:*
  - *the eigenvalues of $E$ are distinct and with negative real part and such that $t_c$ in* (3.33) *is less or equal to the prefixed one;*
  - *the region $S_\sigma$ contains $T_0$;*
  - *the region $S_\rho$ is contained in $T_\rho$;*
- *the control law (see Fig. 3.2) $u(t, \epsilon) : \wp_t \times T_0 \to \wp_u$:*
  - *if $\epsilon \notin \mathring{S}_\rho$, equals to:*

$$u = \begin{cases} \lceil U \rceil, & if \quad v \cdot b(p,t) \geq 0 \\ \lfloor U \rfloor, & if \quad v \cdot b(p,t) < 0 \end{cases} \tag{3.39}$$

*where:*

$$v = B^T P \epsilon, \ P \text{ is defined in } (3.14) \tag{3.40}$$

$$U = \frac{\left[\hat{y}^{(n)} - \sum_{i=1}^{n} a_i(p,t)\hat{y}^{(i-1)}\right] - d(p,t) + \sum_{i=1}^{n} (a_i(p,t) + k_i)\epsilon_i}{b(p,t)} \tag{3.41}$$

$$\lfloor U \rfloor = max\{u \in \wp_u : \ u < U \, \forall p \in \wp_p\} \tag{3.42}$$

$$\lceil U \rceil = min\{u \in \wp_u : \ u \geq U \, \forall p \in \wp_p\} \tag{3.43}$$

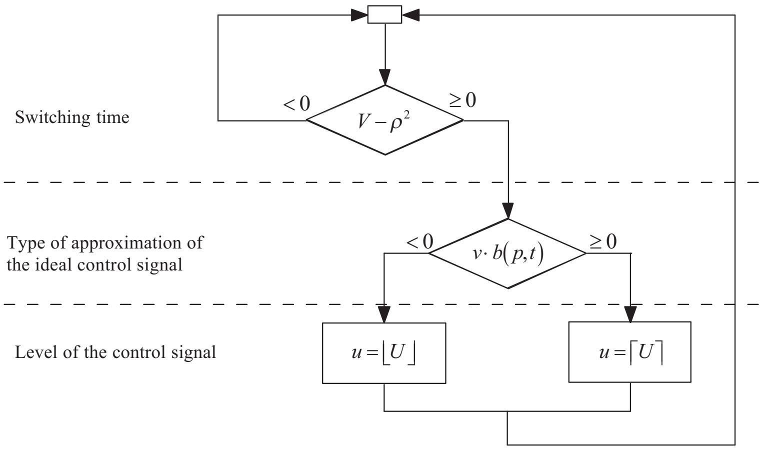


Figure 3.2: Control Algorithm (CA).

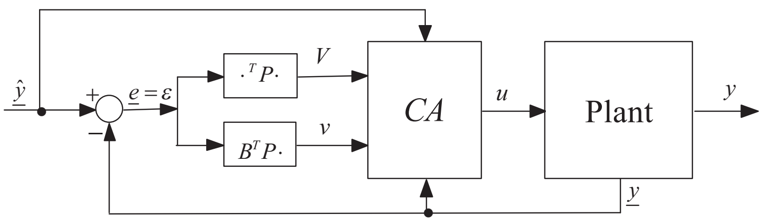


Figure 3.3: Scheme of the closed loop system.

– *if* $\epsilon \in \mathring{S}_\rho$, *equals to the last value assumed on the* $S_\rho$ *boundary.*

$$(3.44)$$

**Proof 6** *The proof easily follows from Lemma 6 observing that, for the hypothesis* (3.2) *the control* $u$ *computed with* (5.19) *provides a signal* $w$*, given by* (3.7)*, satisfying condition* (3.32).

The scheme of the closed loop system is shown in Fig. 3.3, where $\underline{f}$ denotes $\begin{bmatrix} f & \dot{f} & \dots & f^{(n-1)} \end{bmatrix}^T$.

As regards the tracking error and the convergence velocity, we state and prove the following theorems.

**Theorem 4** *If the values* $k_i$, $i = 1, \dots, n$ *in the control law of Theorem 3 are chosen such that the eigenvalues* $\lambda_i$, $i = 1, \dots, n$ *of* $E$ *are distinct, with negative real part and satisfy*

$$\sum_{j=1}^{n} \lambda_j^{i-1} \bar{\lambda}_j^{i-1} \le \left( \frac{\bar{\epsilon}_i}{\rho} \right)^2 \quad \bar{\epsilon}_i \in \mathbb{R} \quad \forall i = 1, \dots, n, \tag{3.45}$$

*then the tracking error* $\epsilon$ *converges into the region*

$$T_\rho = \left\{ \epsilon \in \mathbb{R}^n : \, |\epsilon_i| \le \bar{\epsilon}_i \in \mathbb{R}^+ \quad \forall i = 1, \dots, n \right\}. \tag{3.46}$$

**Proof 7** *Since the matrix $E$ is in reachability canonical form, the matrix of its eigenvectors is*

$$Z = \begin{pmatrix} 1 & 1 & \dots & 1 \\ \lambda_1 & \lambda_2 & \dots & \lambda_n \\ \cdot & \cdot & \dots & \cdot \\ \lambda_1^{n-1} & \lambda_2^{n-1} & \dots & \lambda_n^{n-1} \end{pmatrix} \tag{3.47}$$

*From* (3.8) *and* (3.14) *it follows that the semi-length $\bar{\epsilon}_i$ of the edges of the hyper-rectangle $T_\rho$, for Lemma 4, are*

$$\rho \sqrt{\sum_{j=1}^{n} \lambda_j^{i-1} \bar{\lambda}_j^{i-1}} \quad \forall i = 1, \dots, n, \tag{3.48}$$

*and then the proof.*

**Theorem 5** *If the eigenvalues of $E$ are distinct, with negative real part and with magnitude $\|\lambda_i\| = M, \forall i = 1, \dots, n$, and it is desired to assign only $\bar{\epsilon}_1$ and $\bar{\epsilon}_2$, a non-conservative choice of $\rho$ and $M$ is*

$$\rho = \frac{\bar{\epsilon}_1}{\sqrt{n}} \quad M = \frac{\bar{\epsilon}_2}{\bar{\epsilon}_1}. \tag{3.49}$$

*Furthermore, if the eigenvalues of $E$ have magnitude $M$ and relative phase shift of $\pi/n$ (Butterworth eigenvalues) then $\epsilon$ converges into $T_\rho$ in a time not greater than*

$$t_c = \ln \frac{\sigma}{\rho} \left( M \cos \frac{\pi(n-1)}{2n} \right)^{-1} \tag{3.50}$$

**Proof 8** *The proof directly follows from Theorem 4 noting that*

$$\sum_{j=1}^{n} \lambda_j^{i-1} \bar{\lambda}_j^{i-1} = n M^{2(i-1)} \quad \forall i = 1, \dots, n, \tag{3.51}$$

*and the eigenvalue with the greatest real part is*

$$-M \exp \left( j \frac{\pi(n-1)}{2n} \right). \tag{3.52}$$

**Remark 13** *Under the same hypotheses of Theorem 5, it results*

$$\bar{\epsilon}_i = \rho \sqrt{n} M^{i-1} \quad \forall i = 1, \dots, n. \tag{3.53}$$

## 3.5 Discussion

### 3.5.1 Characteristics of the control law

The control algorithm has the following characteristics

- It guarantees the plant out to practically track a given sufficiently regular reference trajectory with prefixed maximum values of the tracking error and its derivatives.

- It is robust with respect to disturbances and uncertain parameters, and then the knowledge of the plant and of the disturbance does not need to be accurate.

This is obtained choosing a control signal depending on three quantities:

1. the value $V$ of a suitable Lyapunov function, in order to decide the switching time;

2. the value $v$ of a linear function of the tracking error and of its derivatives, in order to decide if the level must be the nearest admissible level to the nominal control for excess or defect;

3. the value $w$ of deviation from the ideal error model, in order to decide the level of the control signal.

**Remark 14** *If the coefficients $a_i(p,t)$, $b(p,t)$ and the disturbance $d(p,t)$ dependence on the parameter $p$ is multi-linear and $\wp_p$ is an hyper-rectangle, then $\lfloor U \rfloor$ and $\lceil U \rceil$ in* (5.19) *will be always in correspondence of vertices of $\wp_p$ (see [30]).*

### 3.5.2 Existence and uniqueness of the solution

Consider the differential equation (3.4) which describes the closed loop system composed by the linear plant and the controller

$$\dot{\epsilon} = f(\epsilon) = E\epsilon - Bw. \tag{3.54}$$

In this section we examine the proprieties of existence and uniqueness of the solutions of such equation, in different scenarios:

- the error trajectory stays inside the region $S_\rho$;

- the error trajectory stays outside $S_\rho$.

#### Analysis inside $S_\rho$

The differential equation (3.54) is piecewise continuous in $t$ and locally Lipschitz in $\epsilon$ on $S_\rho$. On the $S_\rho$-boundary all the trajectories enter $S_\rho$ because $\dot{V}(\epsilon) < 0$. It results from (5.24) that $\epsilon$ either is always contained in $\mathring{S}_\rho$ and the control signal will definitely be constant or it continually passes in a finite time from a boundary point to another distinct one, with control signal switching every time a boundary point will be reached. In any case, the differential equation (3.54) admits a unique Caratheodory solution for every $\epsilon_0 \in S_\rho$.

### Analysis outside $S_\rho$

Consider the switching surface $\mathcal{S} = \{\epsilon : \ v = B^T P\epsilon = 0\}$ an the regions $\Omega^- = \{\epsilon : \ v < 0\}$, $\Omega^+ = \{\epsilon : \ v > 0\}$. If $\epsilon_0 \in \Omega^+ \cup \Omega^-$ and the solution does not cross the switching surface $\mathcal{S}$, the equation (3.54) admits a unique Caratheodory solution.

Conversely, let us consider the behavior of the system on the switching surface. Let us indicate with $w^+$ and $w^-$ the values of w (3.7) respectively in case $v > 0$ and $v < 0$. Based on the Theorem 3, it results $w^+ > 0$ and $w^- < 0$.

Since $f$ in (3.54) is a locally bounded, measurable vector-valued function, the differential equation (3.54) can be replaced by the differential inclusion

$$\dot{\epsilon} \in F(\epsilon) = \begin{cases} f^-(\epsilon) = E\epsilon - Bw^-, & \epsilon \in \Omega^-; \\ f^+(\epsilon) = E\epsilon - Bw^+, & \epsilon \in \Omega^+; \\ E\epsilon - Bw, w \in [w^-, w^+], & \epsilon \in \mathcal{S}. \end{cases} \tag{3.55}$$

It is easy to recognize that $f^+$ and $f^-$ are locally Lipschitz in $x$ in the regions $\Omega^-$ and $\Omega^+$. It results (see Section 2.4.3) that the solution of the differential equation (3.54) exists and is unique if

$$\forall \epsilon \in \mathcal{S} \Rightarrow f_N^-(\epsilon) > 0 \quad or \quad f_N^+(\epsilon) < 0. \tag{3.56}$$

In the following the proof of the existence and uniqueness of the solution is drawn for the case $n = 2$. A similar approach can be applied to the case $n > 2$. Consider the expression of $f_N(\epsilon)$

$$f_N(\epsilon) = P_{21}\epsilon_2 - P_{22}(k_1\epsilon_1 + k_2\epsilon_2 + w), \tag{3.57}$$

where $P_{i,j}$ indicates the $(i, j)$-element of the matrix $P$. In particular, $\forall \epsilon \in \mathcal{S}$ we have

$$f_N(\epsilon) = \epsilon_2(P_{21} - P_{22}k_2 + k_1 P_{22}^2/P_{21}) - P_{22}w. \tag{3.58}$$

It results that

$$f_N^+(\epsilon) < 0 \Leftrightarrow \epsilon_2 < Hw^+ \tag{3.59}$$

$$f_N^-(\epsilon) > 0 \Leftrightarrow \epsilon_2 > Hw^- \quad \epsilon \in \mathcal{S} \tag{3.60}$$

where $H = P_{22}/(P_{21} - P_{22}k_2 + k_1 P_{22}^2/P_{21})$. Observe that $H = \frac{\alpha}{\omega^2}$, where $\alpha$ and $\omega$ are the real part and the natural frequency of the eigenvalues of $P$. Since $P$ is an hurwitz matrix, it follows that $H > 0$ and that $Hw^- < Hw^+$. From that we have proved that the solution exists and is unique since (3.56) is satisfied. In Fig. 3.4 we show the segments of $\mathcal{S}$ where chattering exists (note that the upper and lover extremes of the segments vary as well as $w$ ($w^-$ and $w^+$) varies with $u$, $\epsilon$ and $\hat{y}$).

Consider now the case when $\epsilon$ enters $S_\rho$. It is easy to recognize that the solution is always unique except the case when the trajectory of $\epsilon$ slides over $\mathcal{S}$ before entering $S_\rho$. In fact, the value of the control $u$ assumed once $\epsilon$ touches $S_\rho$ can be arbitrarily chosen between the ones assumed during the sliding motion.

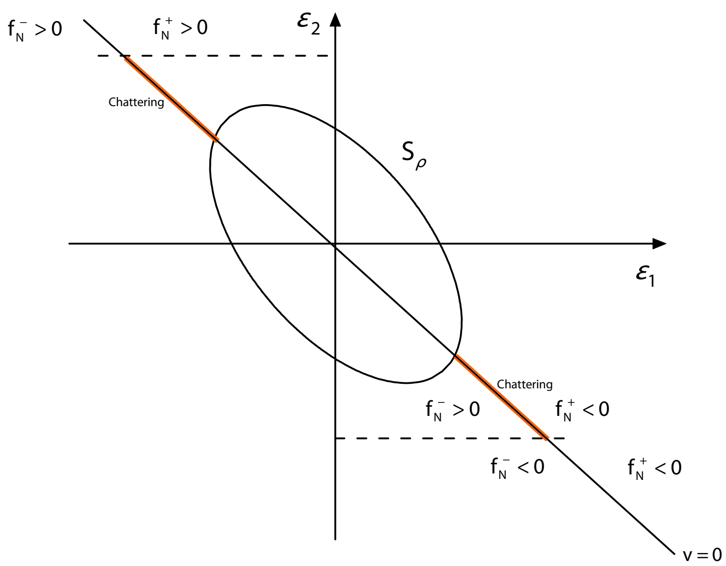


Figure 3.4: Regions of chattering over $\mathcal{S}$.

**Discussion**

As a summary of the analysis presented in the previous paragraphs, we state the following

- the solution to (3.54) exists everywhere in $\mathbb{R}^n$, and for every initial condition;
- there can be sliding motion over $\mathcal{S}$, but it will stop as soon as $\epsilon$ touches $S_\rho$. This event will happen in a finite time since the derivative of the Lyapunov function $V$ is negative along $\mathcal{S}$;
- the solution is unique except in the case when the trajectory enters $S_\rho$ sliding on $\mathcal{S}$.

**Remark 15** *In the hypothesis of possible sliding on $\mathcal{S}$, if the initial part of the reference trajectory is chosen such that $\epsilon(0) \in S_\rho$ then the evolution of $\epsilon$ will be always contained in $S_\rho$ and therefore the control signal will never chatter. If, for example, the plant has the following initial conditions*

$$y(0) = y_0,\; y^{(i)}(0) = 0 \quad \forall i = 1, \ldots, n-1, \tag{3.61}$$

*in order to avoid the chattering it is sufficient that the initial part of the reference signal satisfies the condition*

$$|\hat{y}(0) - y_0| < \frac{\rho}{\sqrt{p_{11}}}, \quad \hat{y}^{(i)}(0) = 0 \quad \forall i = 1, \ldots, n-1, \tag{3.62}$$

*where $p_{11}$ is the $(1,1)$-element of $P$.*

### 3.5.3 Choice of the control signal

This section describes how to choose the control signal range. The minimum $u_-$ and maximum $u_+$ levels of $u$ needed to satisfy Theorem 3 depend on the nominal model of the plant, on the uncertain parameters $p$, on the reference trajectory "variability" (amplitude of $\hat{y}$ and its $n$ derivatives), on the regions $T_0$ (initial errors), $T_\rho$ (tolerable final errors).

Consider first the case when $\epsilon(t_0) \in S_\rho$. It is easy to verify that the maximum and minimum values of the control signal $u$ to satisfy the Theorem 3 must respect the following inequalities

$$u_+ \geq \hat{U}_+ + U_{\epsilon,+} = \max_{t>t_0,\, p\in\wp_p} \hat{U} + \max_{t>t_0,\, p\in\wp_p,\, \epsilon\in S_\rho} U_\epsilon \tag{3.63a}$$

$$u_- \leq \hat{U}_- + U_{\epsilon,-} = \min_{t>t_0,\, p\in\wp_p} \hat{U} + \min_{t>t_0,\, p\in\wp_p,\, \epsilon\in S_\rho} U_\epsilon \tag{3.63b}$$

where

$$\hat{U} = \frac{\left[\hat{y}^{(n)} - \sum_{i=1}^{n} a_i(p,t)\hat{y}^{(i-1)}\right] - d(p,t)}{b(p,t)} \qquad U_\epsilon = \frac{\sum_{i=1}^{n} (a_i(p,t) + k_i)\epsilon_i}{b(p,t)} \tag{3.64}$$

The design rule (3.63) is similar to the one used for the relay controller, but it also utilizes information about the plant model (and not only the gain).

This is due to the fact that the control algorithm is designed to imposed strict specifications about the closed loop dynamics.

The terms $U_{\epsilon,+}$ and $U_{\epsilon,-}$ are calculated tacking into account the error specifications and $\wp_p$. Moreover, if the hypotheses of Remark 14 are satisfied, since $U_\epsilon$ is a linear function with respect to $\epsilon_i$, $i = 1, \ldots, n$, then the maximum $U_{\epsilon,+}$ and minimum $U_{\epsilon,-}$ will correspond to two points on the boundary of $\wp_p \times S_\rho$.

The terms $\hat{U}_+$ and $\hat{U}_-$ instead depend on the reference trajectory $\hat{y}$. If such values have a too high magnitude, it could be useful to scale the reference trajectory velocity, for example in a linear manner (see [57]), realizing a new reference signal

$$\tilde{y}(t) = \hat{y}(t/c), \quad c > 1. \tag{3.65}$$

Choosing the value of $c$ in a suitable manner it is possible to respect (3.63) without increasing the extreme values of $\wp_u$. In fact, in this case $\hat{U}$ becomes:

$$\hat{U} = \frac{\left[c^{-n}\hat{y}^{(n)} - \sum_{i=1}^{n} a_i(p,t)c^{-i+1}\hat{y}^{(i-1)}\right] - d(p,t)}{b(p,t)} \tag{3.66}$$

Observe that if $\epsilon(t_0) \notin S_\rho$ then the control law of Theorem 3 requires to apply a signal $u$ able to impose the error $\epsilon$ to have an initial transient (which carries $\epsilon$ to enter $S_\rho$) characterized by the dynamic matrix $E$. Clearly, if the dynamics the controller imposes is very different from the one of the plant (3.1), then the control signal to apply during the transient must assume values that have high magnitude. Thereby the chosen extreme levels, obtained satisfying only (3.63) could not be enough. In order to solve this inconvenient it can be useful to modify the reference trajectory with and initial joint trajectory so that, with the available levels $\wp_u$, there would be an acceptable "driven transient". To this end, and also to provide a way to calculate $\dot{\hat{y}}$ and $\ddot{\hat{y}}$, the following method can be used.

#### Joint trajectory

If the reference signal $\hat{y}$ is characterized by a bounded band, the output of the Butterworth filter with accessible state and with an appropriate value of the cutting frequency $\omega_d \in \mathbb{R}^+$ practically provides $\hat{y}^{(i)}$, $i = 0, \ldots, n$.

Moreover, if the initial condition of the filter is chosen such that $\epsilon(t_0) \in S_\rho$ then the controller will impose that the error will never escape from the ellipse $S_\rho$. In fact only two cases can happen:

- $\epsilon$ is always contained in $S_\rho$ and the control signal $u$ is definitely constant (see Fig. 3.5a);
- $\epsilon$ continually passes in a finite time from a boundary point of $S_\rho$ to another distinct one, with switching of the control signal $u$ every time a boundary point is reached (see Fig. 3.5b).

Therefore, choosing in a suitable manner the filter band $\omega_d$ and the scaling factor $c$ it is possible to create a reference trajectory which is acceptable for the available extreme levels and with a transient that is practically known in advance. The scheme of the whole control system will be the one in Fig. 3.6.

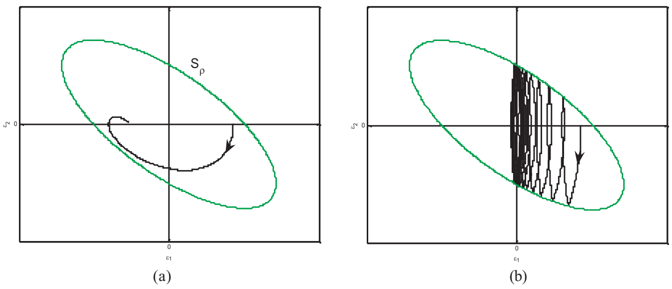


Figure 3.5: Error portraits.

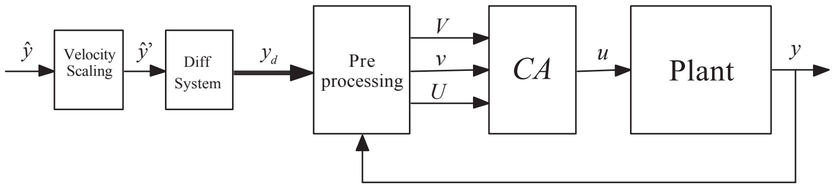


Figure 3.6: Scheme of the closed loop system.

## 3.6 Multi-valued control

The Theorem 3 is valid even if the control signal may assume only a finite number $l$ of levels

$$u_- = u_1 < u_2 < \cdots < u_l = u_+ \tag{3.67}$$

and, in particular, two levels (the classical levels of the relay controller). As regards the steady-state tracking error and the convergence velocity, it is possible to use levels "greater" than the ones provided by (5.19), e.g. only the extreme levels. The intermediate levels are useful to reduce the amplitude of the control signal (and often the power peaks) and the average switching frequency. This is due to the fact that using the levels provided by (5.19), the escape velocity from $S_\rho$ diminishes.

Moreover, note that the control signal's amplitude and switching frequency increase as the parameters uncertainties increase (see (5.19)). Such inconvenient can be reduced identifying the plant parameters.

**Remark 16** *It is easy to prove that, if the plant has order one and* $\wp_u = \{U_-, U_+\}$*, the controller of Theorem 3 becomes a classical relay control with hysteresis* $\rho$*.*

### 3.6.1 Numerical examples

Consider the nominal linear plant

$$\ddot{y} + \dot{y} + y = u \tag{3.68}$$

with a control input that may assume only values in

$$\wp_u = \left\{ \begin{array}{ccccc} -1.2 & -0.6 & 0.0 & +0.6 & +1.2 \end{array} \right\}. \tag{3.69}$$

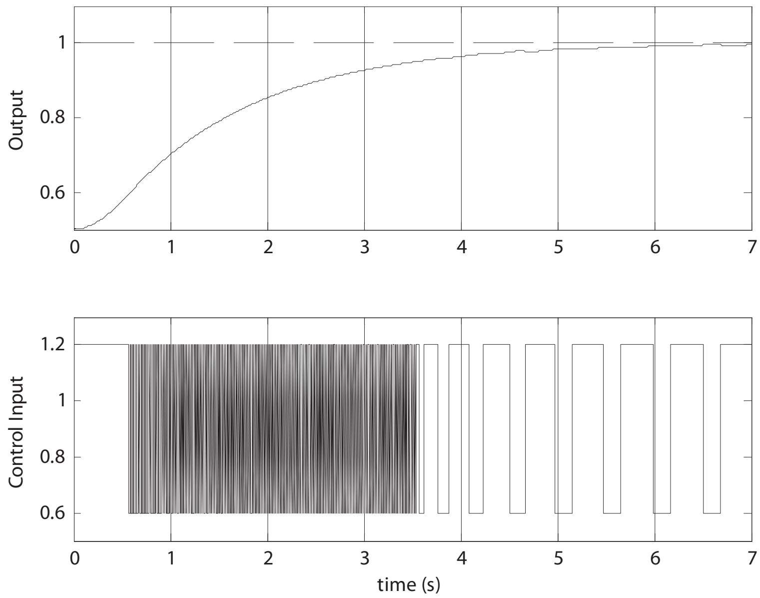


Figure 3.7: Output and control signals. Case A.

We want to impose a steady-state tracking error

$$|\epsilon_1| \leq \bar{\epsilon}_1 = 0.05, \quad |\epsilon_2| \leq \bar{\epsilon}_2 = 0.05. \tag{3.70}$$

We designed a controller with Butterworth eigenvalues with $M = 1$ and $\rho = 0.05/\sqrt{2}$ (see Theorem 5). With this controller we consider three cases illustrating the presented theory.

**Reference signal $\hat{y}(t) = 1$ and initial conditions $y(0) = 0.5$, $\dot{y}(0) = 0$**

In Figs. 3.7 and 3.8 the output $y$, the control $u$ and the error $\epsilon$ are shown. It can be noted that there is an infinitely fast switching of the control signal in the transient because $\epsilon$ slides on $v(\epsilon) = 0$. However, when $\epsilon$ enters $S_\rho$ the control signal switches only whenever $\epsilon$ reaches a boundary point.

Consequently, the proposed control law performs better than the classical sliding mode control, since the phenomenon of chattering is disallowed after the convergence time $t_c$, which can be defined a priori.

Observe, moreover, that the $t_c$ value given by (3.50) results 3.75s and it results a good estimation of the real value 3.44s.

**Reference signal $\hat{y}(t) = 1$ and initial conditions $y(0) = 1$, $\dot{y}(0) = 0.2$**

The error $\epsilon$ converges into $S_\rho$ without sliding motion (see Figs. 3.9 and 3.10).

**Reference signal $\hat{y}(t) = cos(0.5t)$ and initial conditions $y(0) = 0.97$, $\dot{y}(0) = 0$**

Figs. 3.11 and 3.12 show that there is not infinitely fast switching of the control signal because $\epsilon$ is always contained in $S_\rho$. This is in accordance with Remark 15.

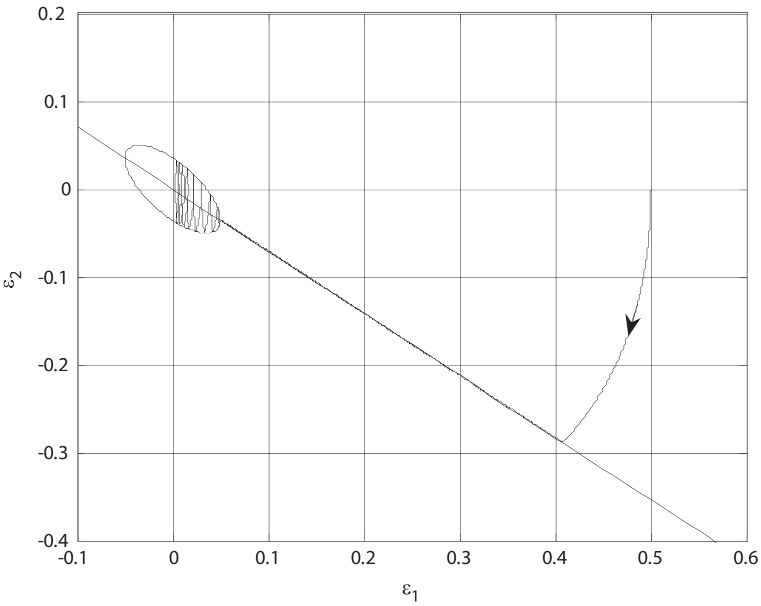


Figure 3.8: Tracking error. Case A.

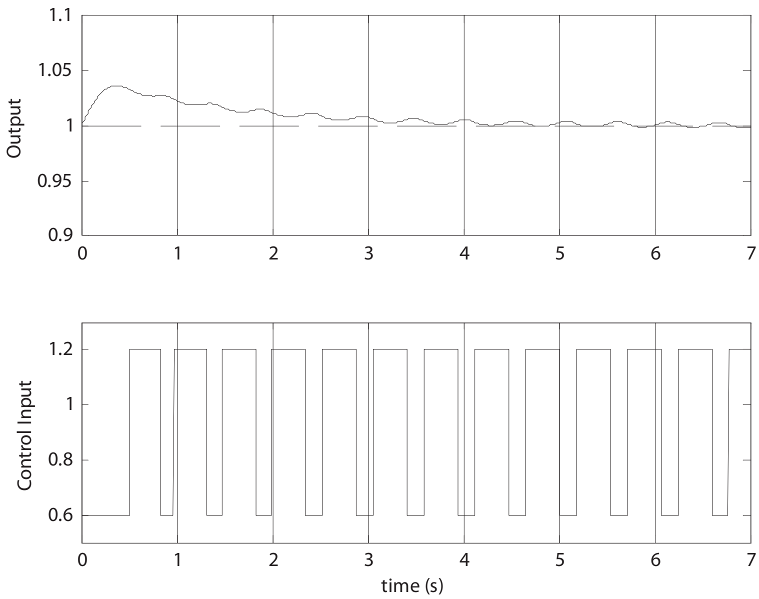


Figure 3.9: Output and control signals. Case B.

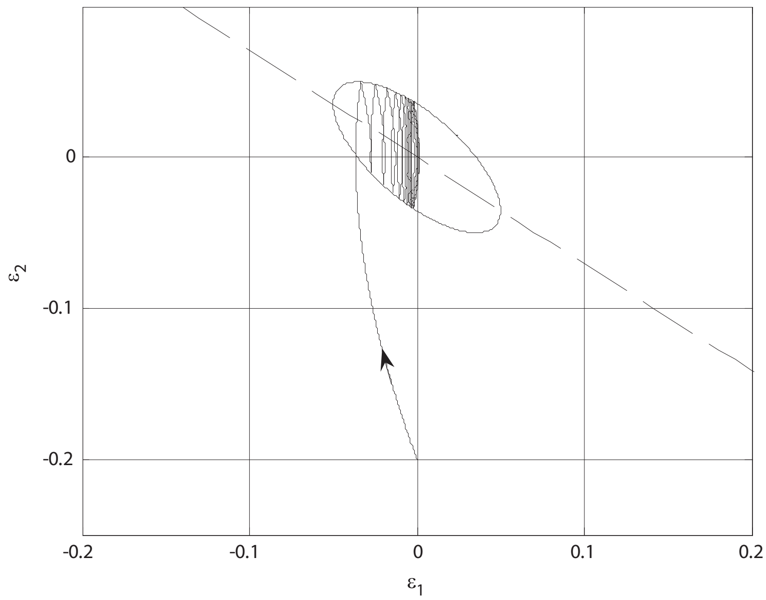


Figure 3.10: Tracking error. Case B.

Moreover, it is important to note that, considering only the extreme values of the control

$$\wp_u = \{ \ -1.2 \quad +1.2 \ \}, \tag{3.71}$$

the output is practically identical to that shown in Fig. 3.11 while there is a consistent increase in the average switching frequency of the control signal (see Fig. 3.13).

## 3.7 Conclusion

In this chapter a new methodology for the design of control laws with finite valued control signals has been presented. This methodology allows designing controllers which guarantee the practical tracking of sufficiently regular reference trajectories for SISO linear plants subject to disturbances and parametric uncertainties.

The formulated theorems allow imposing prescribed maximum limits at the convergence time, the tracking error and its derivatives, limiting or deleting the sliding mode.

A simple example has been presented to put on evidence the advantages obtained using the proposed method, compared to either sliding mode and classical relay control approaches. Such advantages can be also obtained in controlling plants with order greater than two.

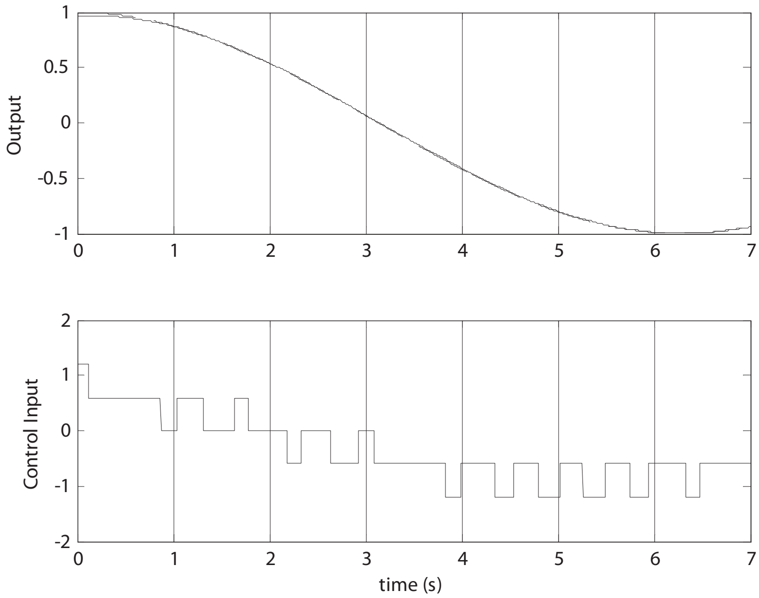


Figure 3.11: Output and control signals. Case C.

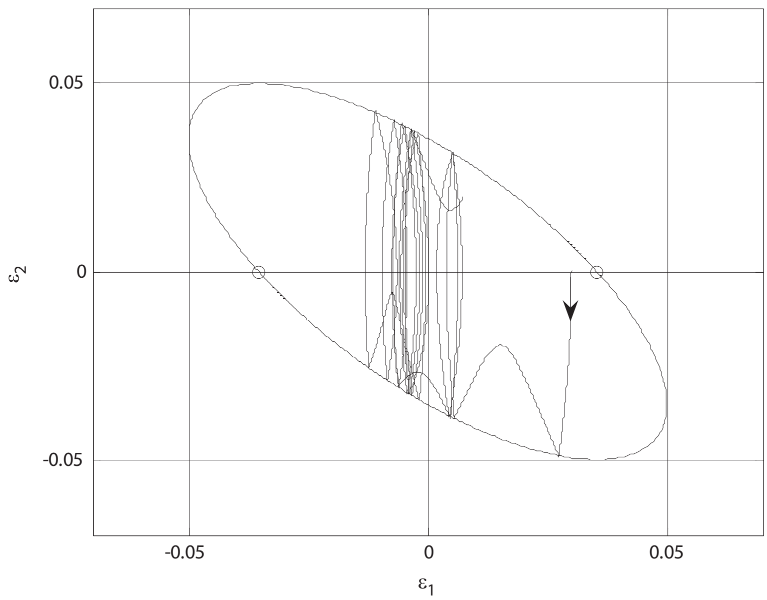


Figure 3.12: Tracking error. Case C.

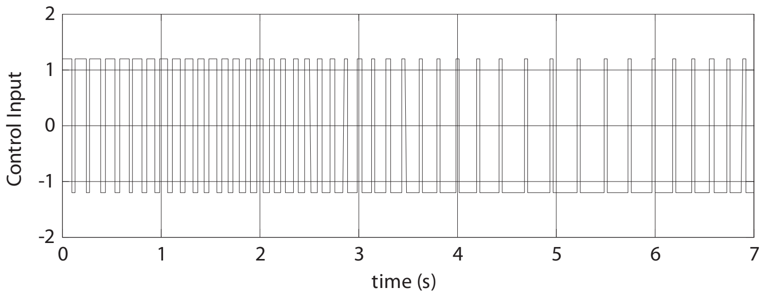


Figure 3.13: Control signal if there are available only the extreme values. Case C.

# Chapter 4

# Optimal filters for the delayed estimation

This chapter presents a new method for the optimal design of filters and control systems. This method is applicable when a certain amount of delay or latency in the estimation of a signal affected by noise can be tolerated or in the case the desired output of the plant to be controlled is known with a certain anticipation. The method is based on the minimization of an appropriate quality index with respect to two design parameters of the filter or the control system, which in part have already been designed with one of the numerous literature methods. As exemplification, considering the class of Butterworth systems the proposed method is used to determine some design formulas and to show the consistent improvements obtained. The proposed method is illustrated through two significant examples, one of noise filtering and another regarding tracking control of a reference trajectory characterized by an assigned band. The proposed theory is then applied to design the optimal differentiation system which provides the derivatives of the reference trajectory for the implementation of the multi-valued control law of Section 3.6. Finally, the application of the optimal filters to the estimation of the trajectory of mobile phone users is presented.

## 4.1 Introduction

The noise which alters the output signal of a system can either come from the system itself (endogenous or internal noise) or from other systems (exogenous or external noise). In ideal conditions, the output signal $\hat{y}$ is produced by an ideal system subjected to an ideal input signal $\hat{u}$.

In real conditions, the output signal $y_m$ is produced by a real system, with parametric and/or structural uncertainties, also subjected to other exogenous and endogenous signals, said disturbances, acting in input, output and in inner points (see Fig. 4.1). The interactions between disturbances and input, output and inner signals can be of several types: additive, multiplicative, etc. The parametric and structural uncertainties can be bounded, time-invariant, etc. If the system with its uncertainties, the signal $\hat{u}$ and the disturbances are so that $y_m = \hat{y} + r$, with $R(\omega)$ external to the band of $\hat{Y}(\omega)$ - $R(\omega)$ and $\hat{Y}(\omega)$ respectively denote the spectrums of the signals $r(t)$ and $\hat{y}(t)$ - then the noise $r$

can be reduced and in some cases removed, without altering $\hat{y}$, through the use of an appropriately designed linear filter (see Fig. 4.2).

Literature proposes various methods for the design of filters which allow imposing constraints on the magnitude and/or on the phase of the frequency response (see, for example, [92] and [72]). The Butterworth filters have maximally flat magnitude at $\omega = 0$ (see [18] and [81]). In [11] [3] [62] methods to assign an arbitrary magnitude of the filter frequency response are presented. The Bessel filters have maximally flat group delay at $\omega = 0$ (see [75]). In order to impose a maximally flat group delay along the whole pass-band it is possible to use symmetric FIR filters [33], nearly symmetric FIR filters (with reduced delay) [81], or linear phase IIR filters [74]. Allpass filters consent to obtain prescribed group delay characteristics (see, for example, [13]). In [52] a method for imposing group delay and magnitude constraints is presented. Since in many cases a delay in the estimation of a signal, whose measure is affected by noise, can be tolerated (e.g. for the estimation of the location of a cellphone or a vehicle [26], in many signal processing and communication systems [35]), it can be interesting, in order to obtain better performance, to design a filter such that the filter output $y(t)$ is considered to be an estimation of $\hat{y}(t-T)/G$ instead of $\hat{y}(t)$, where $G$ and $T$ are constant gain and delay.

An analogue argument can be made for the design of a feedback control system in which it is desired that the plant output $y$ becomes equal or proportional to the desired signal $\hat{y}$ (see Fig. 4.3). Noting that in many cases the desired output $\hat{y}$ of the plant to be controlled is known with a certain anticipation (thinking about manufacturing processes [22], automobile driving, missile trajectory control, vehicle suspension system) [86] [85] [45] [79], the feedback control system can be more appropriately commanded not with the signal $\hat{y}(t)$ but with $G\hat{y}(t+T)$, where $G$ is a constant gain and $T$ is a constant anticipation.

From the above considerations, it follows that the performance of a filter or a feedback control system can be improved if a gain $G$ and a delay or anticipation $T$ of the input signal are introduced as further design parameters.

The preview control was first proposed in [86], in which the information about the reference signal was formulated in deterministic/stochastic terms. The problem was then solved in LQ and $H^\infty$ terms, both for discrete and continuous systems. In the discrete case, the problem of control with anticipated reference and filtering for the delayed estimation was studied by various authors (see e.g. [53] and [54]). However, the results presented in these works allow designing controllers or filters that are generally difficult to implement and with performance which are difficult to predict if the anticipation or the delay vary. In the continuous case, some work was developed using the LQ (see e.g. [9] and [64]) and $H^\infty$ formulation (see [68] [63] [84] [61] [67]). The performance of a $H^\infty$ preview controller was also evaluated using the game theory [82]. However, the proposed controllers are very complex and have implementation problem due to the need of real time calculus of integrals involving exponentials of time-varying matrices . Literature proposes methods for the solution of the minimum mean square error problem for linear continuous time-varying systems with current and time-delay measurements (see e.g. [95]). However, the proposed results are based on the Kalman approach and are valid only in the hypothesis of uncorrelated Gaussian noises.

In this chapter a new method for the optimal design of filters and control systems is presented [20]. Such method is applicable when a certain amount of

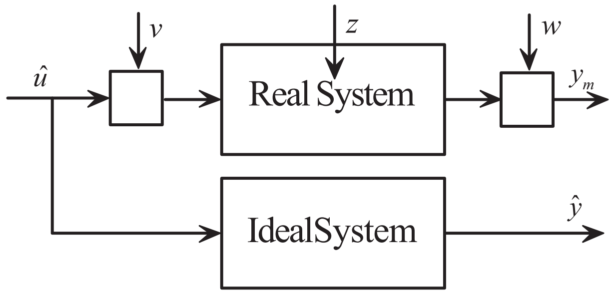


Figure 4.1: Scheme of the systems which generate $y_m$ and $\hat{y}$.

delay or latency in the estimation of a signal affected by noise can be tolerated or in the hypothesis the desired output of the plant to be controlled is known with a certain anticipation. The method proposed in this chapter is based on a frequency approach, suggested by the following considerations.

- The class of desired signals which a plant must track, especially when it is low powered, cannot always be considered polynomial. As it is well-known, a generic signal is almost always better approximated with a truncated Fourier series (of the repeated signal) than with a truncated Taylor series or a Lagrange polynomial interpolation (see e.g. example in Section 4.4.2 and [22]). Therefore it is more realistic to hypothesize that the desired output of a feedback control system belongs to a class of signals characterized by an assigned band, as done in the filtering theory.

- It is a common conviction that, if a signal is contained in the band of the feedback control system or the filter, the error $e(t) = \hat{y}(t) - y(t)$ is tolerable. This is generally not true. For example, for a 4-th order Butterworth low-pass filter, the output related to a sinusoidal input in the 3dB-band of the filter can have a phase delay close to -180 degrees (for the frequencies close to the cut-off frequency). Consequently, the error is not lower than 29% (as one might believe) but can also be close to 170%.

Starting from filters and feedback control systems designed with the numerous literature results (see, for example, [92] [72] [83] [10]), various methods for determining the values of the new design parameters gain $G$ and delay (or anticipation) $T$, through the minimization of the norm of the system frequency error in a $L^p(]0, +\infty[, \mu)$ space, are presented in the chapter. As exemplification, limiting the structure of the filters and of the feedback control systems to the Butterworth systems, some formulas in order to determine the optimal gains and delays will be provided. In this way the obtained consistent improvements will be shown. Such results will also be used to design an efficient feedback control system for tracking a trajectory characterized by an assigned band instead of polynomial and to immediately evaluate the performance of the derived system.

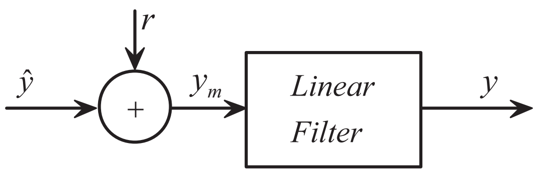


Figure 4.2: Scheme of a linear filter for reduce the noise.

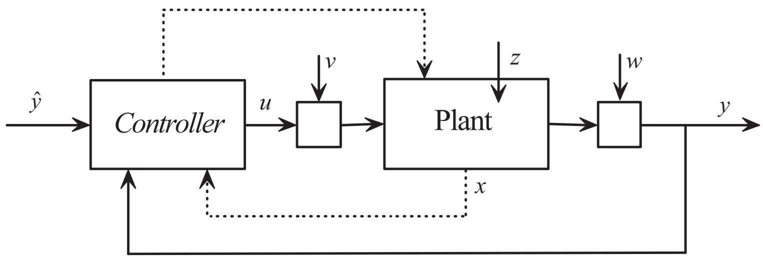


Figure 4.3: Scheme of a feedback control system.

## 4.2 Problem statement and main results

Consider the continuous-time, SISO (Single Input Single Output), asymptotically stable feedback control system of order $n \in \mathbb{N}$, defined by the following transfer function

$$W(s) = \frac{\sum_{j=0}^{n} b_j s^j}{s^n + \sum_{i=0}^{n-1} a_i s^i} \tag{4.1}$$

where

$$a = \begin{pmatrix} a_0 & a_1 & \dots & a_{n-1} \end{pmatrix} \in \mathbb{R}^n, b = \begin{pmatrix} b_0 & b_1 & \dots & b_n \end{pmatrix} \in \mathbb{R}^{n+1}. \tag{4.2}$$

Suppose, for simplicity, that the system has unit gain and 3dB-band $B_{sy} = [0, \omega_{sy}]$. Moreover, suppose that the desired output $\hat{y}$ has bounded band $B_{si} = [0, \omega_{si}]$ and is known with a sufficient anticipation.

Since the magnitude $M(\omega) = |W(j\omega)|$ and the delay $D(\omega) = -arg(W(j\omega))/\omega$, $\omega \in B_{si}$, are variable in $B_{si}$, we can think to pre-process the reference signal through a system with constant gain $G \in \mathbb{R}$ and anticipation $T \in \mathbb{R}$. If the values of $G$ and $T$ are chosen in order to minimize the square errors

$$\int_0^{\omega_{si}} (G^{-1} - M(\omega))^2 d\omega, \quad G \in \mathbb{R}, \tag{4.3a}$$

$$\int_0^{\omega_{si}} (T - D(\omega))^2 d\omega, \quad T \in \mathbb{R}, \tag{4.3b}$$

it is possible to use the following theorem.

**Theorem 6** *The values $\hat{G}$ and $\hat{T}$ which minimize the square errors* (4.3) *result*

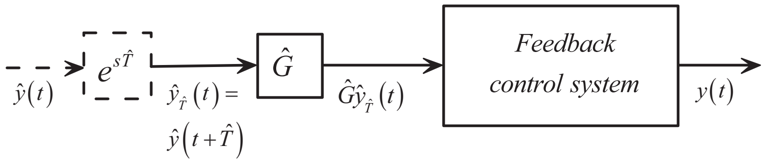


Figure 4.4: Scheme of the pre-processing system connected to a feedback control system.

$$\hat{G} = \frac{1}{\bar{M}}, \quad \bar{M} = \frac{1}{\omega_{si}} \int_0^{\omega_{si}} M(\omega)d\omega, \tag{4.4a}$$

$$\hat{T} = \bar{D} = \frac{1}{\omega_{si}} \int_0^{\omega_{si}} D(\omega)d\omega \tag{4.4b}$$

**Proof 9** *The first result in* (4.4) *easily follows taking into account that*

$$\frac{d}{dG} \int_0^{\omega_{si}} (G^{-1} - M(\omega))^2 d\omega = -2G^{-3} + 2G^{-2} \int_0^{\omega_{si}} M(\omega)d\omega. \tag{4.5}$$

*The last result in* (4.4) *follows in analogue manner.*

**Remark 17** *If $\hat{T} \leq 0$, it is easy to realize the pre-processing system of $\hat{y}$. If $\hat{T} > 0$, the pre-processing can be realized using the scheme of Fig. 4.4 if the desired output is known with at least an anticipation of $\hat{T}$. The advanced knowledge of $\hat{y}$ is guaranteed in many control systems of manufacturing processes, automobile driving, etc.*

**Remark 18** *In the hypothesis that system* (4.1) *is a filter and a delay in the estimation of $\hat{y}(t)$ from $y_m(t) = \hat{y}(t) + r(t)$ - r(t) is a measurement noise and/or an external signal - is tolerable, then it can be appropriate to consider he filter output, with input $y_m(t)$, as an estimation of $\hat{y}(t - \hat{T})/\hat{G}$ instead of $\hat{y}(t)$.*

In order to evaluate the performance improvement obtained using the proposed pre-processing system (see Remark 17) and in order to provide a general method to obtain the optimal values $\hat{G}$ and $\hat{T}$, it is necessary to introduce a measure of the error between desired and effective output. For such reasons, consider the normed vectorial space $L^p(]0, \omega_{si}[, \mu)$ where $p \in [1, +\infty]$ and $\mu$ is the easure of density $\theta \in L_{LOC}(]0, \omega_{si}[)$, $\theta \geq 0$ - $L_{LOC}(]0, \omega_{si}[)$ is the space of locally summable functions $\theta : ]0, \omega_{si}[ \to \mathbb{R}$ - and consider the error measurement

$$\epsilon(G, T) = \|1 - GM(\omega)e^{j\omega(T - D(\omega))}\|_{L^p(]0, \omega_{si}[, \mu)} \tag{4.6}$$

$$= \left( \int_0^{\omega_{si}} \|1 - GM(\omega)e^{j\omega(T - D(\omega))}\|^p \theta(\omega) d\omega \right)^{1/p} \tag{4.7}$$

The following general optimization problem can be formulated.

**Problem 3** *Assigned: system* (4.1), *desired output band $B_{si} = [0, \omega_{si}]$, $p \in [1, +\infty]$, $\theta \in L_{LOC}(]0, \omega_{si}[)$, $\theta \geq 0$, determine the values $\hat{G}$ and $\hat{T}$ which minimize the error* (4.6).

As exemplification, we suppose $p = 2$. In this hypothesis the following result can be stated.

**Theorem 7** *The solution to Problem 3 is obtained choosing $\hat{T}$ so that the following function*

$$S(T) = \left( \int_0^{\omega_{si}} M(\omega) \cos \omega(T - D(\omega))\theta(\omega) d\omega \right)^2, \quad T \in \mathbb{R} \tag{4.8}$$

*is maximized and $\hat{G}$ equals to*

$$\hat{G} = \frac{\int_0^{\omega_{si}} M(\omega) \cos \omega(\hat{T} - D(\omega))\theta(\omega) d\omega}{\int_0^{\omega_{si}} M(\omega)^2 \theta(\omega) d\omega}. \tag{4.9}$$

*Moreover, the optimal value of the error results*

$$\epsilon(\hat{G}, \hat{T}) = \sqrt{\int_0^{\omega_{si}} \theta(\omega) d\omega - \frac{S(\hat{T})}{\int_0^{\omega_{si}} M(\omega)^2 \theta(\omega) d\omega}}. \tag{4.10}$$

**Proof 10** *It is easy to prove that*

$$\epsilon(G, T) = \int_0^{\omega_{si}} (1 - GM(\omega) e^{j\omega(T - D(\omega))})(1 - GM(\omega) e^{-j\omega(T - D(\omega))})\theta(\omega) d\omega \tag{4.11}$$

$$= \int_0^{\omega_{si}} \theta(\omega) d\omega + G^2 \int_0^{\omega_{si}} M(\omega)^2 \theta(\omega) d\omega - 2G \int_0^{\omega_{si}} M(\omega) \cos \omega(T - D(\omega))\theta(\omega) d\omega. \tag{4.12}$$

*Imposing the condition of minimum with respect to $G$, it follows that*

$$G = \frac{\int_0^{\omega_{si}} M(\omega) \cos \omega(T - D(\omega))\theta(\omega) d\omega}{\int_0^{\omega_{si}} M(\omega)^2 \theta(\omega) d\omega}. \tag{4.13}$$

*Substituting this value in* (4.11) *and minimizing with respect to $T$, the proof easily follows.*

**Remark 19** *Through the Theorem 7, Problem 3 is reduced to the one of finding the maximum of the function $S(T)$ in* (4.8) *with respect to only one variable: the delay $T$. Note that the delay $\hat{T}$ which maximizes the function* (4.8) *provides the angular coefficient of the line $\phi = -\hat{T}\omega$ which "better" interpolates the phase diagram* $\arg W(j\omega)$ *in the interval $B_{si} = [0, \omega_{si}]$.*

**Remark 20** *The above method is still valid in case the density function $\theta$ has some impulses, in order to give more weight to particular frequencies in $B_{si}$.*

**Remark 21** *If the feedback control system or the filter* (4.1) *has some degrees of freedom, then the optimum of the error measurement* (4.6) *can be done in contemporary with respect to those degrees of freedom too. Clearly, the possible improvements can be obtained at the expense of more complex and onerous optimization algorithms (taking also into account that it is anyway needed to guarantee certain specifications about robustness, disturbance insensitivity, etc).*

## 4.3 Optimal design of Butterworth systems

Generally, Problem 3 can only be numerically solved. In this section we then consider only a class of systems of particular interest, the low-pass systems with Butterworth structure

$$W(s) = \frac{\omega_{sy}^n}{\prod_{i=0}^{n-1}\left(s - \omega_{sy} e^{j\frac{\pi}{2}(1+\frac{1+2i}{n})}\right)}. \tag{4.14}$$

Moreover, we suppose that the desired output $\hat{y}$ has a band equals to the one of the system ($B_{si} = B_{sy}$), $\theta(\omega) = 1\,, \omega \in B_{si}$ and $p = 2$. In these hypotheses, the following theorem can be formulated.

**Theorem 8** *Let $\hat{G}_{1,n}$ and $\hat{T}_{1,n}$ be the gain and the delay which resolve Problem 3 for system (4.14), $B_{si} = [0, \omega_{si}]$, $\omega_{si} = 1$, and for a given $n \in \mathbb{N}$. Then the values $\hat{G}_n$ and $\hat{T}_n$ which solve the same problem for $B_{si} = [0, \omega_{si}]$, $\omega_{si} \neq 1$ are*

$$\hat{G}_n = \hat{G}_{1,n} \quad \hat{T}_n = \frac{\hat{T}_{1,n}}{\omega_{si}}. \tag{4.15}$$

**Proof 11** *From (4.6), with the change of variables $\omega = w\omega_{si}$ and or the hypothesis that $\theta(\omega) = 1\,, \omega \in B_{si}$, ir results*

$$\begin{aligned}
\epsilon(G,T)^2 &= \omega_{si}\int_0^1 \|1 - GM(w\omega_{si})e^{jw\omega_{si}(T - D(w\omega_{si}))}\|^2 dw && (4.16)\\
&= \omega_{si}\int_0^1 \|1 - GM_{1,n}(w)e^{jw(T_{1,n} - D_1(w))}\|^2 dw && (4.17)\\
&= \omega_{si}\epsilon_{1,n}(G, T_{1,n})^2, && (4.18)
\end{aligned}$$

*where*

$$\begin{aligned}
W_{1,n}(s) &= \frac{1}{\prod_{i=0}^{n-1}\left(s - e^{j\frac{\pi}{2}(1+\frac{1+2i}{n})}\right)}, && (4.19)\\
M_{1,n}(\omega) &= |W_{1,n}(j\omega)|, && (4.20)\\
D_{1,n}(\omega) &= -\arg W_{1,n}(j\omega)/\omega, && (4.21)\\
T_{1,n} &= T\omega_{si}. && (4.22)
\end{aligned}$$

*Thus, the proof easily follows.*

The above theorem allows to facilitate the resolution of Problem 3. In fact, in regard to the optimal values $\hat{G}_{1,n}$ and $\hat{T}_{1,n}$, the following result can be stated.

*The optimal values $\hat{G}_{1,n}$ and $\hat{T}_{1,n}$, $n = 1, \ldots, 10$, and the related errors $\epsilon_{1,n} = \epsilon_{1,n}(\hat{G}_{1,n}, \hat{T}_{1,n})$, determined using Theorem 7 and the Matlab Optimization Toolbox [1], are reported in Table 4.1.*

**Remark 22** *In Table 4.1 we also report the values of the errors $\epsilon_{1,n}^0 = \epsilon_{1,n}(1,0)$ obtained without considering the designed pre-processing system. Confronting $\epsilon_{1,n}$ and $\epsilon_{1,n}^0$ the consistent improvement obtained using the proposed modification to the feedback control system can be observed.*

| $n$ | 1 | 2 | 3 | 4 | 5 | 6 | 7 | 8 | 9 | 10 |
|---|---|---|---|---|---|---|---|---|---|---|
| $\hat{T}_{1,n}$ | 0.86 | 1.55 | 2.24 | 2.92 | 3.60 | 4.29 | 4.98 | 5.67 | 6.36 | 7.06 |
| $\hat{G}_{1,n}$ | 1.122 | 1.069 | 1.047 | 1.033 | 1.024 | 1.016 | 1.009 | 1.002 | 0.996 | 0.990 |
| $\epsilon_{1,n}$ | 0.109 | 0.096 | 0.100 | 0.113 | 0.131 | 0.150 | 0.169 | 0.189 | 0.209 | 0.228 |
| $\epsilon^0_{1,n}$ | 0.463 | 0.788 | 1.069 | 1.282 | 1.416 | 1.473 | 1.470 | 1.431 | 1.387 | 1.361 |

Table 4.1: Optimal values of the parameters $T$ and $G$.

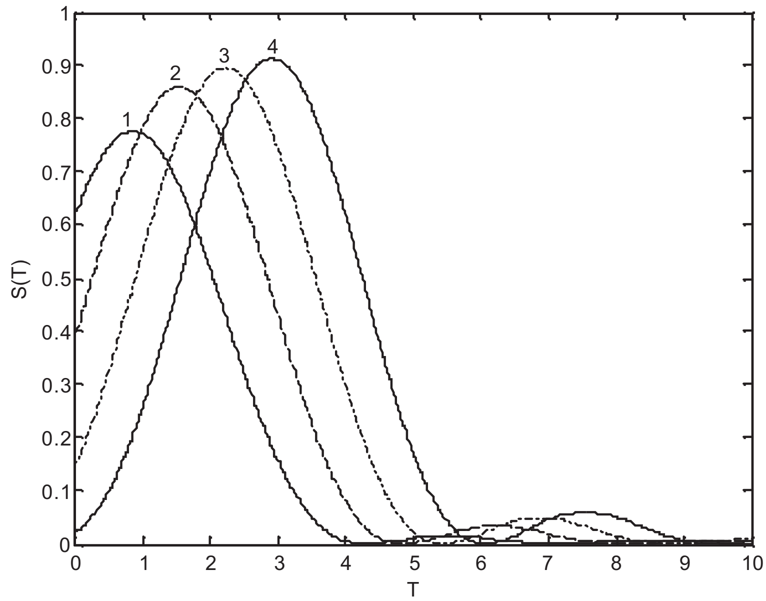


Figure 4.5: $S(T)$, $T \in [0, 10]$s, for $n = 1, \ldots, 4$.

**Remark 23** *It is important to note that the filtering systems which distorts the least the frequency components inside the band $B_{si}$ has order 2 (see the values of $\epsilon_{1,n}$ in Table 4.1).*

**Remark 24** *It is interesting to analyze the trend of the function $S(T)$ (4.8) (see Fig. 4.5 for $n = 1, \ldots, 4$). These diagrams point out the problems in the analytical determination of the optimal delay $\hat{T}$ because of many local maximus. Moreover, these diagrams allow to easily obtain, given a sub-optimal value of $T$ different from $\hat{T}$, the optimal value $\hat{G}$ and the related error $\epsilon$.*

Fig. 4.6 shows the errors

$$|1 - \hat{G}_{1,n} M_1(\omega) e^{j\omega(\hat{T}_{1,n} - D_1(\omega))}|^2 \tag{4.23}$$

$$|1 - M_1(\omega) e^{-j\omega D_1(\omega)}|^2 \,, \omega \in [0, 1] \,, n = 1, \ldots, 4, \tag{4.24}$$

using and not using the proposed pre-processing system. From them it is possible to understand how big the errors are, also for optimized systems like the Butterworth ones, for certain frequencies in the band (even not only the ones close to the cut-off frequency) and how it is possible to reduce them using the proposed simple pre-processing system.

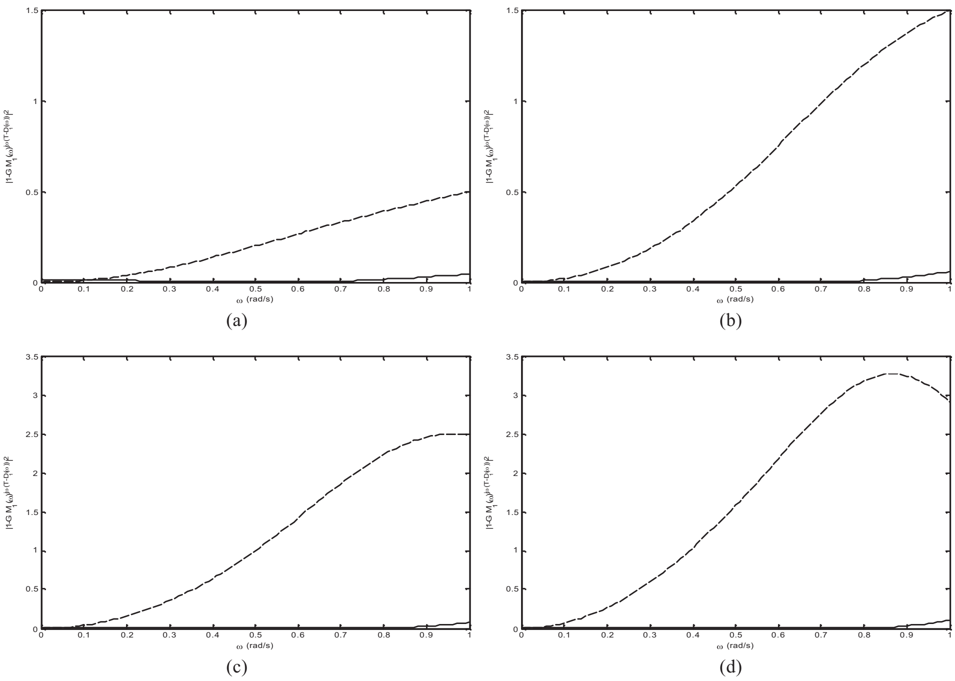


Figure 4.6: Errors of the normalized Butterworth systems of order 1 (a), 2 (b), 3(c), 4(d) considering (solid line) and not considering the pre-processing system (dashed line).

| $n$ | 1 | 2 | 3 | 4 | 5 | 6 | 7 | 8 | 9 | 10 |
|---|---|---|---|---|---|---|---|---|---|---|
| $\hat{T}_{1,n}$ | 0.92 | 1.51 | 2.14 | 2.78 | 3.44 | 4.10 | 4.76 | 5.42 | 6.09 | 6.75 |
| $\hat{G}_{1,n}$ | 1.135 | 1.079 | 1.056 | 1.043 | 1.035 | 1.030 | 1.026 | 1.023 | 1.020 | 1.018 |
| $\epsilon_{1,n}$ | 0.113 | 0.100 | 0.114 | 0.136 | 0.161 | 0.186 | 0.211 | 0.236 | 0.260 | 0.285 |

Table 4.2: Optimal values of the parameters $T$ and $G$ calculated through Theorem 6.

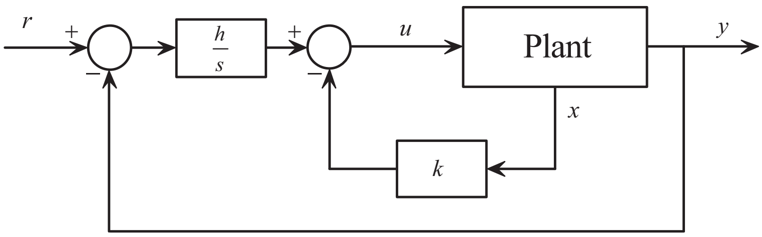


Figure 4.7: Control scheme with state feedback and integral action.

**Remark 25** *As regards the same Butterworth systems used to obtain Table 4.1, the values $\hat{G}$ and $\hat{T}$, determined applying Theorem 6, and the related errors $\epsilon$ are reported in Table 4.2. Such errors are not too different from the ones calculated using Theorem 7. For non-Butterworth systems, especially for systems with non-minimum phase or with low damping poles, the improvement obtained applying Theorem 7 is more consistent. Consider, for example, a feedback control system with $W(s) = \frac{1}{s^2+0.8s+1}$. For such a system, applying the pre-processing system derived by Theorem 6, for $\omega_{si} = 1$, we obtain $\epsilon = 0.216$. If the pre-processing system is instead designed using Theorem 7, we obtain $\epsilon = 0.167$.*

**Remark 26** *If the plant to be controller (of order $n_p$) is controllable, characterized by a transfer function without zeros and its state vector is available, it is easy to prove (see for example [28] and [29]) that through the control scheme with state feedback and integral action of Fig. 4.7, the reference-output system, with an opportune choice of $h \in \mathbb{R}$ and $k \in \mathbb{R}^{n_p}$, can become a Butterworth system (4.14) of order $n = n_p + 1$. Therefore its performance can be greatly improved if the reference $r(t)$ is not imposed to be equal to $\hat{y}(t)$, as it commonly happens, but equal to the output of the pre-processing system of Fig. 4 with input $\hat{y}(t)$, where $\hat{G}$ and $\hat{T}$ are easily calculable using Table 4.1 and Theorem 8.*

## 4.4 Explanatory examples

### 4.4.1 Noise filtering

Consider a signal $\hat{y}$ with spectrum $[0, 0.25]$rad/s corrupted by an additive noise $r$ with spectrum in $[0, 100]$rad/s (see Figs. 4.8, 4.9 and 4.10). Consider the Butterworth filtering systems of order $n = 1, \ldots, 10$, with $\omega_{sy} = 0.25$rad/s, where the optimal delays $\hat{T}_n$ and gains $\hat{G}_n$ are obtained applying Theorem 8 and Table 4.1.

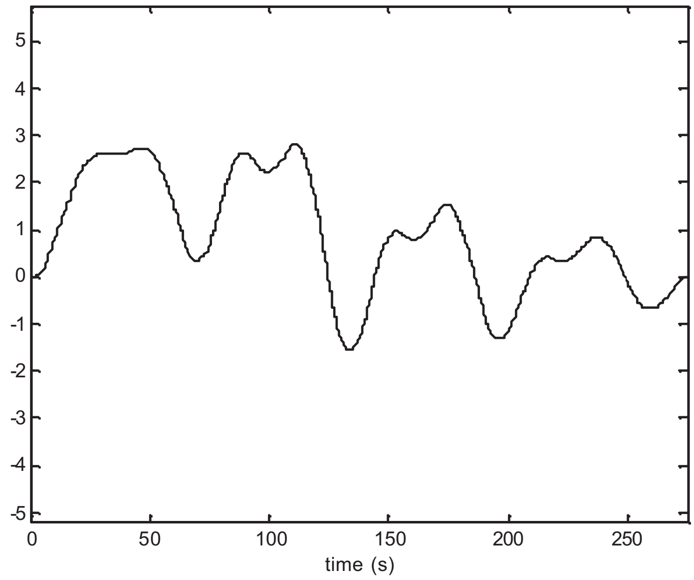


Figure 4.8: Signal $\hat{y}$.

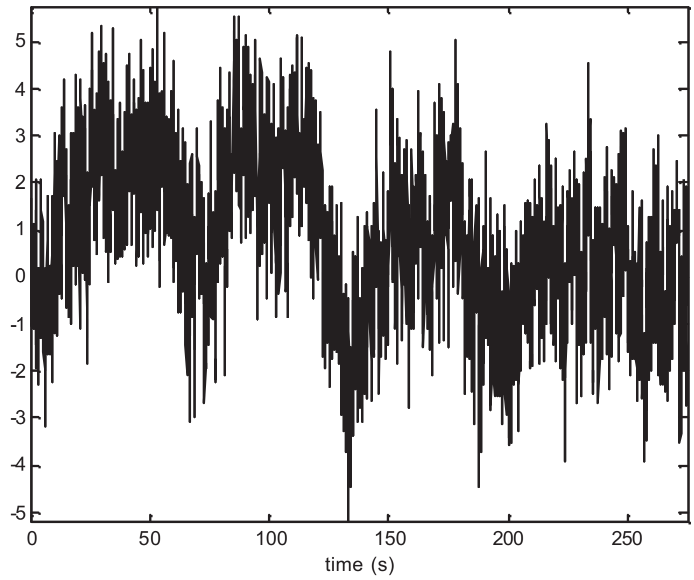


Figure 4.9: Signal $y = \hat{y} + r$.

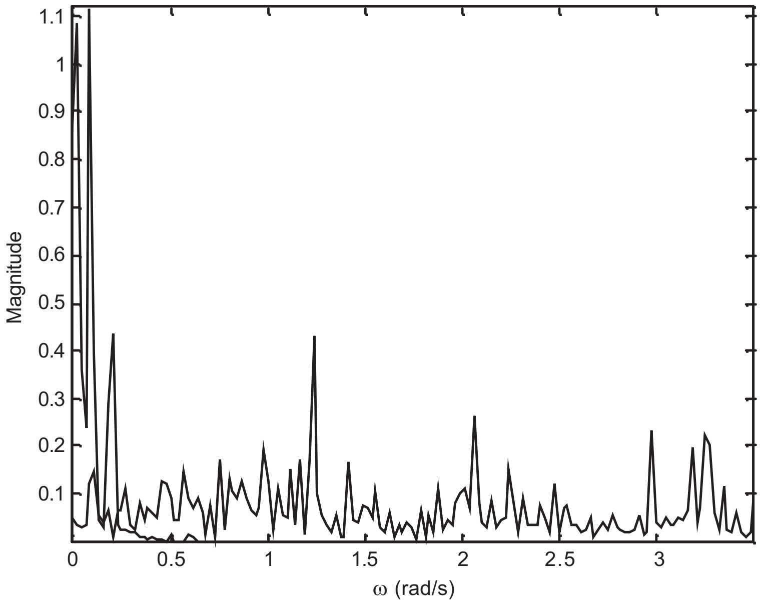


Figure 4.10: Spectrums of signal $\hat{y}$ (solid line) and noise $r$ (dotted line), limitedly to the interval $[0, 3.5]$rad/s.

As example, Fig. 4.11 shows the percentage errors made by the third order filter with and without considering the delay $\hat{T}_3$ and the gain $\hat{G}_3$. From the figure the improvement obtained with the proposed method can be clearly observed. In Fig. 4.12 signal-to-noise ratios of the input signal and the filters' output signals

$$SNR_{IN} = \frac{RMS(\hat{y})}{RMS(r)} \quad SNR_{OUT} = \frac{RMS(\hat{y})}{RMS(\hat{y} - y)}, \tag{4.25}$$

with and without considering the delays $\hat{T}_n$ and the gains $\hat{G}_n$ are reported. From the figure, it results that

- without considering the delays $\hat{T}_n$ and the gains $\hat{G}_n$, the filter that damages the least has order 1;
- for a sufficiently high value of $n$, the filter without considering the delay and the gain may even worsen the signal-to noise ratio.

### 4.4.2 Control system

We want to design a controller for a planar laser scanner which uses two galvanometers (see Fig. 4.13) [19]. Clearly for such a system the reference trajectories can be much better characterized in frequency rather then polynomial terms.

We start defining a dynamical model of deflection of a galvanometer's mirror. Let $\theta$[rad] be the angular position of the mirror, $i$[A] be the absorbed current and

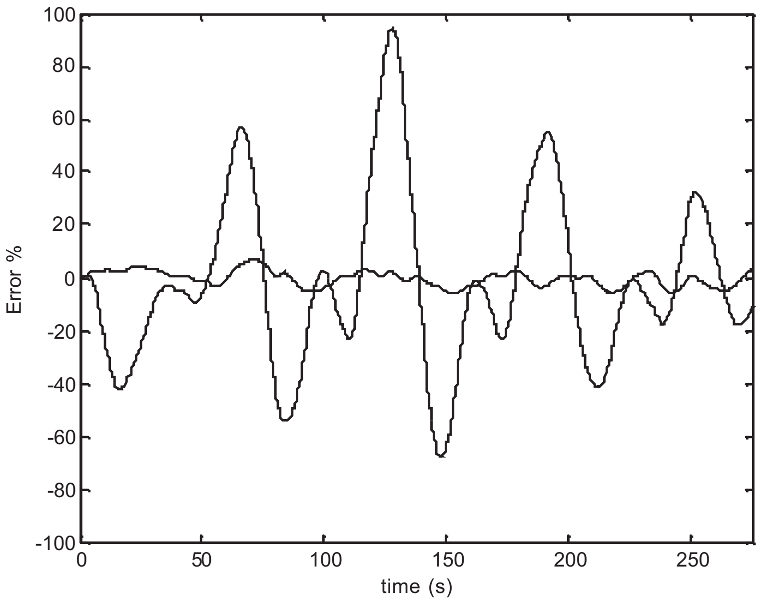


Figure 4.11: Errors made by the third order filter with (solid line) and without considering the delay $\hat{T}_3$ and the gain $\hat{G}_3$ (dotted line).

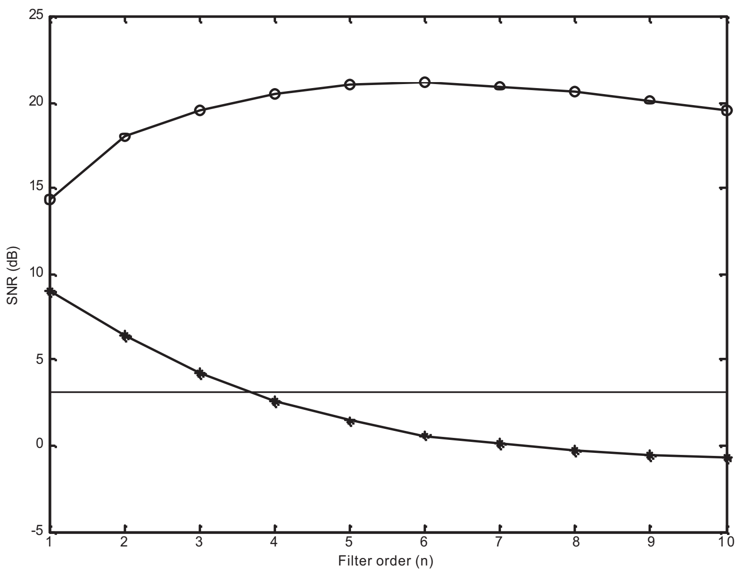


Figure 4.12: Signal-to-noise ratios. Input SNR (dotted line); Output SNR: $T = 0$, $G = 1$ (*), $T = \hat{T}_n$, $G = \hat{G}_n$ ().

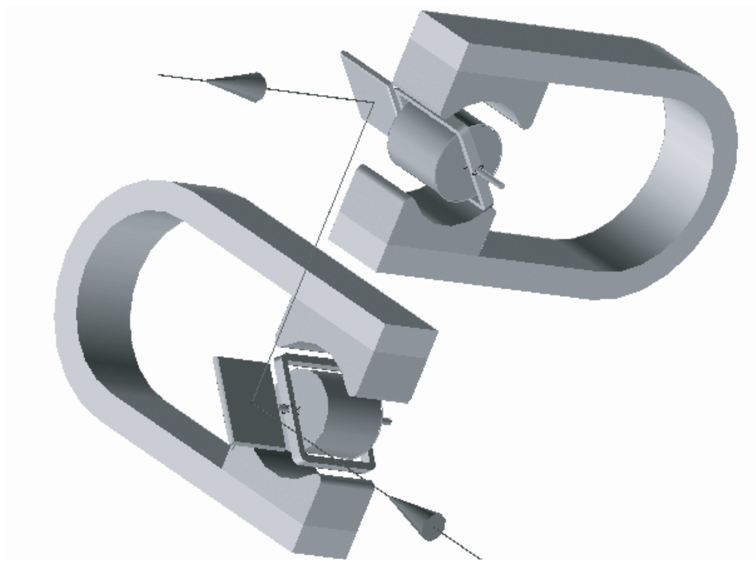

Figure 4.13: Laser beam deflected by the two galvanometers.

$u$[V] be the voltage applied to the galvanometer. Imposing $x = \begin{pmatrix} \theta & \dot{\theta} & i \end{pmatrix}^T$, a possible model of the galvanometer results

$$\dot{x} = \begin{pmatrix} 0 & 1 & 0 \\ -K_t/J & -K_a/J & K_i/J \\ 0 & -K_v/L & R/L \end{pmatrix} x + \begin{pmatrix} 0 \\ 0 \\ 1/L \end{pmatrix} u, \tag{4.26}$$

$$y = \begin{pmatrix} 1 & 0 & 0 \end{pmatrix} x, \tag{4.27}$$

where realistic values of the parameters are

$$R = 1.4\Omega \tag{4.28}$$
$$L = 55\mu H \tag{4.29}$$
$$K_v = 0.036Vs \tag{4.30}$$
$$J = 3.3 \cdot 10^{-7} Kgm^2 \tag{4.31}$$
$$K_i = 0.036Nm/A \tag{4.32}$$
$$K_a = 2.8 \cdot 10^{-4} Nms \tag{4.33}$$
$$K_t = 0.20Nm. \tag{4.34}$$

We want to design a control system of the mirror's angular position, when the desired trajectory is characterized by the band $[0, 2\pi 150]$rad/s. Based on the considerations proposed in Remark 26, such problem can be resolver through the control scheme of Fig. 4.7, with

$$h = 398 \quad k = \begin{pmatrix} 0.613 & -3.55 \cdot 10^{-2} & -1.31 \end{pmatrix} \tag{4.35}$$

so that the feedback system has a dynamic characterized by a 4-th order Butterworth system with unit gain and $\omega_{sy} = 2\pi 150$rad/s, and the pre-processing system of Fig. 4.4, with delay $\hat{T} = 3.10$ms and gain $\hat{G} = 1.033$, determined applying Theorem 8 and Table 4.1.

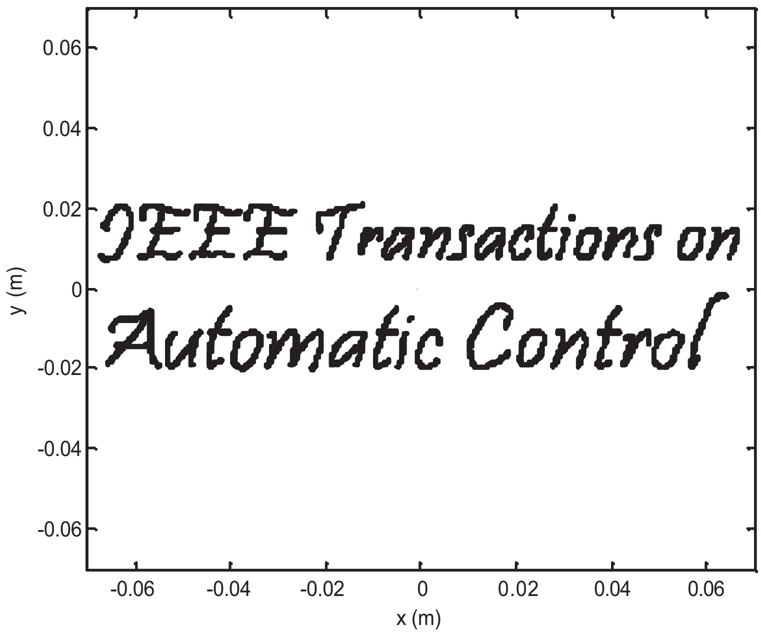


Figure 4.14: Writing to be realized.

It is important to note that the in-band error $\epsilon$, considering the pre-processing system, results about 11 times smaller with respect to the error without pre-processing (see Table 4.1 for $n = 4$). Consequently the consistent improvement in performance is evident.

The designed controller has been applied to both the galvanometers of the planar laser scanner. In Fig. 4.14 an example of writing to be realized, with scanning speed 2m/s is shown. Fig. 4.15 shows the desired trajectories for the feedback control systems of the two galvanometers, obtained from the writing to be realized with appropriate joint trajectories, covered with disabled laser beam.

Figs. 4.16 and 4.17 show the writings obtained with the designed feedback control system, considering and not considering the pre-processing system. These graphs are a further confirmation of the consistent improvement obtained using the proposed simple pre-processing system.

## 4.5 Application to the multi-valued control

The proposed theory of optimal filter for the delayed estimation can be suitably applied to the generation of the reference trajectory's derivatives, needed for the implementation of the control law of the Theorem 3 presented in the Chapter 3. In fact, it can be observed that the reference trajectory $\hat{y}$ is usually characterized by a bounded band. Then, the output of the Butterworth derivative filter

$$W(s) = \frac{\omega_{sy}^n s^n}{\prod_{i=0}^{n-1}\left(s - \omega_{sy} e^{j\frac{\pi}{2}(1+\frac{1+2i}{n})}\right)}. \tag{4.36}$$

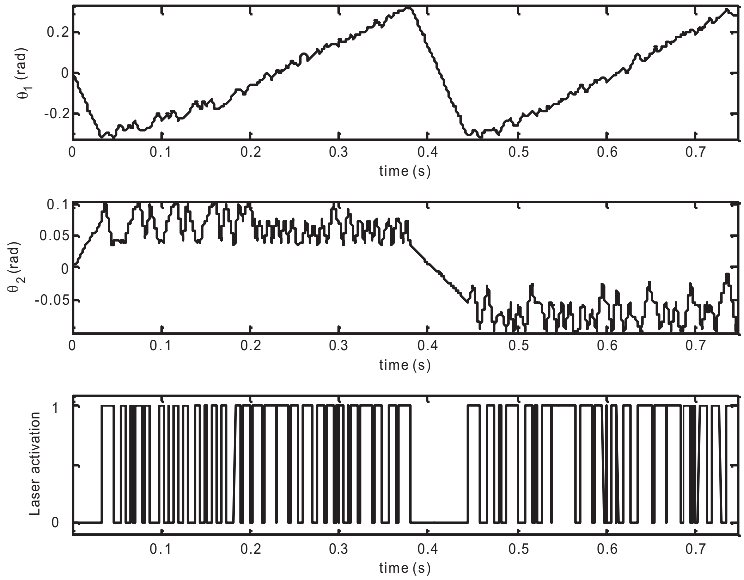


Figure 4.15: Galvanometer and laser activation reference trajectories.

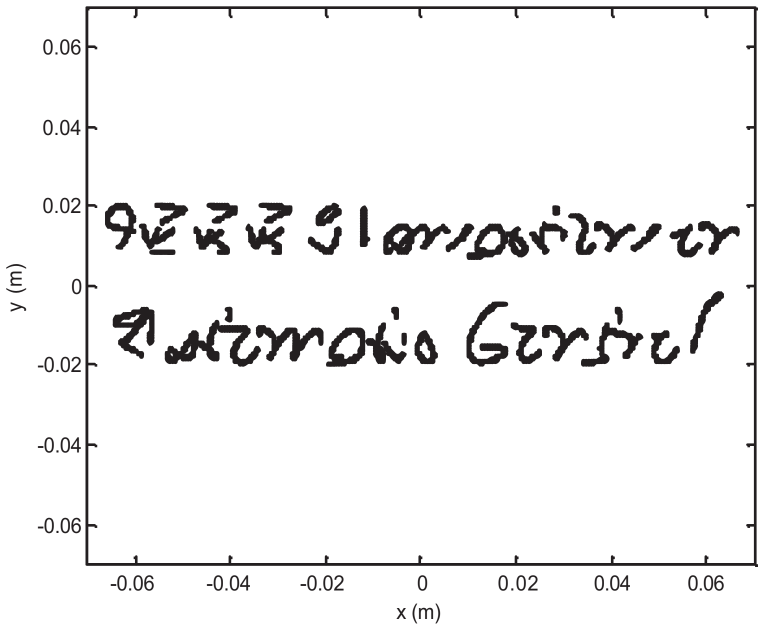


Figure 4.16: Writing obtained without pre-processing the reference signals of the galvanometers.

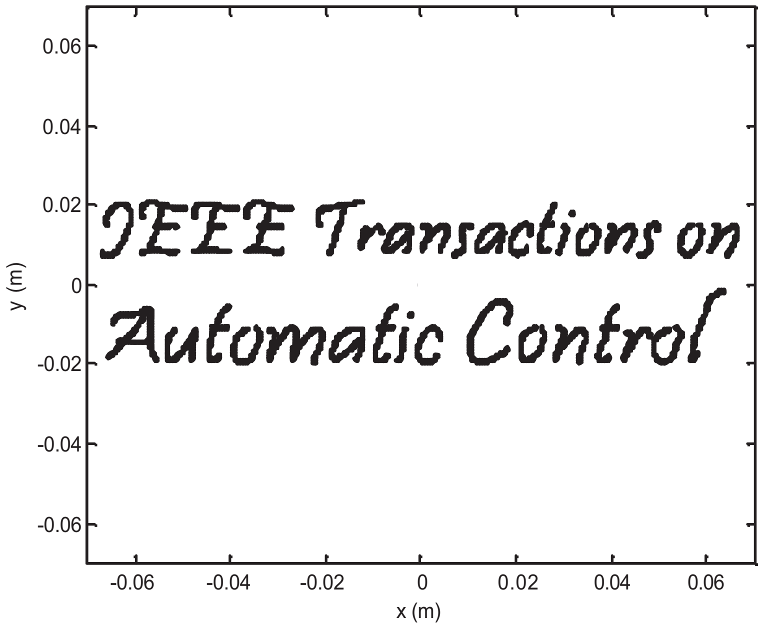


Figure 4.17: Writing obtained pre-processing the reference signals of the galvanometers.

with an appropriate value of $\omega_{sy} \in \mathbb{R}^+$ can be used to practically provide the $n$-th derivative of the reference $\hat{y}$.

Since the reference trajectory is usually known with a certain advance, it becomes important to take into account the delay introduced by the filters (4.36) (at the varying of $n$) so that the signal $\hat{y}$ and its "calculated" derivatives are phased in time. The structure of the differentiation block becomes the one in Fig.4.18. The choice of the delays for the $n-1$ anticipators can be done according to the minimization of the errors

$$\epsilon(G,T) = \|(j\omega)^n - GM(\omega)e^{j\omega(T-D(\omega))}\|_{L^p(]0,\omega_{si}[,\mu)} \tag{4.37}$$

$$= \left(\int_0^{\omega_{si}} \|(j\omega)^n - GM(\omega)e^{j\omega(T-D(\omega))}\|^p \theta(\omega) d\omega\right)^{1/p}. \tag{4.38}$$

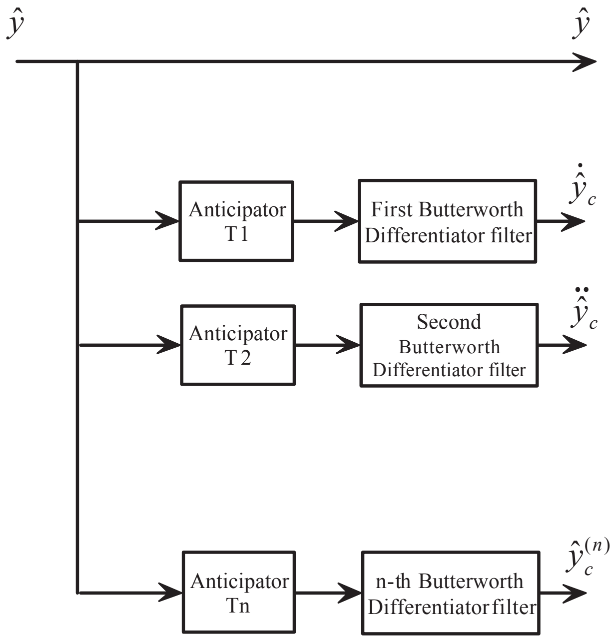


Figure 4.18: Differentiation block.

## 4.6 Application to the tracking of mobile phones

In this section we describe how the proposed results on the design of optimal filters have been utilized for significantly improving the performance in the estimation of the cellphone location. Moreover we present the application of the locationing systems for realizing dynamic maps of urban mobility for the "Real Time Rome" project, developed by the MIT SENSEable City Laboratory.

### 4.6.1 LocHNESs platform

LocHNESs (Localizing and Handling Network Event Systems) is a software platform developed in collaboration with Telecom Italia for the evaluation of statistics, such as real time road traffic estimation, based on the anonymous monitoring of the ME movements. The functional elements that constitute the LocHNESs are presented in Fig. 4.19 and will be described in more detail in the following paragraphs. The LocHNESs platform is based on the localization of events that occur on the mobile network (call in progress, SMS sending, handover, etc.) thanks to the use of external probes. These probes are installed on the Abis interfaces, i.e. the interfaces that link the BTS to the Base Station Controller (BSC). These probes analyze all the signalling messages and send a notification of the detected events. The key data detected by LocHNESs through the Abis interface are MEASurement RESult [2] messages, which are used to report the results of radio channel measurements made by the BTS (uplink measurements) and the measurement reports received by the BTS from the ME (downlink measurements) to the BSC. The MEASurement RESult message contains GSM parameters such as the average signal quality (RXQUAL) as measured by both ME and BTS, the received signal strength (RXLEV) as measured by the BTS (uplink measurement), the received signal strength on the serving BTS and on the neighbouring BTSs as measured by the ME (downlink measurement) and the actual Timing Advance (TA). The MEASurement RESult message related to each active connection (ME in the state "connected") is sent to the BSC every 480 ms, allowing LocHNESs to determine the complete trajectory of the call with the same time resolution. In order to reduce the computational load of the platform, however, the number of events notified to LocHNESs for each call is reduced by the probes according to a fixed sampling ratio (for example 1:10, i.e. with a time resolution of 4.8 s). Using the above data, the LocHNESs platform produces aggregated traffic maps in raster form: the area under analysis is split into a number of contiguous square pixels of varying size (typically 250x250 m in urban areas and 500x500 m in extra-urban areas ). For each pixel the platform estimates a number of parameters, such as the average speed in the four quadrants (North West, North East, South East and South West) of a Cartesian reference system centred in the centre of the pixel, the total average speed, the number of moving users, etc. In order to have real time applications for vehicular traffic these traffic maps are constantly updated with a given periodicity (for instance, every 5 minutes). It is important to note that the LocHNESs platform complies with the 2002 Directive by the European Parliament and Council on privacy . At no time could individual users be identified based on the collected and analyzed data. In this sense, we hope that this project might stimulate a dialogue on the responsible access to locational data and on how it could provide value-added services, such as traffic

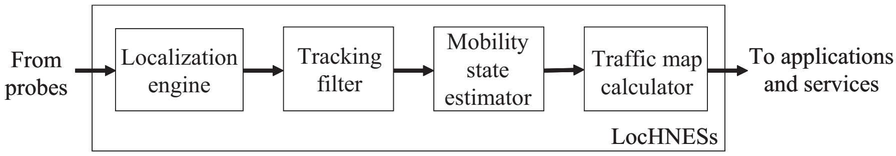


Figure 4.19: Functional structure of the LocHNESs platform.

monitoring, to local and regional communities.

### Localization engine

The Localization engine estimates the instantaneous position of each ME involved in a call using the data extracted from the MEASurement RESult messages, received from the probes. Location is calculated using an Enhanced Cell Id with Timing Advance algorithm (E-CI+TA) [65], named DFL (Data Fit Location); its principal components are the following:

- Network database - it is a database that contains all the parameters coming from the planning and dimensioning process of the entire mobile network (Cell identifiers, i.e. CGI, BSIC and number of BCCH carrier, BTSs latitude, longitude and height, BTS antennas azimuth and tilt, BTS transmission power and losses, etc.);
- Antennas database - it is a database that contains the complete radiation patterns (both in the H and V plane) of all the antennas mounted on the BTSs;
- Propagation model - it allows to calculate the mean received power as a function of different parameters such as the operating frequency, the ME-BTS distance, the ME and BTS heights above the ground, the building density and typology, etc.. The Localization engine, in particular, uses the COST-Hata propagation model, described in [37], which does not require the knowledge of the area morphology and of the building typology with obvious advantages for computational speed.

For each call, the Localization engine, through the probes, receives the signal strength level (RXLEV) measured by the ME on the serving BTS and on a maximum of six adjacent BTSs, the cell identifiers (LAC and CI) of the received BTSs and the actual TA. The DFL algorithm works as follows:

1. through the identifiers received and using the Network database, it obtains the geographic position of the BTSs involved in the measurement;
2. starting from these positions and using the antenna beam widths extracted from the Antennas database, it defines an area in which the ME is supposed to be located with high probability based on simple geometric considerations;
3. it further bounds the search area using the intersection with the TA ring;
4. it identifies a grid in this new search area ;

5. for each point $p$ of the grid, it calculates the mean power received by the ME from every BTS involved in the measurement ($Pc_i(p)$) using the proper parameters of the Network database, the radiation patterns contained in the Antennas database and the propagation model;

6. for each point $p$ of the grid and considering the i-th BTS, it calculates the error function $e_i(p) = Pm_i - Pc_i(p)$, where $Pm_i$ is the power measured by the ME on the i-th BTS;

7. it estimates the ME position $p^*$, finding the point $p$ that minimizes the mean square error

$$\|e(p)\|^2 = \sum_i (Pm_i - Pc_i(p))^2.$$

**Tracking filter**

The Tracking filter estimates the complete trajectory of the MEs, and the related speed, starting from a sequence of punctual localizations received, with the associated time-stamps, from the Localization engine. It consists of the following blocks:

- Sampler - it receives the sequence of ME position estimates, then removes the incorrect localizations (according to an associated numeric code set by the DFL algorithm) and finally resamples the remaining ones with a fixed step;

- Latitude and Longitude Estimators - they are two ad-hoc designed processing systems able to estimate the covered position (and speed) trajectories along the two directions, attenuating the measurement noises. Since the filtering system can work off-line, it is possible to use the approach proposed in Section 4.2 to improve the attenuation of the noise.

  Regarding the position estimation, the processing algorithm used is a combination of two low-pass Butterworth filters. One filter works from the first to the last sample of the locations sequence, and gives a time-delayed estimation of the position trajectory, in order to take into account the delays occurring in the data acquisition, processing and filtering. The other filter works in an analogue way but in the opposite direction (from the last to the first sample of the sequence). The delays of the two filters have been selected according to Table 4.1, and the values of the cut-off bandwidths have been optimally tuned based on training data (with both ME-estimated and GPS locations available, see for instance Fig 4.20). A combination algorithms is used to correctly merge the filtered sequences in order to obtain an estimation of the position trajectory which is homogenous along the whole observation window.

  Regarding speed estimation, a similar processing algorithm is used, but it utilizes a filter composed by an ideal-differentiator and a second-order law-pass filter. This filter allows to both attenuate the noise and differentiate the locations sequence in order to extract the speed trajectory.

- Combiner - it merges the two components to give an estimation on the complete trajectory. As regards the speed trajectory estimation, the result

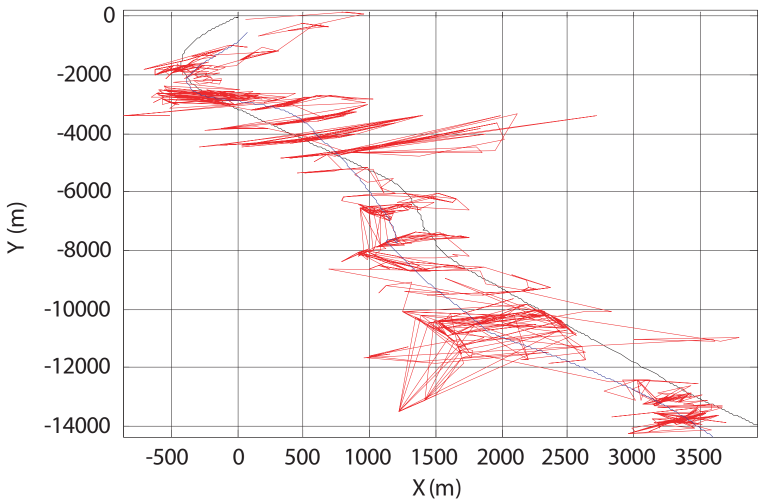


Figure 4.20: Example of trajectory to be estimated (black line). Punctual localizations (red lines) and estimated path (blue line).

is also combined with the output of a first-order low-pass filter which gives another speed estimation, starting from the instantaneous displacements between subsequent samples of the estimated position trajectory.

**Mobility state estimator**

The Mobility state estimator separates the set of calls made by "moving ME" from the set of calls made by "not moving ME" . The adopted algorithm calculates the average ME speed $v_{av}$ in the time interval $T_w$ (said evaluation window) and compares this speed with a reference threshold $v_t$: the ME is evaluated as "moving" if $v_{av} > v_t$. The evaluation window $T_w$ and the threshold speed $v_t$ have been obtained through an empirical analysis with the following considerations:

1. $T_w$ has been obtained minimizing $P(N|M)$, that is the probability of considering as "not moving" a ME who is "moving", whatever is the threshold speed $v_t$;

2. given $T_w$, $v_t$ is obtained minimizing a linear combination of $P(N|M)$ and $P(M|N)$, this last being the probability of estimating as "moving ME" a ME who is "not moving ME", i.e. minimizing the function $wP(N|M) + (1 - w)P(M|N)$, $w \in [0, 1]$.

The minimization of this combination is needed due to the trade-off between these two probabilities, i.e. as $v_t$ increases, $P(N|M)$ increases consequently whereas $P(M|N)$ decreases and vice versa.

Finally, calls lasting less than $T_w$ are discarded, whereas calls lasting more than $nT_w$ (with $n \geq 2$) are considered as they are $n$ different calls making it possible to correctly estimate the mobility state even if it changes during the same call.

**Traffic map calculator**

The Traffic map calculator produces the traffic maps for the entire area monitored by the platform. This is accomplished using the set of calls considered by the Mobility state estimator as made by "moving ME" in the time interval $\Delta T$ that ends when these maps are produced; the value for this interval determines the confidence of the calculated statistics and consequently has to be accurately chosen. Practically it depends on the number of calls it includes and finally on all the parameters linked to the telephone traffic density such as the area type, the time of the day, etc. As previously said, these traffic maps are periodically updated in order to have real time estimations.

As an example, we describe the algorithm used by this module to produce the traffic maps for the average speed:

1. it splits the trajectory of the calls made in the time interval $\Delta T$ among the different pixels where the trajectory is located;

2. it calculates the average ME speed for each share of the trajectory, i.e.

$$v_{ij} = \frac{1}{cardI_{ij}} \sum_{m \in I_{ij}} v_{ijm}, \tag{4.39}$$

   where $i$ identifies the $i$-th pixel, $j$ identifies the $j$-th ME and $I_{ij}$ represents the set of different ME$j$ speed estimations in the $i$-th pixel;

3. it calculates the total average speed value for the $i$-th pixel, i.e.

$$v_i = \frac{1}{cardI_i} \sum_{j \in I_i} v_{ij}, \tag{4.40}$$

   where the set $I_i$ represents the indexes of the ME$j$ located in the $i$-th pixel.

Similarly, the Traffic map calculator obtains the maps of the average speed in each of the four quadrants (North West, North East, South East and South West) of a Cartesian reference system centered in the center of the pixel and the analogous maps of the maximum speeds.

### 4.6.2 Real Time Rome

The Real Time Rome project [25] was developed by the MIT SENSEable City Laboratory for the 10th International Architecture Exhibition of the Venice Biennale in collaboration with the Italian cellphone carrier Telecom Italia. The project aimed at creating an integrated approach to urban monitoring [26], by developing a mobile equipment (ME) location-based monitoring for a whole city - in this case Rome, Italy. The key features of the system are the following:

- it uses high resolution and high definition data over extensive urban areas, whose collection has been made possible by Telecom Italia's innovative LocHNESs (Localizing and Handling Network Event Systems) software platform;

- it monitors a very large portion of the city of Rome over a very complex street network;

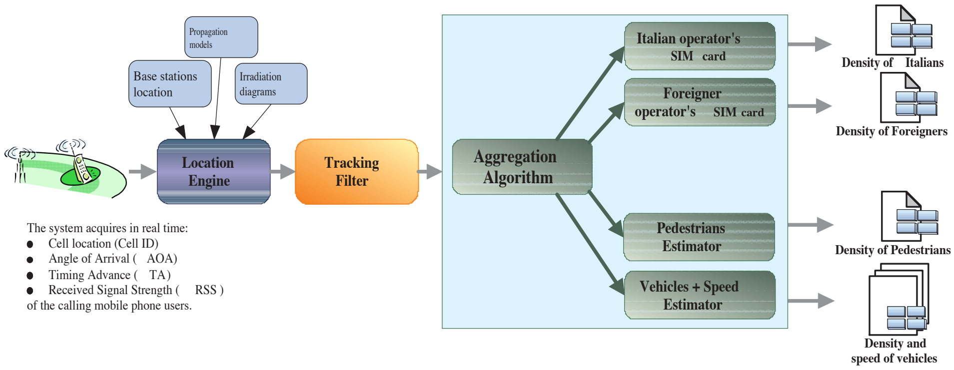


Figure 4.21: Location system.

- it integrates the cellphone data with other type of real time information, such as the position of taxis and buses.

The initial aim of the project was to make a proof of concept for the Venice Biennale and as such focussed more on artistic visualization than on the use of this information in real time in the city. However, this integrated approach seems to open a new way to monitor urban traffic in real time and, more generally, to develop a real-time control system for cities [24].

### LocHNESs data in Rome

Telecom Italia installed the platform LocHNESs and the related probes on a group of BSC located in Rome, covering an area of approximately $100Km^2$ in the north-east of the city. The area was divided into a grid of 250 x 250 m squares and the traffic maps were produced every 5 minutes, as described in section 4.6.1.

Moreover, some ad-hoc algorithms were added to obtain maps related to the number of pedestrians and the number of foreigners. The former was calculated summing the number of MEs estimated to be in each pixel of the grid and considered "not moving MEs" by the Mobility state estimator; the latter was calculated considering the trajectories of those MEs whose IMSI (International Mobile Subscriber Identity) numbers were related to foreigners Mobile Network Operators (see location system Fig. 4.21).

### Voice and data traffic in Rome

A further Telecom Italia server provided the voice and data traffic (expressed in Erlang) served by each of the BTSs located in the urban area of Rome (about 450 directional antennas covering about $47Km^2$). This data was localized and collected with a sampling period of 15 minutes [76].

### System architecture

In this section a description of the system architecture, the data collection, transfer and processing is presented (see Fig. 4.22). Three servers were set up by Telecom Italia , Atac and Samarcanda to provide locational data, both using

SFTP transfer and UDP datagrams transfer. A database was designed and ran on MySQL in the SENSEable City Lab server at MIT, both with some Java applications which collected the data from the externals servers, pre-processed them providing the results to an internal SFTP server.

A description of a more general real time processing platform is given in [27].

Six computers at the Venice Biennale exhibit continuously accessed the SENSEable City Lab FTP server and ran Java software (developed using Processing, and OpenGL) to visualize the different dynamic maps of the city in real-time, using Google maps as background. Furthermore, three computers connected to three audio streaming sources (coming from the three audio sensors installed in Rome) played locational traffic noise in time-synchronization with the visual software.

Among the different visualizations developed for the project, here it is presented the dynamic map of the vehicular traffic, obtained by means of the mobile phone data, processed using the LocHNESs platform. The software in Fig. 4.23 visualizes the locational data of mobile phone callers travelling in vehicles. It focuses on the area around the Stazione Termini and the Grande Raccordo Anulare (Rome's ring road). The software crates a layer on the top of the map, showing 250 x 250 m pixels whose colours are related to vehicle speeds. Red indicated areas where traffic is moving slowly, green shows areas where vehicles is moving quickly. The software also shows an arrow in the centre of the pixel whose direction is the dominant direction of travel and magnitude is proportional to the related speed.

Another interesting visualization developed for the project is the one depicted in Fig. 4.24. This software shows the changing positions of Atac buses and Samarcanda taxis indicated by yellow points, and the relative densities of mobile phone users, represented by the red areas. An algorithm is used to acquire and update the location of buses and taxis in real time. It also estimates buses and taxis paths based on the previous locations, drawing a yellow tail on the map. The algorithm acquires the pedestrian locational data every 5 minutes, showing a red layer on the top of the map (areas colored by a deeper red have a higher density of pedestrians).

## 4.7 Conclusion

In this chapter a new method for the optimal design of filters and control systems and for the evaluation of their performance has been presented. This method is applicable when a delay in the estimation of a signal affected by noise can be tolerated or in case the desired output of the plant to be controlled is known with a certain anticipation.

The new method is based on the minimization of an appropriate quality index, with respect to two design parameters of the filter of the feedback control system, which in part have already need designed with the numerous literature results. As exemplification, considering the class of Butterworth systems, the proposed method has been used to determine some design formulas and to show the obtained consistent improvements.

Different examples of noise filtering and of control for tracking a reference trajectory characterized by a given band have illustrated the advantages of the proposed approach.

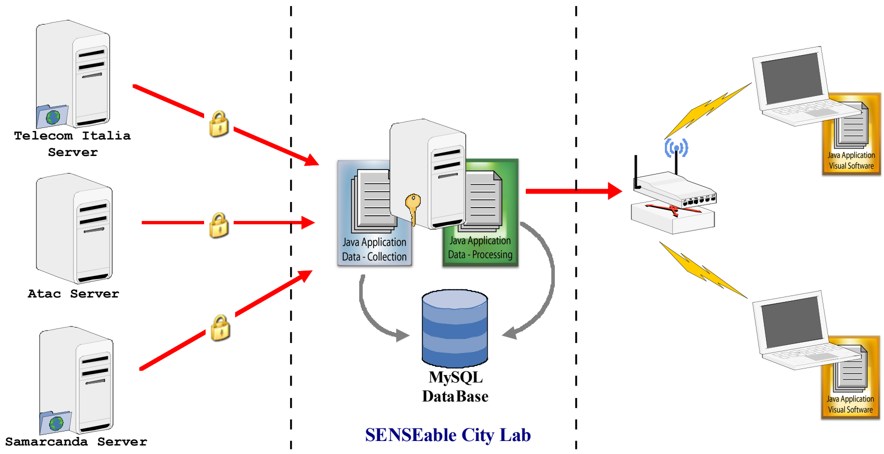


Figure 4.22: Real Time Rome system architecture.

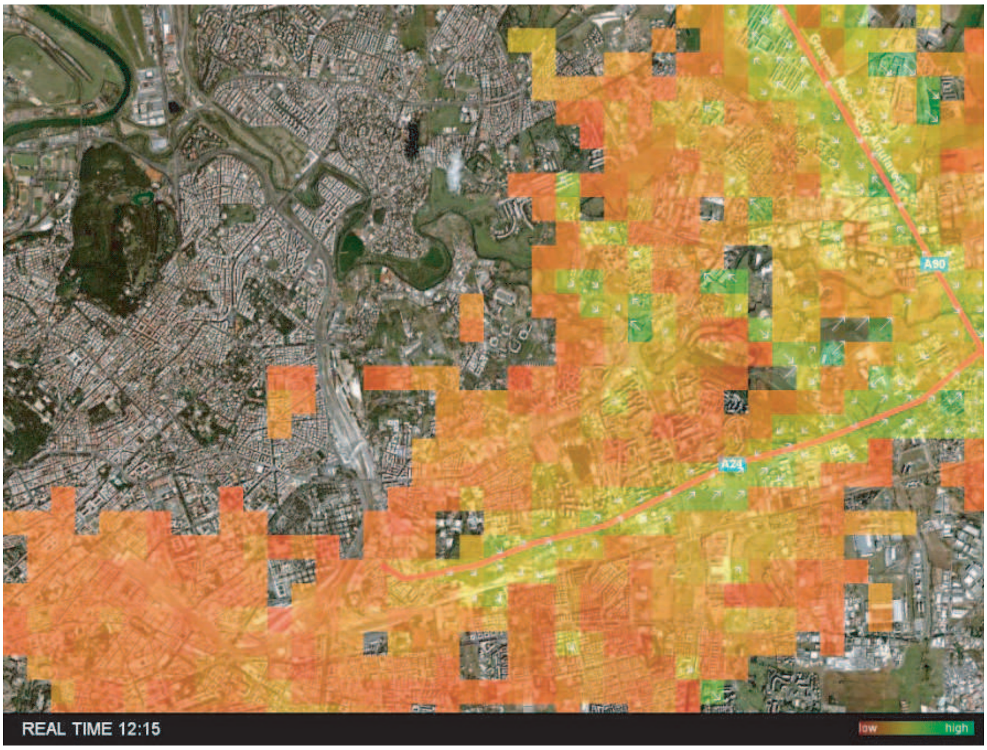


Figure 4.23: Real Time Rome dynamic map: Where is traffic moving?

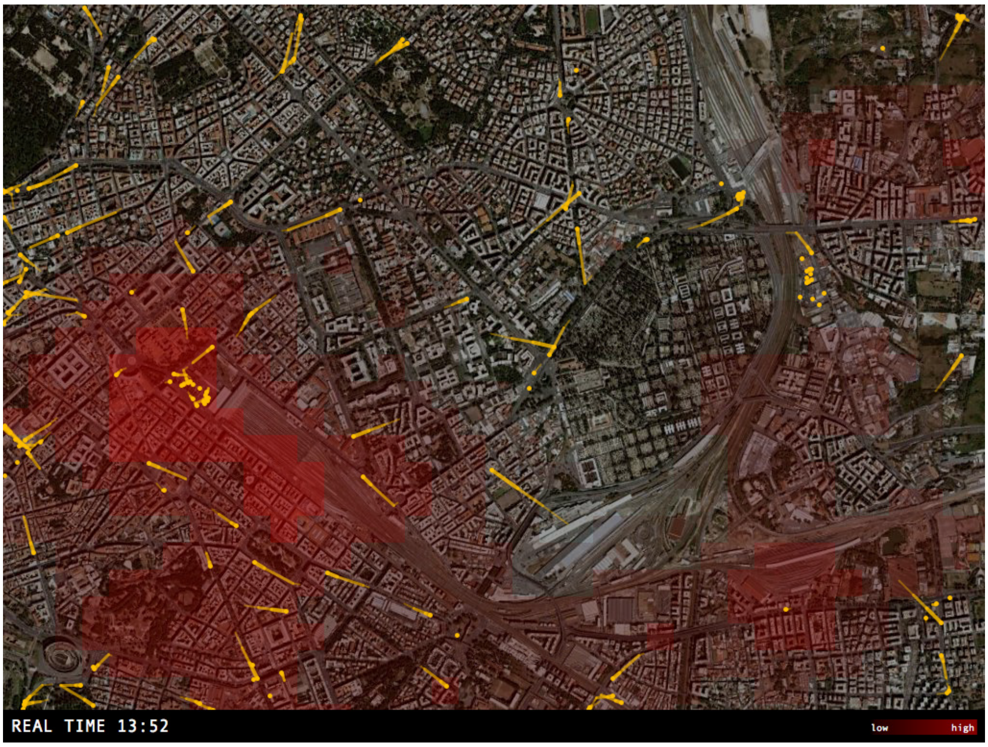


Figure 4.24: Real Time Rome dynamic map: Connectivity: Is public transportation where the people are?

# Chapter 5

# Multi-valued controller implementation and experiments

The chapter deals with the digital realization of the multi-valued control law and the key issues associated with its microprocessor implementation. It presents the realization of a prototypal embedded system, realized through a microprocessor, which implements the control law characterized by a fixed and quantized control set (see Section 3.6). The efficiency of the design method and of the technology utilized for the realization are shown through a very interesting application: a temperature control system of a ceramic kiln.

## 5.1 Introduction

Before the widespread deployment of microprocessor systems, the control laws which were usually utilized for controlling plants were chosen depending on the characteristics of the simple analogical and/or digital circuits which could be used to realize them, limiting the number of design specifications. In the last years, the increasing use of microprocessors in the industrial field has enabled the addiction of further functionalities to the control systems: check control, monitoring and remote communication of the most important process information, improvement of the user interface, chance of setting many operation modes, etc (see [80]; [12] [48]).

In spite of the microprocessors potentialities, the classical PID and relay control laws are still widely used. On the one hand, the wide use of such traditional control laws and the scepticism still now observed with respect to their replacement are mainly due to the well proofed characteristics of simplicity in design (see [98], [94], [71] for some PID tuning techniques, see [87], [47], [32] for some relay controllers synthesis techniques) and to their good efficiency regarding robustness and accuracy. On the other hand, for all the applications characterized by traditional control specifications, the cost-reliability combination offered by these controllers is still valid, so the only notable innovation is their digital implementation.

With the realization of more complex plants and conducing an effort in managing in a more integrated manner: production, security, environmental preservation, etc, it is therefore necessary to introduce new methodologies in the control system design, which make use of more complex, non linear and partially logical control laws. Such methodologies, which consent to obtain improvements in performance and efficiency of the controlled plants, generally require more accurate models of the plants (which require specific knowledge about the process and/or modeling and identification methodologies) and new theoretical results. However, many literature theoretical results are often hardly applicable to solve concrete problems because they refer to unusual plants or because they consider analogical implementations (which are not always realizable at affordable costs).

It follows that in some cases it is important to evaluate if a controller, provided by a promising theory, can be implemented using standard (or standardizable with low cost) hardware/software technologies, without reducing the expected theoretical improvements (see e.g. [8], [93], [56], [36]).

This chapter describes the implementation of the control law proposed in Chapter 3 using an embedded control system, and, with reference to the test case of the ceramic kiln control, presents the performance of the proposed controller compared to other controllers and to the theoretical expectations.

## 5.2 Ceramic kiln control

The ceramic manufacturing process is composed of several steps, among them the ceramic firing, which significantly determines the final characteristics of a ceramic object. Changes in the physical state and the progressive and continuous chemical reactions that fix the final properties of the ceramics take place during the firing process. Consequently, the ceramic firing requires specific temperature trajectories, which depend on the type and thickness of the ware, kiln cross section, kind of coat, paint, etc [14].

A temperature kiln controller is in charge of providing the control signal needed to impose the kiln temperature to track the reference one, respecting some specifications about the tracking error. Such specifications can regard bounds on the error and also its derivatives; the latter thing allows satisfying process vital specifications; in fact, small but fast temperature variations with respect to the reference can generate stress and shock in the fired ceramic objects (see [77]; [66]; [42]). The ability of imposing such constraints characterizes the kiln performance and then the kind of firing processes it is able to handle.

Electrical kilns, like many other power industrial plants, both for constructive simplicity and in order to minimize the operation cost, are commanded by means of relays which activate resistors (heat-ing elements) and ventilation systems (cooling elements) in a discrete way [49]. Two control techniques are usually adopted in such cases. One technique is based on the PID controller whose output defines the duty cycle of a relay control signal, accordingly to a Pulse-Width Modulation (PWM) technique. This controller guarantees a steady state tracking (if it is well designed starting from the plant model knowledge) but needs the control signal to switch every sampling period. Moreover, the available design rules for such controller do not allow to impose constraints both on the tracking error and its derivative, because the reference trajectory generally cannot be approximate with a polynomial. The other adopted solution is based on the classical relay controller, which allows the practical regulation of the plant output to a specific set-point, with switching of the control signal every time the absolute value of the error becomes greater than an acceptable value. This kind of controllers provides good performance only if the plant to be controlled is approximable with a first order system and if the reference is constant [87]. In the kiln case, however, the performance of the whole system mainly depends on the plant, reducing the possibility of imposing strict constraints on the reference trajectory and on the tracking error [32].

Based on the fact that it is quite easy to separately command the available on-off actuators by means of different relays, we can think to use a different type of control law that is able to utilize such further control levels to improve the overall performance. This section presents a new kiln digital controller developed at the Embedded Industrial Microcontrollers Laboratory of the University of Naples Federico II, Italy. The controller is based on an algorithmic law characterized by a control signal which may assume more that two levels (see Chapter 3.7). Such controller allows the practical tracking of the reference trajectory, guaranteeing prefixed maximum limits to the temperature tracking error and its derivative. Like the PID controller, the proposed controller makes use of the plant model knowledge (even if some uncertainties in the knowledge of the parameters is allowed) but it consents to strongly reduce the control signal amplitude and switching frequency because it makes use of more levels and the control signal only switches when the error becomes not tolerable. This thing allows guaranteeing a long life to the actuators and inducting less stress and shock in the manufactured ceramic objects. Moreover, the proposed controller is robust with respect to external disturbances and plant uncertain parameters.

The rest of the chapter is structured as follows. Section 5.3 describes the model of the electric kiln used for the experimentations and the control specifications. The practical tracking problem is then presented. Section 5.4 describes the proposed solution to the control problem. Section 5.5 deals with the development of an embedded controller, based on the proposed solution, to be applied to the electric kiln. The differences between the experimental results obtained using the standard (pre-existent) controller and the new controller are shown in Section 5.6. The reported results clearly prove the advantage in using the new controller, even if only two control levels are used.

## 5.3 Preliminaries

### 5.3.1 Model of the kiln used for the experimentations

Let $u$ [W] be the heating power and $\theta_0$, $\theta_k$, $\theta_e$ [$^o$C] be the temperature of the object internal to the kiln, the kiln and the external environment. A second order firing model is the following

$$\dot{x} = \begin{pmatrix} -\frac{K_o+K_k}{C_k} & \frac{K_o}{C_k} \\ \frac{K_o}{C_o} & -\frac{K_o}{C_o} \end{pmatrix} x + \begin{pmatrix} \frac{1}{C_k} & \frac{K_k}{C_k} \\ 0 & 0 \end{pmatrix} \begin{pmatrix} u \\ \theta_e \end{pmatrix} \tag{5.1}$$

where

- $x = \begin{pmatrix} \theta_k & \theta_o \end{pmatrix}^T$ is the state vector;

- $C_k$ is the kiln thermal capacity;
- $K_k$ is the thermal conductance between kiln and external environment;
- $C_o$ is the object thermal capacity;
- $K_o$ is the thermal conductance between object and kiln.

Results of experimentations on the available electric kiln provided the following values of the plant parameters:

$$C_k = 3000 J/^oC \tag{5.2a}$$
$$K_k = 2.3 W/^oC \tag{5.2b}$$
$$C_o \in [50, 200] J/^oC \tag{5.2c}$$
$$K_o \in [0.5, 2.0] W/^oC. \tag{5.2d}$$

The uncertain parameters are due to different thermal capacities and conductances of the objects which can be inserted into the kiln. There is also a disturbance due to the external environment temperature

$$\theta_e \in [10, 30]^oC. \tag{5.3}$$

### 5.3.2 Desired trajectory

It this section we characterize the family of possible desired temperature trajectories $\hat{\theta}$. The firing process of a tile involves several steps. The first important step is the heating up, characterized by a rate which depends on the thermal conductivity, moisture and gas evolution during drying and material decomposition, quartz transformation, low viscosity liquid phase formation and solid state reactions. The soaking time at maximum temperature depends on the rate of dissolution of crystalline components while controlled cooling is essential to prevent thermal stress being included in the ceramic object [14]. Fig. 5.1 shows an example of firing trajectory. At the beginning there is a growing trend, with 200$^o$C/h thermal gradient, up to 500C. Then there is a reduction of the gradient to 100$^o$C/h between 500 and 600$^o$C in order to allow the compete combustion of a certain quantity of organic substances and the evacuation of all gases, preventing the enamel to start fusing. After this stage, there is a new growing trend, with 160$^o$C/h average thermal gradient, up to 1050$^o$C. The temperature is then held constant for approximately an hour. It follows a quick cooling stage up to 500$^o$C with -220$^o$C/h thermal gradient and a further slower cooling stage, in order to avoid the creation of tensions in the ceramic objects because of the quartz transformation.

### 5.3.3 Control specifications

In order to specify the control requirements, we make use of the concept of tracking error vector:

$$\epsilon = \begin{pmatrix} \epsilon_1 & \epsilon_2 \end{pmatrix}^T, \quad \epsilon_1 = \hat{\theta} - \theta, \quad \epsilon_2 = \dot{\epsilon}_1. \tag{5.4}$$

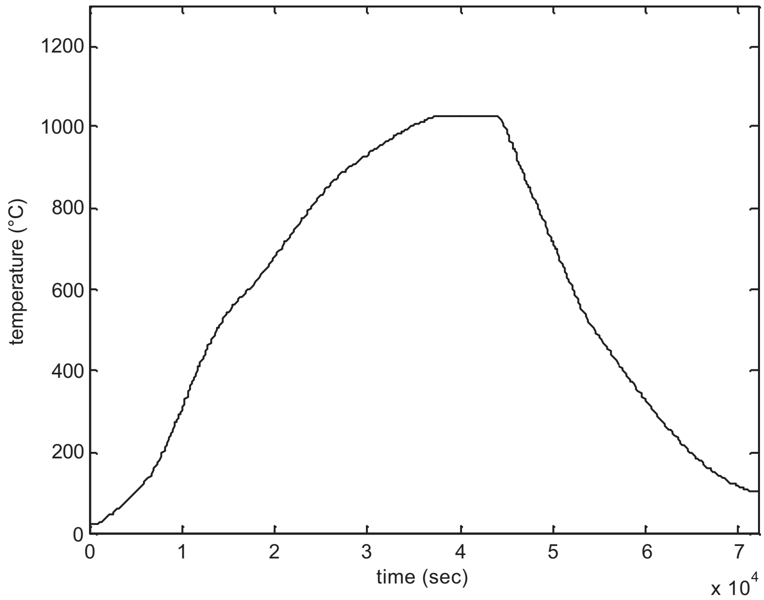


Figure 5.1: Reference trajectory.

Consequently, the tolerable error in tracking the reference trajectory can be specified by two upper bounds

$$\bar{\epsilon}_1 = \max_t |\hat{\theta} - \theta|, \quad \bar{\epsilon}_2 = \max_t |\dot{\hat{\theta}} - \dot{\theta}|. \tag{5.5}$$

Observe that the specification about the maximum value of the temperature velocity error $\epsilon_2$ plays a main role in this application. In fact small but fast temperature variations around $]\hat{\theta} - \bar{\epsilon}_1, \hat{\theta} + \bar{\epsilon}_1[$, especially in the critic stages of the firing process, could create alterations in the ceramic objects, e.g. black core, black bubble, preheating breaks, carbonate decomposition, etc (see [77]; [66]; [42]). In our experimentations we considered the following bounds

$$\bar{\epsilon}_1 = 50^o C, \quad \bar{\epsilon}_2 = 50^o C/h = 0.014^o C/s. \tag{5.6}$$

### 5.3.4 Practical tracking control problem statement

**Problem 4** *Given the plant* (5.1)*, a reference trajectory* $\hat{\theta}(t)\,, t > t_0$*, and a region*

$$T_\rho = \left\{ \epsilon \in \mathbb{R}^2 : \quad |\epsilon_1| \leq \bar{\epsilon}_1, \quad |\epsilon_2| \leq \bar{\epsilon}_2 \right\} \tag{5.7}$$

*of tolerable errors, design a controller, characterized by an actuation signal* $u \in \wp_u$ *that may assume a finite number of levels* $u_- = u_1 < u_2 < \cdots < u_l = u_+$*, which guarantees that*

$$\epsilon \in T_\rho, \quad \forall t > t_0, \quad \forall \epsilon(t_0) \in T_\rho, \tag{5.8}$$

*robustly with respect to the plant uncertain parameters* (5.2) *and disturbance* (5.3)*.*

## 5.4 Control problem solution

To solve the problem, we rewrite the plant model as follows

$$\frac{\ddot{\theta}}{\omega_n^2(p(t))} + \frac{2\zeta(p(t))}{\omega_n(p(t))}\dot{\theta} + \theta = Gu + d(p(t), t), \tag{5.9}$$

where

$$\zeta = \frac{C_k K_o + C_o(K_o + K_k)}{2\sqrt{C_k C_o K_k K_o}} \tag{5.10}$$

$$\omega_n = \sqrt{\frac{K_k K_o}{C_k C_o}} \tag{5.11}$$

$$G = \frac{1}{K_k} \tag{5.12}$$

$$p = \begin{pmatrix} C_o & K_o \end{pmatrix}^T \tag{5.13}$$

$$p \in \wp_p = [50, 200] \times [0.5, 2.0] \tag{5.14}$$

$$d = \theta_e, \quad d \in \wp_d = [10, 30] \tag{5.15}$$

Then, the problem is solved using the following theorem

**Theorem 9** *It is possible to solve the Problem 4*

- *choosing*

$$\rho = \bar{\epsilon}_1\sqrt{2}/2 \quad M = \bar{\epsilon}_2/\bar{\epsilon}_1 \tag{5.16}$$

$$k_1 = M^2 \quad k_2 = \sqrt{2}M \tag{5.17}$$

$$P = \begin{pmatrix} 1 & \frac{\sqrt{2}}{2M} \\ \frac{\sqrt{2}}{2M} & \frac{1}{M^2} \end{pmatrix} \tag{5.18}$$

- *with the following control law*
  - *if* $V = \epsilon^T P \epsilon \geq \rho^2$, $u(t)$ *is equal to:*

$$u = \begin{cases} \lceil U \rceil, & if \quad v \geq 0 \\ \lfloor U \rfloor, & if \quad v < 0 \end{cases} \tag{5.19}$$

*where:*

$$v = B^T P \epsilon, \tag{5.20}$$

$$U = \frac{\ddot{\hat{\theta}} + 2\zeta\omega_n\dot{\hat{\theta}} + \omega_n^2(\hat{\theta} - d) + (k_1 - \omega_n^2)\epsilon_1 + (k_2 - 2\zeta\omega_n)\epsilon_2}{G\omega_n^2} \tag{5.21}$$

$$\lfloor U \rfloor = max\{u \in \wp_u : \ u < U \ \forall p \in \wp_p\} \tag{5.22}$$

$$\lceil U \rceil = min\{u \in \wp_u : \ u \geq U \ \forall p \in \wp_p\} \tag{5.23}$$

  - *if* $V < \rho^2$, $u(t)$ *is equal to the last value assumed on the boundary of* $S_\rho = \{x \in \mathbb{R}^2 : \ V \leq \rho^2\}$.

(5.24)

**Proof 12** *The proof easily derives from Theorem 3.*

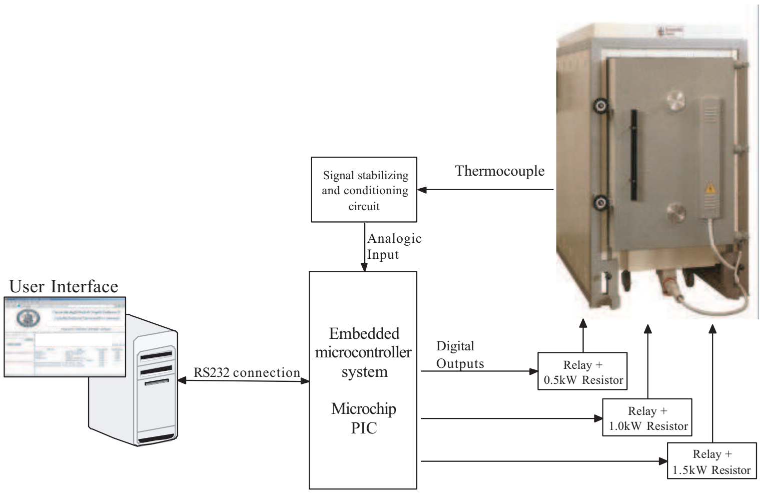


Figure 5.2: Realized feedback control system.

## 5.5 Embedded control system

Based on the proposed solution to the control problem, a feedback control system was developed at the Embedded Industrial Microcontrollers Laboratory of the University of Naples Federico II, Italy. Fig. 5.2 shows a schematics of the implemented control scheme. The key issues involved in the design and implementation of the embedded controller are described in the following subsections.

### Choice of the embedded system

A 8-bit microprocessor Microchip PIC with 20MHz clock, 8K flash program memory (14-bit words), 256B EEPROM data memory, 368B data memory (see [59]) was selected for the development of the embedded system. Such microcontroller is equipped with 10-bit AD converter [58], used for the acquisition of the transduced object temperature. The realized embedded system is shown in Fig. 5.3.

### Choice of the sensors and actuators

The used temperature sensor was a K-type thermocouple, connected to the microcontroller by means of a signal stabilizing and conditioning circuit realized through operational amplifiers.

The actuation part of the control was realized by means of Kanthal resistors, activated by 15A 250V AC relays. The value of the resistors depends on the control requirements and was designed taking into account the rule described in Section 3.5.3.

Based on the chosen reference trajectory and control requirements, we calculated the functions $\max_{p\in\wp_p} \hat{U} + U_{\epsilon,+}$ and $\min_{p\in\wp_p} \hat{U} + U_{\epsilon,-}$ (see Fig. 5.4)

From the figure it results that the needed maximum and mini-mum levels of the control signal can be chosen as $u_+ = 3.0$ KW and $u_- = 0.0$ KW.

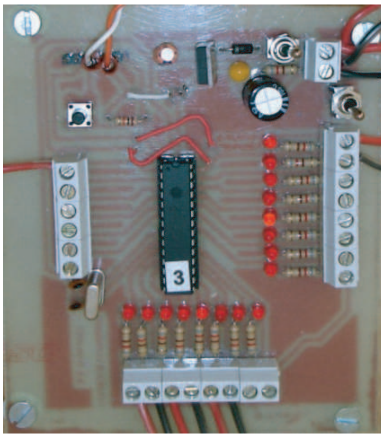

Figure 5.3: Realized embedded system.

We decided to use three heating elements (Kanthal resistors) of powers:

$$0.5\text{KW}\,,1.0\text{KW}\,,1.5\text{KW} \tag{5.25}$$

Such actuators, activated according to suitable combinations, allow obtaining the following seven equal-spaced control levels:

$$\wp_u = \left\{ \begin{array}{ccccccc} 0.0 & 0.5 & 1.0 & 1.5 & 2.0 & 2.5 & 3.0 \end{array} \right\} \text{KW}. \tag{5.26}$$

**Remark 27** *Note that Fig. 5.4 also shows that, for almost all the time, it is more appropriate to use control levels lower than the extreme ones.*

### Implementation of the Control algorithm

A scheme of the control algorithm is presented in Algorithm 1. All the algebraic operations have been implemented using 16 bits, in order to reduce rounding problems. Using the selected hardware, the control algorithm is able to run at a sampling rate up to 1KHz. In the following subsections some technical issues about the algorithm implementation are presented.

### Choice of the sampling period

In order to correctly select the most appropriate sampling period, the following was taken into account.

- If the sampling period of the control algorithm is too big with respect to the dominant time constant of the plant, the delay within which the control switches could cause the temporary escape of $\epsilon$ from $S_\rho$.
- The sampling period must not be chosen too small to avoid unneeded tests, which do not pro-duce switching.

**Algorithm 1** Control algorithm

**Require:** $\wp_u$ {Vector of the control input values}
**Require:** $\bar{\epsilon}_1$, $\bar{\epsilon}_2$ {Tracking error vector specifications}
**Require:** $\zeta$,$\omega_n$,$G$,$\wp_p$,$\wp_d$ {Plant parameters and their uncertainties}
  **calculusControllerParameters**($\bar{\epsilon}_1$,$\bar{\epsilon}_2$, $\rho$, $M$, $P$, $k_1$, $k_2$, $T_c$)
  $iu = 1$ {Index in the vector of the input values $\wp_u$}
  **loop**
    {Execution of the task every Tc seconds}
    **readReference**($\hat{\theta}$, $\dot{\hat{\theta}}$, $\ddot{\hat{\theta}}$) {Read reference trajectory and its derivatives}
    $\theta$=**readOutput**() {Read the actual value of the output variable}
    $\dot{\theta}$=**calculusDerivative**($\theta$, $\theta_{prec}$) {Calculus of the derivative of the output}
    $\epsilon$=**calculusEps**($\theta$,$\dot{\theta}$,$\hat{\theta}$,$\dot{\hat{\theta}}$) {Calculus of the tracking error}
    $V$=**calculusV**($P$,$\epsilon$) {Value of the Lyapunov function}
    **if** $(V - \rho^2) < 0$ **then**
      **continue** {Tracking error internal to the ellipse $S_\rho$}
    **else**
      {Tracking error external to the ellipse $S_\rho$}
      $v$=**calculusv**($B$,$P$,$\epsilon$) {Value of the switching function}
      **calculusU**($\zeta$,$\omega_n$,$G$,$\wp_p$,$\wp_d$ ,$k_1$, $k_2$,$\epsilon$,$\hat{\theta}$, $\dot{\hat{\theta}}$, $\ddot{\hat{\theta}}$, $U_{min}$, $U_{max}$) {Calculus of the two extremes $U_{max}$ and $U_{min}$ of the nominal control, based on the uncertainties}
      **if** $(v >= 0)$ **then**
        {Choice of the admissible control level above $U_{max}$}
        **while** ($iu < length(\wp_u)$ and $\wp_u(iu) < U_{max}$) **do**
          $iu = iu + 1$
        **end while**
      **else**
        {Choice of the admissible control level below $U_{min}$}
        **while** ($iu > 0$ and $\wp_u(iu) > U_{min}$) **do**
          $iu = iu - 1$
        **end while**
      **end if**
      $u$=$\wp_u(iu)$ {Chosen control level}
    **end if**
    $\theta_{prec}$=**savePrevious**($\theta$) {Save the previous values of the output (for the calculus of the derivative)}
  **end loop**

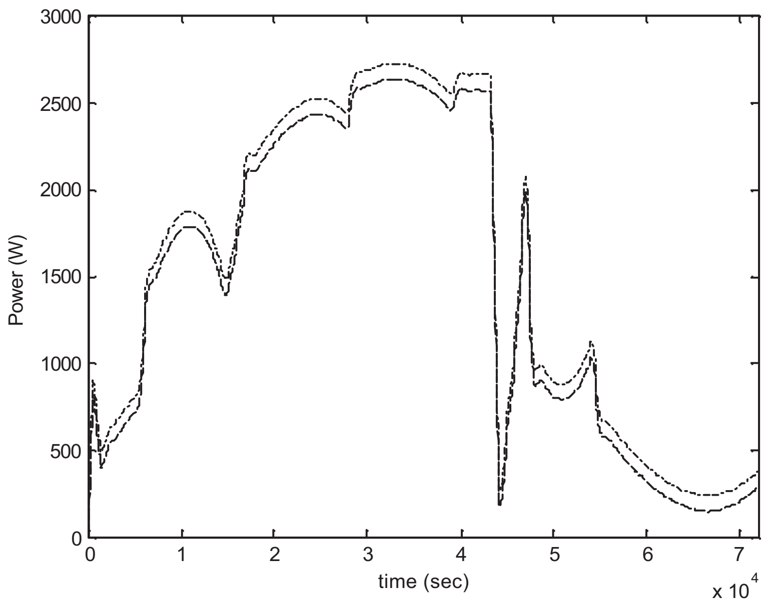


Figure 5.4: Diagram of $\max_{p\in\wp_p} \hat{U} + U_{\epsilon,+}$ and $\min_{p\in\wp_p} \hat{U} + U_{\epsilon,-}$, used for the control levels design.

- There is a strong correlation between the amplitude of the region $T$, the accuracy of the used sensors and the sampling period. Therefore, if small errors are required, it will be necessary to use more accurate sensors and a smaller sampling period.

Based on the above considerations, the control specifications and the kiln's model parameters, an appropriate sampling period was selected to be $T_c = 30$ s.

**Calculus of the reference trajectory's derivatives**

As regards the calculus of the derivatives of the reference trajectory, it can be observed that $\hat{\theta}$ is usually characterized by a bounded band. Then, the output of the Butterworth filter with accessible state and with an appropriate value of $\omega_d \in \mathbb{R}^+$:

$$\dot{x} = \begin{pmatrix} 0 & 1 & 0 \\ 0 & 0 & 1 \\ -\omega_d^3 & -2\omega_d^2 & -2\omega_d \end{pmatrix} x + \begin{pmatrix} 0 \\ 0 \\ \omega_d^3 \end{pmatrix} \hat{\theta} \tag{5.27}$$

$$\theta_d = \begin{pmatrix} 1 & 0 & 0 \\ 0 & 1 & 0 \\ 0 & 0 & 1 \end{pmatrix} x \tag{5.28}$$

can be used to practically provide $\hat{\theta}, \dot{\hat{\theta}}$ and $\ddot{\hat{\theta}}$. In the case of the trajectory of Fig. 5.1, a good choice of $\omega_d$ is 0.004rad/s.

### Calculus of $\dot{\theta}$

The control algorithm requires the knowledge of $\dot{\theta}$. Because a sensor able to measure $\dot{\theta}$ was unavailable, its value is calculated through a numeric derivative algorithm, with 10 s sample step, which appropriately uses the three previous samples and the current one.

### User interface

A RS232 serial interface was added to the microcontroller in order to upload the plant parameters, control specifications and reference trajectory into the microprocessor. The interface allows to connect the embedded system to a PC where such information can be edited. Moreover, the microcontroller is also used for monitoring and storing the firing process information.

## 5.6 Experimental results

This section describes the results of some experimental tests performed applying the prototypal controller to the available electric kiln.

### Test 1

The reference trajectory of Fig. 5.1 was applied. Figs. 5.5 and 5.6 show the measured object temperature and the errors $\epsilon_1$ and $\epsilon_2$ obtained using the designed controller. Moreover, Fig. 5.7 shows the control signal. The depicted experimental results show that the performance of the prototyped controller meet pretty well the theoretical expectations in terms of accuracy and robustness.

### Test 2

In case of firing of a large number of similar objects, it would be appropriate to plan a preliminary identification procedure of the plant uncertain parameters. In such a case it is possible to obtain a reduction of the amplitude and the switching frequency of the control signal (see (5.19)). To illustrate this fact, Fig. 5.8 shows the control signal in case:

$$\wp_p = [70,\ 120] \times [0.6,\ 1] \tag{5.29}$$

The use of more control levels and a reduction of the total switching number from 83 to 50 can be clearly observed.

### Test 3

It the following a comparison between the results obtained utilizing the proposed and the relay controller (with hysteresis $\bar{\epsilon}_1 = 50\text{C}$), if only the extreme levels

$$\wp_u = \left\{ \begin{array}{cc} 0.0 & 3.0 \end{array} \right\} \text{KW} \tag{5.30}$$

are available, is reported. As it can be noted (see Figs. 5.9, 5.10 and 5.11) the performance of the relay controller are worsen and the error is hardly ever inside the admissible region $T$. This is due to the fact that, as it is well known,

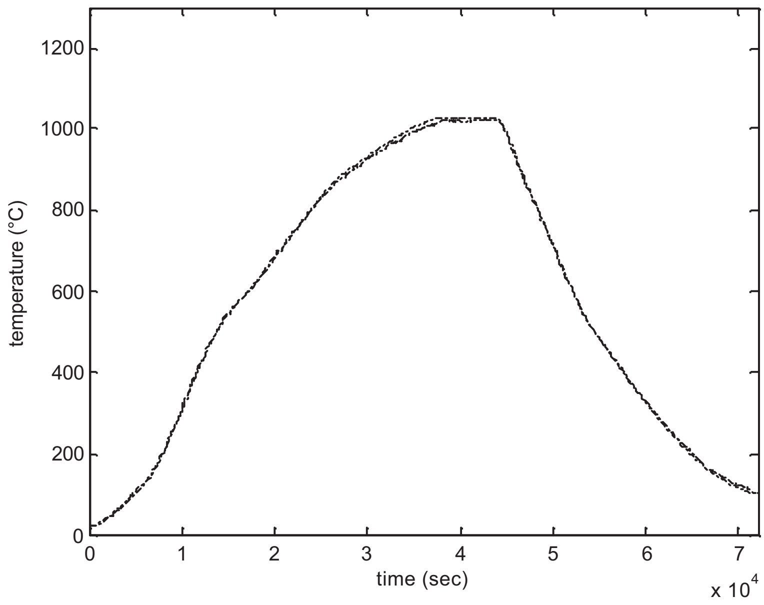


Figure 5.5: Reference trajectory (dashed line) and effective temperature obtained using the proposed controller (solid line), considering the control levels (5.26).

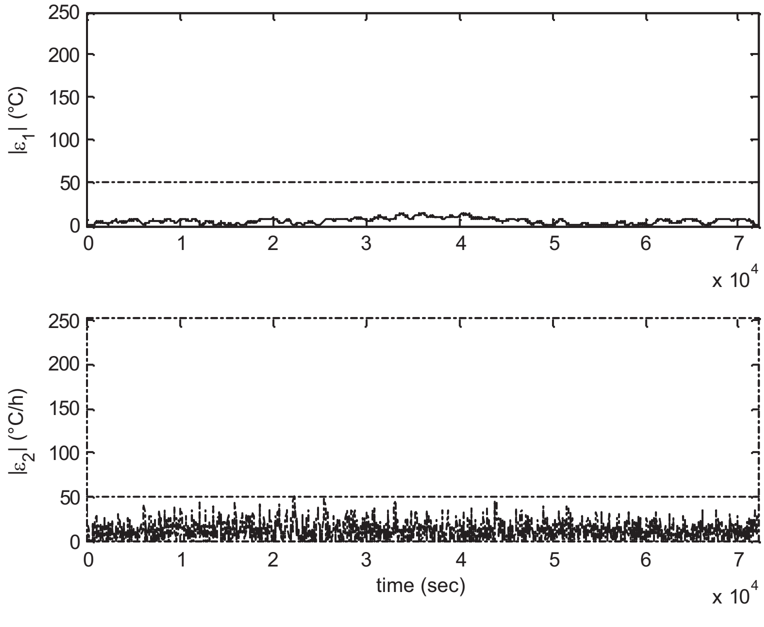


Figure 5.6: Obtained tracking error and its derivative (solid lines) and their maximum tolerable values (dash-dotted lines), considering the control levels (5.26).

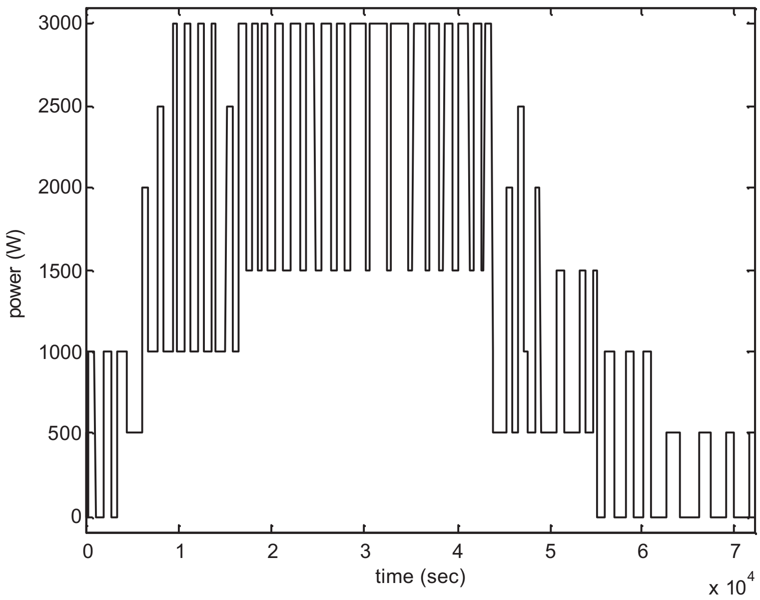


Figure 5.7: Applied multi-valued control signal in case of uncertainties (5.2), considering the control levels (5.26).

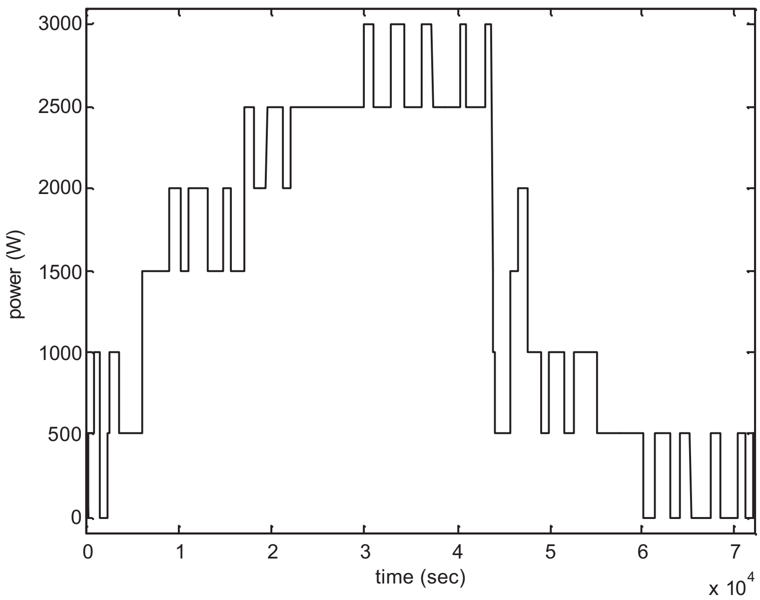


Figure 5.8: Applied multi-valued control signal in case of uncertainties (5.29), considering the control levels (5.26).

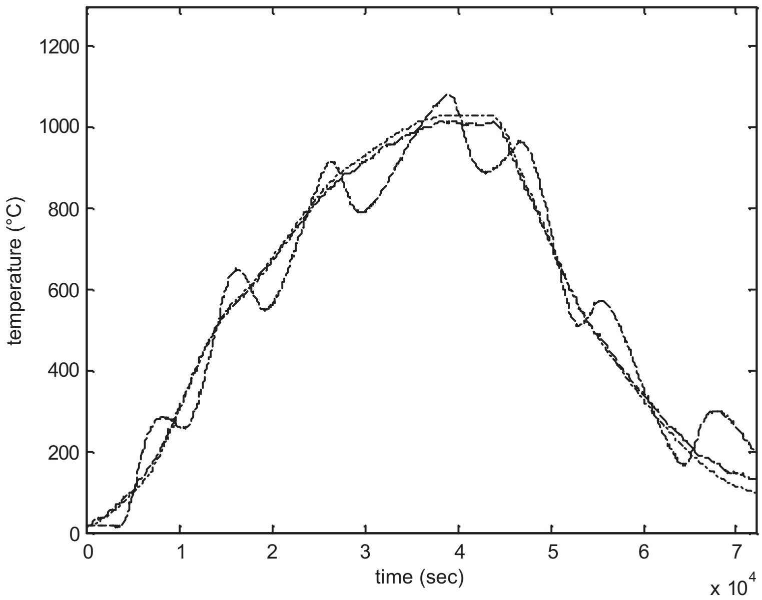


Figure 5.9: Reference trajectory (dash-dotted line) and effective temperatures utilizing the relay controller (dashed line) and the proposed controller (solid line), considering the control levels (5.30).

the relay controller guarantees good performance only if the plant can be approximated with a first order system. On the contrary, the proposed controller allows respecting the control specifications (5.6) also using only two control levels (5.30).

## 5.7 Conclusion

In this chapter the design of an embedded system which implements a new multi-valued controller for ceramic kilns has been presented. The key issues regarding the digital realization, in particular, the choice of actuators, sensors and the control algorithm implementation have been discussed. Numerous experimental results on an available electric kiln have shown the substantive advantage of the proposed solution with respect to the relay controller. Besides, important reductions in the switching number can be obtained using the proposed controller and many control levels. The proposed controller can easily be generalized to be used in different applications where a decisional control is required.

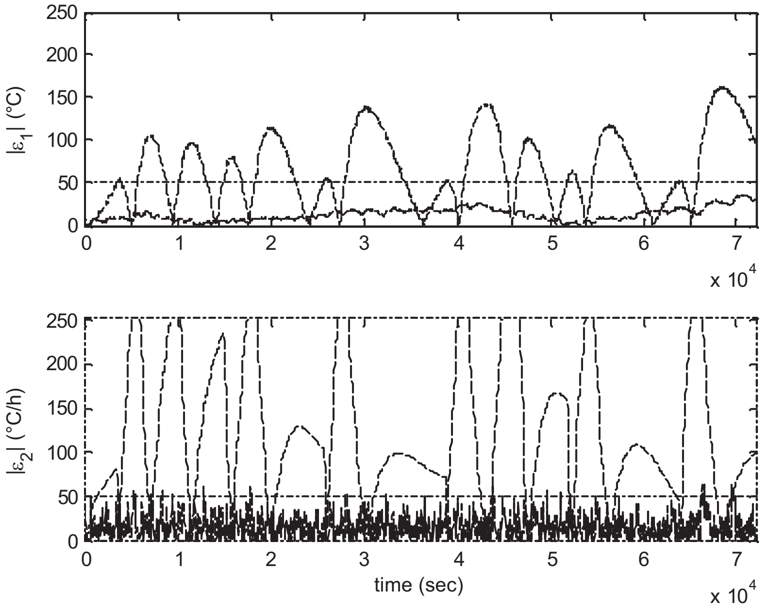


Figure 5.10: Tracking error and its derivative utilizing the relay controller (dashed line) and the proposed controller (solid lines), considering the control levels (5.30). Maximum tolerable values (dash-dotted lines) .

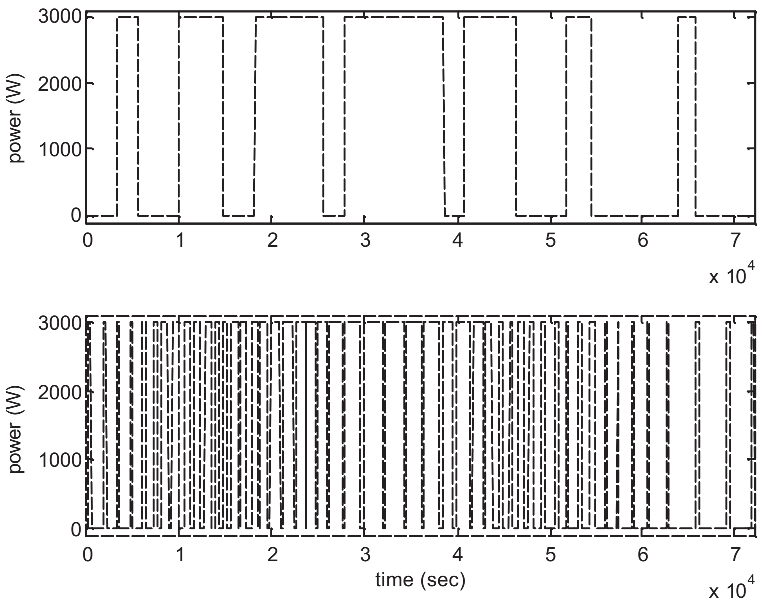


Figure 5.11: Applied control signals utilizing the relay controller (dashed line) and the proposed controller (solid line), considering the control levels (5.30).

# Chapter 6

# Conclusions and Discussion

Multi-valued control systems have been considered in this thesis and topics concerning analysis, design and implementation issues have been studied. It only remains to summerize, and give some concluding remarks from a retrospective viewpoint together with topics for future research.

### Summary

A variety of plants with high parametric uncertainties are usually controlled with signals that may assume only a finite number of values, in order to simplify actuator's construction and minimize the operation cost. This thesis has dealt with the problems concerning the multi-valued control laws, ranging from the analysis, to the design and implementation issues.

New design technique have been developed, based on the concept of practical stability, which refers to the behavior of the system over a finite time interval and which requires the state of such system, given some initial conditions, to remain within prescribed bounds in that time interval. The thesis has analyzed the two classes of problems arising in this framework: finite-time stability and practical stability. The finite-time stability (FTS) problem has been presented in Section 2.2, and two approaches have been discussed for the analysis of FTS of a linear continuous system, respectivelly based on quadratic Lyapunov functions and polyhedral Lyapunov functions. The practical stability problem has instead been presented in Section 2.3.

The second chapter has also analyzed the discontinuous control systems, and in particular the problem arising in the definition of solutions to discontinuous right hand side differential equations.

Chapter 3 has proposed a novel method for the design of controllers that allow to solve the practical stability problem. The proposed controller is robust with respect to the plant's uncertain parameters and disturbances, and guarantees to follow the reference trajectory with prefixed values of the tracking error and of its derivatives until $n-1$, where $n$ is the order of the plant.

The case when the control input set is quantized has been treated in Section 3.6 and several examples have been discussed.

Chapter 4 has dealt with the problem of defining the optimal structure of a filter, when it is supposed that a certain delay in the estimation is tolerable.

The main contribution has been the formulation of an optimal filter design problem, and its application to the class of Butterworth filters. The proposed theory has then been applied to design the optimal differentiation system which provides the derivatives of the reference trajectory for the implementation of the multi-valued control law of Section 3.6.

The theory presented in the forth chapter has also been investigated to design optimal control systems for tracking reference signals, known with a certain advance, providing that an appropriate pre-processing system can be applied to the reference trajectory.

Finally, the application of the optimal filters to the estimation of the trajectory of mobile phone users has been presented in Section 4.6, with reference to the collaboration with Telecom Italia Lab and the Massachusetts Institute of Technology SENSEable City Laboratory and the test bed deployed in the city of Rome.

The digital realization of the new multi-valued control law has been addressed in Chapter 5 and all the key issues associated with its microprocessor implementation have been discussed. The efficiency of the design method and of the technology utilized for the realization have been shown through the application of the developed embedded control system at the problem of temperature control in a ceramic kiln.

**Remarks and future research**

There are many interesting problems and open questions about multi-valued control systems beyond the scope of this thesis. Some remarks together with subjects for future research closely related to the topics in this thesis will briefly be given in the following.

The Theorem 5 in Chapter 3 allows tuning the control parameters in case it is required to bound the error and its derivative. It is interesting to note that the convergence time also depends on the location of the eigenvalues of $E$ in the complex plane, and can almost independently be chosen. Conversely, if the convergence time is not important for the application, the degree of freedom left in the definition of location of the eigenvalues on $E$ in the complex plane can be used to impose a bound on the second derivative of the tracking error, in case the plant has order greater than three.

The theory proposed in Chapter 3 can potentially be extended to a wider class of systems. In order to generalize the synthesis technique proposed in Chapter 3 to the case of multivariable systems, the effect of the different input signals on the outputs must be accurately taken into account, because of the coupling effects. Considering, instead, discrete-time systems (digitalized plants), it must be taken into account that the sampling period plays a crucial role. In fact it constraints the dimension of the domain of admissible errors, since, if it is not well defined, could cause the tracking error escaping the domain during a sampling period and not allowing the control signal to avoid it.

Since an identification of the plant is needed in order to tune the control parameters (even if some uncertainties are tolerated), it would be interesting to evaluate the possibility to implement an on-line identification procedure and analyze how the pair controller-identificator behaves in terms of stability and performance of the closed loop system. In general, having an accurate knowledge of the plant helps the control algorithm in the choice of the control signal, that, as pointed out in Section 3.6, allows reducing the average switching frequency and the power peaks.

I look forward to tackle the above problems in the future.

# Bibliography


[1] *Optimization Toolbox 3, User's Guide.* The Mathworks, Inc., Natick, MA, 2007.

[2] 3GPP TS 08.58. 3rd generation partnership project; technical specification group gsm edge radio access network; base station controller - base transceiver station (bsc - bts) interface; layer 3 specification (release 1999).

[3] A. Alkhairy. Design of optimal iir filters with arbitrary magnitude. *IEEE Transactions on Circuits and Systems II: Analog and Digital Signal Processing*, 42(9):618–620, 1995.

[4] F. Amato, R. Ambrosino, M. Ariola, and F. Calabrese. Finite-time stability of linear systems: An approach based on polyhedral lyapunov functions. In *46th IEEE Conference on Decision and Control*, 2007.

[5] F. Amato, M. Ariola, and C. Cosentino. Finite-Time Stabilization via Dynamic Output Feedback. *Automatica*, 42:337–342, 2006.

[6] F. Amato, M. Ariola, and P. Dorato. Finite-time control of linear systems subject to parametric uncertainities and disturbances. *Automatica*, 37:1459–1463, 2001.

[7] F. Amato, A. Caruso, F. Garofalo, and L. Glielmo. Robust Polyhedral Stability Via Extreme Points Results. In *Proc. $32^{nd}$ Allerton Conference*, pages 89–95, Monticello, IL, 1995.

[8] G. Ambrosino, G. Celentano, and F. Garofalo. Microprocessor implementation of a robust control law for industrial robots. *International Journal of Modelling and Simulation*, 4(4):141–144, 1984.

[9] B.D.O. Anderson and J.B. Moore. *Optimal Filtering.* Englewood Cliffs, NJ: Prentice-Hall, 1979.

[10] B.D.O. Anderson and J.B. Moore. *Optimal Control, Linear Quadratic Methods.* Prentice Hall, 1990.

[11] F. Argenti and E. Del Re. Design of iir eigenfilters with arbitrary magnitude frequency response. In *IEEE Int. Conf. on Acoustics, Speech and Signal Processing*, volume 3, pages 1265–1268, 1998.

[12] A. S. Berger. *Embedded Systems Design: An Introduction to Processes, Tools and Techniques.* CMP Books, 2001.

[13] P.A. Bernhardt. Simplified design of high-order recursive group-delay filters. *IEEE Transactions on Acoustics, Speech, and Signal Processing*, ASSP-28(5):498–503, 1980.

[14] A. Bhattacharya. Optimization of firing parameters for ceramic wares by thermal analysis. *Journal of Thermal Analysis*, 49:1365–1371, 1997.

[15] A. Bicchi, A. Marigo, and B. Piccoli. On the reachability of quantized control systems. *IEEE Transactions on Autom. Control*, 47(4):546–563, 2002.

[16] F. Blanchini. Nonquadratic lyapunov functions for robust control. *Automatica*, 31(3):451–461, March 1995.

[17] R. W. Brockett and D. Leberzon. Quantized feedback stabilization of linear systems. *IEEE Transactions on Autom. Control*, 45(7):1279–1289, 2000.

[18] S. Butterworth. On the theory of filter amplifiers. *Wireless Engineer*, (7):536–541, 1930.

[19] F. Calabrese and G. Celentano. Optimal design of robust control systems with large band reference signals. In *Eurocon 2005 - The International Conference on "Computer as a tool"*, 2005.

[20] F. Calabrese and G. Celentano. Optimal design of filters with delayed estimation and controllers with anticipated reference. Technical report, University of Naples "Federico II", Italy, 2006.

[21] F. Calabrese and G. Celentano. Practical tracking via finite-valued control for uncertain siso plants. Technical report, University of Naples "Federico II", 2006.

[22] F. Calabrese and G. Celentano. Design and realization of a step-nc compliant cnc embedded controller. In *12th IEEE Conference on Emerging Technologies and Factory Automation*, 2007.

[23] F. Calabrese and G. Celentano. A new multi-valued control law for ceramic kilns. In *IEEE International Symposium on Industrial Electronics, submitted*, 2007.

[24] F. Calabrese, K. Kloeckl, and C. Ratti. Wikicity: real-time location-sensitive tools for the city. *IEEE Pervasive Computing*, 2007.

[25] F. Calabrese and C. Ratti. Real time rome. *Networks and Communications Studies*, 2006.

[26] F. Calabrese, C. Ratti, M. Colonna, P. Lovisolo, and D. Parata. A system for real-time monitoring of urban mobility: a case study in rome. *IEEE Communications Magazine, submitted*, 2007.

[27] F. Calabrese, B. Resch, and C. Ratti. An approach towards a real-time data exchange platform system architecture. In *Sixth Annual IEEE International Conference on Pervasive Computing and Communications*, 2008.

[28] G. Celentano. Modal synthesis of multivariable systems with observers of specified order. *Systems and Control Letters*, (3), 1983.

[29] G. Celentano and A. Balestrino. New techniques for the design of observers. *IEEE Transactions on Autom. Control*, (11), 1984.

[30] G. Celentano, F. Garofalo, and L. Glielmo. Stability robustness of interval matrices via Lyapunov quadratic forms. *WSEAS Transactions on Systems*, 38:281–284, 1993.

[31] G. Celentano and R. Iervolino. Finite-valued control law synthesis for nonlinear uncertain systems. In *Proc. IFAC 15th Triennal World Congress*, Barcelona, Spain, 2002.

[32] G. Celentano and R. Iervolino. Finite-valued control design. *WSEAS Transactions on Systems*, 3:2011–2016, 2004.

[33] T. Cooklev and A. Nishihara. Maximally flat fir filters. In *IEEE Int. Symp. Circuits Syst. (ISCAS)*, 1993.

[34] M.J. Corless and G. Leitmann. Continuous state feedback guaranteeing uniform ultimate boundedness for uncertain dynamic systems. *IEEE Transactions on Autom. Control*, 26:1139–1144, 1981.

[35] S. Crisafulli, J. D. Mills, and R. R. Bitmead. Kalman filtering techniques in speech coding. In *ICASSP*, volume 1, 1992.

[36] P. Crnosija, B. Kuzmanovic, and S. Ajdukovic. Microcomputer implementation of optimal algo-rithms for closed-loop control of hybrid stepper motor drives. *IEEE Trans. Industrial Electronics*, 47(6):1319–1325, 2000.

[37] E. Damosso. Digital mobile radio towards future generation systems. Technical report, COST 231 Final Report, 1998.

[38] L. Debnath and P. Mikusinski. *Introduction to Hilbert Spaces with Applications*. Academic Press, 1990.

[39] D. F. Delchamps. Stabilizing a linear system with quantized state feedback. *IEEE Transactions on Autom. Control*, 33(8):916–924, 1990.

[40] P. Dorato. Short time stability in linear time-varying systems. In *Proc. IRE International Convention Record Part 4*, pages 83–87, 1961.

[41] N. Elia and S. K. Mitter. Stabilization of linear systems with limited information. *IEEE Transactions on Autom. Control*, 46(7):1384–1400, 2001.

[42] X. Elias. The formation and consequences of black core in ceramic ware. *Interceram*, 29(3):380, 1980.

[43] F. Fagnani and S. Zampieri. Stability analysis and synthesis for scalar linear systems with a quantized feedback. *IEEE Transactions on Autom. Control*, 48(9):1569–1584, 2003.

[44] F. Fagnani and S. Zampieri. Quantized stabilization of linear systems: complexity versus performance. *IEEE Transactions on Autom. Control*, 49(9):1534–1548, 2004.

[45] A. Farooq and D.J. Limebeer. Path following of optimal trajectories using preview control. In *IEEE Conference on Decision and Control*, 2005.

[46] A. F. Filippov. *Differential Equations with Discontinuous Righthand Sides.* Kluwer Academic Publishers, 1988.

[47] I. Flugge-Lotz. *Discontinuous automatic control.* Princeton University Press, Princeton, NJ, 1953.

[48] M. Frankowiak, R. Grosvenor, and P. Prickett. A review of the evolution of microcontroller-based machine and process monitoring. *International Journal of Machine Tools and Manufacture*, 45:573–582, 2005.

[49] H. Fraser. *The Electric Kiln.* University of Pennsylvania Press, Pennsylvania, 2000.

[50] P. Gahinet, A. Nemirovski, A. J. Laub, and M. Chilali. *LMI Control Toolbox.* The Mathworks Inc, Natick, MA, 1995.

[51] F. R. Gantmacher. *The theory of matrices, Vol. I.* Chelsea, New York, 1959.

[52] R.A. Gopinath. Lowpass delay filters with flat magnitude and group delay constraints. *IEEE Transactions on Signal Processing*, 51(1):182–192, 2003.

[53] M.J. Grimble. $H^\infty$ fixed-lag smoothing filter for scalar systems. *IEEE Transactions on Signal Processing*, 39(9), 1991.

[54] L. Xie H. Zhang and Y.C. Soh. $H^\infty$ deconvolution filtering, prediction, and smoothing: a krein space polynomial approach. *IEEE Transactions on Signal Processing*, 48(3):888–892, 2000.

[55] W. Hahn. *Stability of Motion.* Springer Verlag, Berlin, 1967.

[56] D. He and R.M. Nelms. Fuzzy logic average current-mode control for DC-DC converters using an inexpensive 8-bit microcontroller. *IEEE Trans. Industry Applications*, 41(6):1531–1538, 2005.

[57] J. M. Hollerbach. Dynamic scaling of manipulators trajectories. *ASME J. Dynamic Systems, Measurement, and Control*, 106:102–106, 1984.

[58] Microchip Technology Inc. 10-bit A/D Converter PICmicro Mid-Range MCU Family - Application Notes. 1997.

[59] Microchip Technology Inc. 8-bit CMOS Microcontrollers, PIC16F876 Datasheet. 2003.

[60] U. Itkis. *Control systems of variable structure.* Wiley, New York, 1976.

[61] H. Katoh. $H^\infty$ optimal preview controller and its performance limit. *IEEE Transactions on Autom. Control*, 49(11), 2004.

[62] T. Kobayashi and S. Imai. Design of iir digital filters with arbitrary log magnitude function by wls techniques. *IEEE Transactions on Acoustics, Speech, and Signal Processing*, 38(2):247–252, 1990.

[63] A. Kojima and S. Ishijima. Lq preview synthesis: optimal control and worst case analysis. *IEEE Transactions on Autom. Control*, 44(2):352–357, 1999.

[64] A. Kojima and S. Ishijima. $H^{\infty}$ performance of preview control systems. *Automatica*, 39(4):693–701, 2003.

[65] A. Kupper. *Location-based Services - Fundamentals and Operation*. John Wiley and Sons Ltd, 2005.

[66] J.R. Leigh. *Temperature Measurement and Control*. IET, 1988.

[67] L. Mianzo and H. Peng. A unified framework for lq and $h^{\infty}$ preview control algorithms. In *IEEE Conference on Decision and Control*, 1998.

[68] L. Mirkin. On the $h^{\infty}$ fixed-lag smoothing: how to exploit the information preview. *Automatica*, pages 1495–1504, 2003.

[69] S. Nikitin. Piecewise smooth stabilizing extension. In *Proc. 2nd European Control Conference*, Groningen, The Netherlands, 1993.

[70] S. Nikitin. *Global controllability and stabilization of nonlinear systems*. World Scientific Publishing Co. Pte Ltd, 1994.

[71] J.J.E. Oviedo, T. Boelen, and P. van Overschee. Robust advanced PID control (RaPID): PID tuning based on engineering specifications. *IEEE Control Systems Magazine*, 26(1):15–19, 2006.

[72] L.D. Paarmann. *Design and Analysis of Analog Filters: A Signal Processing Perspective*. Springer, 2001.

[73] B. Picasso, F. Gouaisbaut, and A. Bicchi. Construction of invariant and attractive sets for quantized-input linear systems. In *Proc. Conf. Decision Control*, pages 824–829, Las Vegas, NV, 2002.

[74] S.R. Powell and P.M. Chau. A technique for realizing linear phase iir filters. *IEEE Transactions on Signal Processing*, 39, 1991.

[75] L.R. Rabiner and B. Gold. *Theory and Application of Digital Signal Processing*. Englewood Cliffs NJ:Prentice-Hall, 1975.

[76] J. Reades, F. Calabrese, A. Sevtsuk, and C. Ratti. Cellular census: Explorations in urban data collection. *IEEE Pervasive Computing*, 2007.

[77] G. Bickley Remmey. *Firing Ceramics*. World Scientific, 1997.

[78] R. T. Rockafellar. *Convex Analysis*. Princeton University Press, Princeton, NJ, 1972.

[79] S. H. Roh and Y. Park. Stochastic optimal preview control of an active vehicle suspension. *Journal of Sound and Vibration*, 220(2):313–330, 1999.

[80] A. Sangiovanni-Vincentelli and J. Sifakis. *Embedded Software*. Springer, 2002.

[81] I.W. Selesnick and C.S. Burrus. Maximally-flat lowpass fir filters with reduced delay. *IEEE Transactions on Circuits and Systems II: Analog and Digital Signal Processing*, 45, 1998.

[82] U. Shaker and C.E. de Souza. Continuous-time tracking problems in a $h^\infty$ setting: A game theory approach. *IEEE Transactions on Autom. Control*, 40(5):841–852, 1995.

[83] S.M. Shinners. *Modern Control System Theory and Design.* Wiley-IEEE, 1998.

[84] G. Tadmor and L. Mirkin. $H^\infty$ control and estimation with preview-part i: matrix are solutions in continuous time. *IEEE Transactions on Autom. Control*, 50(1):19–28, 2005.

[85] K. Takaba. A tutorial on preview control systems. In *SICE Annual Conference in Fukui*, 2003.

[86] M. Tomizuka. Optimal continuous finite preview problem. *IEEE Transactions on Autom. Control*, 20(6):362–265, 1975.

[87] Y.Z. Tsypkin. *Relay control systems.* Cambridge University Press, Cambridge, UK, 1984.

[88] V. I. Utkin. Variable structure systems with sliding modes. *IEEE Transactions on Autom. Control*, 22:212–222, 1977.

[89] V. I. Utkin. *Sliding modes in optimisation and control.* Springer-Verlag, New York, 1992.

[90] editor W. S. Levine. *The Control Handbook.* CRC Press, 1996.

[91] L. Weiss and E. F. Infante. Finite time stability under perturbing forces and on product spaces. *IEEE Trans. Auto. Contr.*, 12:54–59, 1967.

[92] S. Winder. *Analog and Digital Filter Design.* Newnes, 2002.

[93] J.X. Xu, H. Hashimoto, J.J.E. Slotine, Y. Arai, and F. Harashima. Implementation of VSS control to robotic manipulators-smoothing modification. *IEEE Trans. Industrial Electronics*, 36(3):321–329, 1989.

[94] Li Yun, Kiam Heong Ang, and G.C.Y. Chong. PID control system analysis and design. *IEEE Control Systems Magazine*, 26(1):32–41, 2006.

[95] H. Zhang, X. Lu, and D. Cheng. Optimal estimation for continuous-time systems with delayed measurements. *IEEE Transactions on Autom. Control*, 51(5):823–827, 2006.

[96] F. Zhao and V. I. Utkin. Adaptive simulation and control of variable-structure control system in sliding regimes. *Technical Report OSU-CISRC-3/95-TR10 - The Ohio State University*, 1995.

[97] G. M. Ziegler. *Lectures on Polytopes.* Springer, NY, 1998.

[98] J. G. Ziegler and N.B. Nichols. Optimal settings for automatic controllers. *Trans. on ASME*, 64:759–768, 1942.